Walter A. Rosenblith New Investigator Award

RESEARCH REPORT

HEALTH EFFECTS INSTITUTE

Number 197
March 2019

Cellular and Acellular Assays for Measuring Oxidative Stress Induced by Ambient and Laboratory-Generated Aerosols

Nga L. Ng, Wing Y. Tuet, Yunle Chen, Shierly Fok, Dong Gao, Marlen S. Tagle Rodriguez, Mitchel Klein, Anna Grosberg, Rodney J. Weber, and Julie A. Champion

Cellular and Acellular Assays for Measuring Oxidative Stress Induced by Ambient and Laboratory-Generated Aerosols

Nga L. Ng, Wing Y. Tuet, Yunle Chen, Shierly Fok, Dong Gao, Marlen S. Tagle Rodriguez, Mitchel Klein, Anna Grosberg, Rodney J. Weber, and Julie A. Champion

with a Critique by the HEI Review Committee

Research Report 197

Health Effects Institute

Boston, Massachusetts

Trusted Science • Cleaner Air • Better Health

Publishing history: This document was posted at *www.healtheffects.org* in March 2019.

Citation for document:

Ng NL, Tuet WY, Chen Y, Fok S, Gao D, Tagle Rodriguez MS, et al. 2019. Cellular and Acellular Assays for Measuring Oxidative Stress Induced by Ambient and Laboratory-Generated Aerosols. Research Report 197. Boston, MA:Health Effects Institute.

 Cameographics, Union, Me., Compositor. Printed by Recycled Paper Printing, Boston, Mass. Library of Congress Catalog Number for the HEI Report Series: WA 754 R432.

Cover paper: made with at least 55% recycled content, of which at least 30% is post-consumer waste; free of acid and elemental chlorine. Text paper: made with 100% post-consumer waste recycled content; acid free; no chlorine used in processing. The book is of permanent archival quality.

CONTENTS

ABOUT HEI

The Health Effects Institute is a nonprofit corporation chartered in 1980 as an independent research organization to provide high-quality, impartial, and relevant science on the effects of air pollution on health. To accomplish its mission, the institute

- Identifies the highest-priority areas for health effects research;
- Competitively funds and oversees research projects;
- Provides intensive independent review of HEI-supported studies and related research;
- Integrates HEI's research results with those of other institutions into broader evaluations; and
- Communicates the results of HEI's research and analyses to public and private decision makers.

HEI typically receives balanced funding from the U.S. Environmental Protection Agency and the worldwide motor vehicle industry. Frequently, other public and private organizations in the United States and around the world also support major projects or research programs. HEI has funded more than 340 research projects in North America, Europe, Asia, and Latin America, the results of which have informed decisions regarding carbon monoxide, air toxics, nitrogen oxides, diesel exhaust, ozone, particulate matter, and other pollutants. These results have appeared in more than 260 comprehensive reports published by HEI, as well as in more than 1,000 articles in the peer-reviewed literature.

HEI's independent Board of Directors consists of leaders in science and policy who are committed to fostering the public–private partnership that is central to the organization. The Research Committee solicits input from HEI sponsors and other stakeholders and works with scientific staff to develop a Five-Year Strategic Plan, select research projects for funding, and oversee their conduct. The Review Committee, which has no role in selecting or overseeing studies, works with staff to evaluate and interpret the results of funded studies and related research.

All project results and accompanying comments by the Review Committee are widely disseminated through HEI's website (*www.healtheffects.org*), printed reports, newsletters and other publications, annual conferences, and presentations to legislative bodies and public agencies.

ABOUT THIS REPORT

Research Report 197, *Cellular and Acellular Assays for Measuring Oxidative Stress Induced by Ambient and Laboratory-Generated Aerosols*, presents a research project funded by the Health Effects Institute and conducted by Dr. Nga Lee (Sally) Ng of the Georgia Institute of Technology, Atlanta, Georgia, and her colleagues. This research was funded under HEI's Walter A. Rosenblith New Investigator Award Program, which provides support to promising scientists in the early stages of their careers. The report contains three main sections.

The HEI Statement, prepared by staff at HEI, is a brief, nontechnical summary of the study and its findings; it also briefly describes the Review Committee's comments on the study.

The Investigators' Report, prepared by Ng and colleagues, describes the scientific background, aims, methods, results, and conclusions of the study.

The Critique, prepared by members of the Review Committee with the assistance of HEI staff, places the study in a broader scientific context, points out its strengths and limitations, and discusses remaining uncertainties and implications of the study's findings for public health and future research.

This report has gone through HEI's rigorous review process. When an HEI-funded study is completed, the investigators submit a draft final report presenting the background and results of the study. This draft report is first examined by outside technical reviewers and a biostatistician. The report and the reviewers' comments are then evaluated by members of the Review Committee, an independent panel of distinguished scientists who have no involvement in selecting or overseeing HEI studies. During the review process, the investigators have an opportunity to exchange comments with the Review Committee and, as necessary, to revise their report. The Critique reflects the information provided in the final version of the report.

HEI STATEMENT
Synopsis of Research Report 197

Cellular and Acellular Assays for Measuring Oxidative Stress Induced by Ambient and Laboratory-Generated Aerosols

BACKGROUND

In this study Dr. Nga (Sally) Ng, who was a recipient of HEI's Walter A. Rosenblith New Investigator Award, and her colleagues characterized and compared the oxidative properties of ambient PM and laboratory-generated secondary organic aerosol (SOA) using in vitro assays. SOA is formed in the atmosphere from the products of photochemical reactions of organic compounds. The chemistry involving the formation of SOA is complex and depends on many factors, such as precursor composition, temperature, humidity, concentration of oxides of nitrogen (NO_x), and existing aerosols.

APPROACH

Dr. Ng studied the relative oxidative activity of resuspended ambient PM and laboratory-generated SOA using a chemical assay (DTT) and a cellular assay (C-DCFH). The former assay assessed the ability of particle extracts to oxidize DTT in a test tube, while the latter assessed the ability of particle extracts to induce ROS production in macrophages grown in culture. Dr. Ng also studied induction of two markers of inflammation (tumor necrosis factor-α and interleukin-6) by SOA.

The ambient PM samples were collected as part of a previous study by the authors. The SOA samples were generated in an environmental chamber in the presence of simulated sunlight and ammonium sulfate (which serves as a seed particle onto which the semivolatile products condense) under different conditions (high and low humidity, high and low NO_x, and presence of redox-active metal). Separate experiments were performed using six organic compounds (SOA precursors) to generate different types of SOA: three precursors are commonly emitted by anthropogenic sources (*m*-xylene, naphthalene, and pentadecane) and three from biogenic sources (isoprene, α-pinene, and β-caryophyllene).

MAIN RESULTS AND INTERPRETATION

Ambient PM There was an association between oxidative potential (DTT assay) and ROS response (C-DCFH assay) for ambient PM collected in summer, but not for PM collected in winter. Some

What This Study Adds

- The study provides a systematic analysis of the ability of ambient particulate matter (PM) and laboratory-generated secondary organic aerosol (SOA) to induce the production of reactive oxygen species (ROS) as measured by both chemical (DTT) and cellular (C-DCFH) assays.
- The results show that all of the types of aerosol tested have the ability to induce production of ROS to some extent. For ambient PM, positive correlations were observed for water-soluble organic compounds, black carbon, and some metals in summer samples. Among the different types of SOA tested, naphthalene-derived SOA had the highest activity in both assays. There was a correlation between cellular ROS production and aerosol carbon oxidation state.
- The results of the SOA activity are novel and point to the need to better understand their effects on human health.

This Statement, prepared by the Health Effects Institute, summarizes a research project funded by HEI and conducted by Dr. Nga Lee (Sally) Ng at the Georgia Institute of Technology, Atlanta, Georgia, and colleagues. Research Report 197 contains both the detailed Investigators' Report and a Critique of the study prepared by the Institute's Review Committee.

constituents of summer PM (water-soluble organic compounds, brown carbon, iron, and titanium), but not of winter PM, were correlated with increased ROS production in the C-DCFH assay.

Laboratory-Generated SOA SOA formed from the photo-oxidation of naphthalene elicited the largest response in both the DTT and C-DCFH assays across all chamber conditions. SOA formed from isoprene oxidation had the lowest DTT activity. For the other precursors, the DTT activities were low. There was more variability in the ROS and inflammatory responses than in the DTT assay across the SOA, with naphthalene-derived SOA showing the largest range in inflammatory responses and isoprene-derived SOA, the lowest response. While there was no clear trend between chamber conditions (high and low NO_x and high and low humidity) and ROS production across the six types of SOA, the investigators reported a positive correlation between ROS production and carbon oxidation state.

CONCLUSIONS

In its independent review of this study by Ng and colleagues, the HEI Review Committee noted that the study provides an overview of whether components or characteristics of PM influence ROS formation. The Committee thought the results indicate that both ambient PM and SOA have some oxidative potential and ability to induce ROS production. While a correlation was observed between the two assays for summer PM samples, for SOA the correlation seemed to be driven by SOA produced by naphthalene, and thus not generalizable. The Committee noted that, because the chemical and cellular assays measure different aspects of oxidative activity, a correlation would not necessarily be expected. The experiments with laboratory-generated SOA also show that ROS production is accompanied by production of inflammatory mediators. However, there was no clear trend between ROS production and SOA precursor identity or formation condition. The Committee noted that biological relevance of these results is not known. However, SOA is a major component of fine particulate matter in many areas of the country, and the results of this study underscore the need to better understand the effects of SOA on human health.

INVESTIGATORS' REPORT

Cellular and Acellular Assays for Measuring Oxidative Stress Induced by Ambient and Laboratory-Generated Aerosols

Nga L. Ng[1,2], Wing Y. Tuet[1], Yunle Chen[3], Shierly Fok[1], Dong Gao[4], Marlen S. Tagle Rodriguez[5], Mitchel Klein[6], Anna Grosberg[5], Rodney J. Weber[2], and Julie A. Champion[1]

[1]*School of Chemical and Biomolecular Engineering, Georgia Institute of Technology, Atlanta, GA;* [2]*School of Earth and Atmospheric Sciences, Georgia Institute of Technology, Atlanta, GA;* [3]*School of Materials Science and Engineering, Georgia Institute of Technology, Atlanta, GA;* [4]*School of Civil and Environmental Engineering, Georgia Institute of Technology, Atlanta, GA;* [5]*Department of Biomedical Engineering, University of California–Irvine, Irvine, CA;* [6]*Rollins School of Public Health, Emory University, Atlanta, GA*

ABSTRACT

INTRODUCTION

Many studies have established associations between exposure to air pollution, or atmospheric particulate matter (PM*), and adverse health effects. An increasing array of studies have suggested oxidative stress as a possible mechanism by which PM-induced health effects arise, and as a result, many chemical and cellular assays have been developed to study PM-induced oxidant production. Although significant progress has been made in recent years, there are still many gaps in this area of research that have not been addressed. Many prior studies have focused on the aerosol of primary origin (e.g., the aerosol emitted from combustion engines) although the aerosol formed from the oxidation of volatile species, secondary organic aerosol (SOA), has been shown to be the predominant type of aerosol even in urban areas. Current SOA health studies are limited in number, and as such, the health effects of SOA are poorly characterized. Also, there is a lack of perspective in terms of the relative toxicities of different SOA systems. Additionally, although chemical assays have identified some SOA constituents associated with adverse health endpoints, the applicability of these results to cellular responses has not been well established.

SPECIFIC AIMS

The overall objective of this study was to better understand the oxidative properties of different types and components of PM mixtures (especially SOA) through systematic laboratory chamber experiments and ambient field studies. The study had four specific aims:

1. To develop a cellular assay optimized for measuring reactive oxygen and nitrogen species (ROS/RNS) production resulting from PM exposure and to identify a robust parameter that could represent ROS/RNS levels for comparison with different endpoints.
2. To identify ambient PM components associated with ROS/RNS production and evaluate whether results from chemical assays represented cellular responses in terms of ROS/RNS production.
3. To investigate and provide perspective on the relative toxicities of SOA formed from common biogenic and anthropogenic precursors under different conditions (e.g., humidity, nitrogen oxides [NO_x], and redox-active metals) and identify bulk aerosol properties associated with cellular responses.
4. To investigate the effects of photochemical aging on aerosol toxicity.

This Investigators' Report is one part of Health Effects Institute Research Report 197, which also includes a Critique by the Review Committee and an HEI Statement about the research project. Correspondence concerning the Investigators' Report may be addressed to Dr. Nga Lee (Sally) Ng, School of Chemical and Biomolecular Engineering and School of Earth and Atmospheric Sciences, Georgia Institute of Technology, 311 Ferst Dr. NW, Atlanta, GA 30322; email: *ng@chbe.gatech.edu*.

Although this document was produced with partial funding by the United States Environmental Protection Agency under Assistance Award CR–83467701 to the Health Effects Institute, it has not been subjected to the Agency's peer and administrative review and therefore may not necessarily reflect the views of the Agency, and no official endorsement by it should be inferred. The contents of this document also have not been reviewed by private party institutions, including those that support the Health Effects Institute; therefore, it may not reflect the views or policies of these parties, and no endorsement by them should be inferred.

* A list of abbreviations and other terms appears at the end of this volume.

METHODS

Ambient PM samples were collected from urban and rural sites in the greater Atlanta area as part of the Southeastern Center for Air Pollution and Epidemiology (SCAPE) study between June 2012 and October 2013. The concentrations of water-soluble species (e.g., water-soluble organic carbon [WSOC], brown carbon [BrC], and metals) were characterized using a variety of instruments. Samples for this study were chosen to span the observed range of dithiothreitol (DTT) activities.

Laboratory studies were conducted in the Georgia Tech Environmental Chamber (GTEC) facility in order to generate SOA under well-controlled photooxidation conditions. Precursors of biogenic origin (isoprene, α-pinene, and β-caryophyllene) and anthropogenic origin (pentadecane, *m*-xylene, and naphthalene) were oxidized under various formation conditions (dry vs. humid, NO_x, and ammonium sulfate vs. iron sulfate seed particles) to produce SOA of differing chemical composition and mass loading. For the naphthalene system, a series of experiments were conducted with different initial hydrocarbon concentrations to produce aerosols with various degree of oxidation. A suite of instruments was utilized to monitor gas- and particle-phase species. Bulk aerosol properties (e.g., O:C, H:C, and N:C ratios) were measured using a high-resolution time-of-flight aerosol mass spectrometer. Filter samples were collected for chemical oxidative potential and cellular measurements. For the naphthalene system, multiple filter samples were collected over the course of a single experiment to collect aerosols of different photochemical aging.

For all filter samples, chemical oxidative potentials were determined for water-soluble extracts using a semi-automated DTT assay system. Murine alveolar macrophages and neonatal rat ventricular myocytes were also exposed to PM samples extracted in cell culture medium to investigate cellular responses. ROS/RNS production was detected using the intracellular ROS/RNS probe, carboxy-2′,7′-dichlorodihydrofluorescein diacetate (carboxy-H_2DCFA), whereas cellular metabolic activity was assessed using 3-(4,5-dimethylthiazol-2-yl)-2,5-diphenyltetrazolium bromide (MTT). Finally, cytokine production, that is, secreted levels of tumor necrosis factor-α (TNF-α) and interleukin-6 (IL-6), were measured post-exposure using an enzyme-linked immunosorbent assay (ELISA). To identify PM constituents associated with oxidative properties, linear regressions between oxidative properties (cellular responses or DTT activity) and aerosol composition (metals, elemental ratios, etc.) were evaluated using Pearson's correlation coefficient, where the significance was determined using multiple imputation and evaluated using a 95% confidence interval.

RESULTS

We optimized several parameters for the ROS/RNS assay, including cell density (2×10^4 cells/well for macrophages and 3.33×10^4 cells/well for cardiomyocytes), probe concentration (10 μM), and sample incubation time (24 hours). Results from both ambient and laboratory-generated aerosols demonstrate that ROS/RNS production was highly dose-dependent and nonlinear with respect to PM dose. Of the dose–response metrics investigated in this study (maximum response, dose at which the response is 10% above the baseline [threshold], dose at which 50% of the response is attained [EC_{50}], rate at which the maximum response is attained [Hill slope], and area under the dose–response curve [AUC]), we found that the AUC was the most robust parameter whose informativeness did not depend on dose range.

A positive, significant correlation was observed between ROS/RNS production as represented by AUC and chemical oxidative potential as measured by DTT for ambient samples collected in summer. Conversely, a relatively constant AUC was observed for ambient samples collected in winter regardless of the corresponding DTT activity. We also identified several PM constituents (WSOC, BrC, iron, and titanium) that were significantly correlated with AUC for summer samples. The strong correlation between organic species and ROS/RNS production highlights a need to understand the contribution of organic aerosols to PM-induced health effects. No significant correlations were observed for other ROS/RNS metrics or PM constituents, and no spatial trends were observed.

For laboratory-generated aerosol, precursor identity influenced oxidative potentials significantly, with isoprene and naphthalene SOA having the lowest and highest DTT activities, respectively. Both precursor identity and formation condition significantly influenced inflammatory responses induced by SOA exposure, and several response patterns were identified for SOA precursors whose photooxidation products share similar carbon-chain length and functionalities. The presence of iron sulfate seed particles did not have an apparent effect on oxidative potentials; however, a higher level of ROS/RNS production was observed for all SOA formed in the presence of iron sulfate compared with ammonium sulfate. We also identified a significant positive correlation between ROS/RNS production and average carbon oxidation state ($\overline{OS}_c$), a bulk aerosol property. It may therefore be possible to roughly estimate ROS/RNS production using this property, which is readily obtainable. This correlation may have significant implications as aerosols have an atmospheric lifetime of a week, during which $\overline{OS}_c$ increases because of atmospheric photochemical aging. Our results suggest that aerosols

might become more toxic as they age in the atmosphere. Finally, in the context of ambient samples, laboratory-generated SOA induced comparable or higher levels of ROS/RNS. Oxidative potentials for all laboratory SOA systems, with the exception of naphthalene (which was higher), were all comparable with oxidative potentials observed in ambient samples.

INTRODUCTION

Exposure to PM is a leading global human health risk (Lim et al. 2012). Over the past few decades, there have been multiple epidemiological studies reporting associations between elevated PM concentrations and increased incidences of cardiopulmonary morbidity and mortality (Anderson et al. 2011; Brunekreef and Holgate 2002; Dockery et al. 1993; Hoek et al. 2013; Li et al. 2008; Lim et al. 2012; Pope et al. 2002; Pope III and Dockery 2006). More recent studies have also found significant associations between cardiopulmonary health effects and particle oxidative potential (Bates et al. 2015; Fang et al. 2016; Weichenthal et al. 2016; Yang et al. 2016). Furthermore, findings from toxicological studies suggest that PM-induced oxidant production, including ROS/RNS, may be a possible mechanism for PM-induced health effects (Castro and Freeman 2001; Gurgueira et al. 2002; Li et al. 2003a; Tao et al. 2003). Specifically, these oxidative species can initiate cellular inflammatory cascades, and prolonged stimulation of these cascades can lead to oxidative stress, cellular damage (e.g., lipid peroxidation, protein oxidation, and nucleic acid alteration), and chronic inflammation for which there is an established link to cancer (Hensley et al. 2000; Philip et al. 2004; Wiseman and Halliwell 1996). Collectively, these findings suggest that a possible link exists between PM exposure and observed health endpoints.

Multiple chemical and cellular assays have been developed to measure PM-induced oxidant production and elucidate constituents responsible for oxidant production (Cho et al. 2005; Fang et al. 2015c; Kumagai et al. 2002; Landreman et al. 2008). In biological systems, ROS/RNS are formed by the reaction between oxygen and reducing agents present in the cell, such as nicotinamide adenine dinucleotide phosphate (NADPH) and nicotinamide adenine dinucleotide (NADH) (Frei 1994). PM species can react with these reducing agents to initiate a series of redox reactions that ultimately produce superoxide anions, which can further react to produce hydrogen peroxides (e.g., Rattanavaraha et al. 2011). This is the basis of cell-free chemical assays, in which an antioxidant species (e.g., dithiothreitol, DTT; ascorbic acid; or other species present in the respiratory tract lining fluid) is used to simulate biologically relevant redox reactions, and anti-oxidant decay provides a measure of the concentration of redox-active species in a sample (Cho et al. 2005; Fang et al. 2015c; Kumagai et al. 2002). Cellular assays, on the other hand, utilize a non-fluorescent probe that reacts with ROS/RNS and produces a fluorescent compound post-reaction. The measured fluorescence is proportional to the concentration of ROS/RNS produced as a result of PM exposure (Landreman et al. 2008). In cellular systems, cells may also generate ROS/RNS as a signaling molecule and/or upregulate antioxidant defenses in response to stimuli (Wiseman and Halliwell 1996), which affects the measured ROS/RNS production. The cellular assay utilized in this study predominantly measures ROS/RNS produced by the cell in response to PM exposure. Redox-active species, the concentration of which is measured by chemical assays, can induce cellular ROS/RNS production and hence may be measured by the cellular assay as well. Furthermore, it may be possible for particle-bound ROS/RNS to diffuse across the cell membrane and react with the ROS/RNS probe. This is the basis of another acellular chemical assay, which has been used previously to study the oxidative properties of PM (Møller et al. 2009). Therefore, there exists some overlap between the types of ROS/RNS measured by both chemical and cellular assays.

Epidemiological studies and various assays have associated numerous PM components with adverse health effects. The potential contributions of metals have been explored extensively as many metals are redox-active and hence may produce ROS/RNS via Fenton-like reactions (Chevion 1988; Frei 1994). Many studies report findings that support the adverse influence of metals on PM-induced health effects. Epidemiological studies have found strong associations between metals, namely iron, nickel, and zinc, and mortality (Burnett et al. 2001). These observations are supported by toxicological studies, where various oxidative properties were found to be most significant in metal-containing samples (Akhtar et al. 2010; Pardo et al. 2015). Strong correlations between oxidative properties (e.g., neutrophil influx and oxidative potential) and water-soluble metals have also been reported (Charrier and Anastasio 2012; Charrier et al. 2015; Huang et al. 2003; Verma et al. 2010). Similarly, organic-carbon constituents have been found to be toxicologically relevant. Studies on the oxidative potential of PM have reported strong correlations between DTT activity and WSOC, as well as polycyclic aromatic hydrocarbons and other oxygenated aromatics, such as humic-like substances (Antinolo et al. 2015; Dou et al. 2015; Li et al. 2003b; Lin and Yu 2011; McWhinney et al. 2013b; Saffari et al. 2014b; Verma et al. 2009, 2012, 2015a, 2015b). Furthermore, inhalation and exposure studies

have found that organic-carbon constituents may play a significant role in PM-induced adverse effects (Hamad et al. 2015; Kleinman et al. 2005). However, many of these inhalation and exposure studies involved limited data sets and low-throughput methods, and the applicability of chemical oxidative potentials to cellular responses has not been established.

Ambient PM consists of a complex mixture of hundreds to thousands of species. Organic aerosols, which constitute a significant portion of PM, can be further divided into two classes of aerosols: primary organic aerosol (POA) and secondary organic aerosol (SOA) (Jimenez et al. 2009; Kanakidou et al. 2005; Zhang et al. 2007). POA is directly emitted as PM from a variety of sources, such as vegetation, fossil fuel combustion, and power plant operation. SOA, on the other hand, is formed from the oxidation of volatile species followed by gas-particle partitioning (Hallquist et al. 2009; Kroll and Seinfeld 2008). Currently, many pollution control strategies and policies are focused on primary emissions. Field studies, however, have shown that mass loadings of SOA often exceed those of POA, even in urban environments (Jimenez et al. 2009; Ng et al. 2010; Zhang et al. 2007). In the past, many health studies focused on primary emissions, such as the PM emitted from diesel and gasoline exhaust (Bai et al. 2001; Kumagai et al. 2002; McWhinney et al. 2013a; Turner et al. 2015), or were conducted on particles that were not representative of ambient exposures (Koike and Kobayashi 2006). More recent studies explored the potential health implications of SOA (Arashiro et al. 2016; Baltensperger et al. 2008; Kramer et al. 2016; Lund et al. 2013; McDonald et al. 2010, 2012; McWhinney et al. 2013b; Platt et al. 2014; Rattanavaraha et al. 2011). The oxidative potentials and cellular responses measured in these studies demonstrated that pure SOA could indeed contribute to PM-induced health effects. However, these studies generally focused on an SOA formed from a single precursor or on SOA generated in a simulated urban environment (Arashiro et al. 2016; Kramer et al. 2016; McDonald et al. 2012; McWhinney et al. 2013b; Rattanavaraha et al. 2011). Furthermore, the large range of oxidative potentials observed for individual SOA systems was largely unexplored (Kramer et al. 2016; McWhinney et al. 2013b). Results from cellular exposure studies also included different measures of response (e.g., ROS/RNS, gene expression, and inflammatory markers) and were inconclusive, with some studies reporting significant response as a result of SOA exposure and others observing little to no response (Arashiro et al. 2016; Baltensperger et al. 2008; Lund et al. 2013; McDonald et al. 2010, 2012). This may, in part, be attributable to the difference in exposure dose explored in each study. Overall, there is a lack of perspective in terms of the relative toxicities of individual SOA systems formed from various precursors, and it is unclear whether responses resulting from SOA exposure are indeed toxic compared with other sources and subtypes of PM. Finally, the potential health implications arising from organic aerosols formed in the presence of redox-active metals have also not been explored, even though this formation condition can be atmospherically relevant as these metals are readily emitted via combustion and various mechanical processes (Charrier and Anastasio 2012; Fang et al. 2015a). Moreover, both components (metals and organics) have been shown to have considerable health effects in previous studies. This formation of organic aerosols in the presence of metals may therefore produce aerosols that are highly detrimental to health. Furthermore, organic aerosols have a lifetime of approximately one week, over which continued photochemical aging can alter their physical and chemical properties. These changes have potential health implications that have not be explored.

SPECIFIC AIMS

The main objectives of this study were to better understand the oxidative properties of different types of PM mixtures, especially SOA, through laboratory-chamber experiments and ambient field studies, as well as to determine whether chemical oxidative potential results were representative of cellular responses. Figure 1 gives an overview of the approaches utilized in this study to assess these objectives. Major gaps in the literature were addressed by using a dose–response approach for assessing cellular responses, considering multiple dose–response parameters, obtaining a large data set for comparison of results of cellular and chemical assays, and systematically investigating SOA generated from a variety of precursor compounds under multiple formation conditions. There were four specific aims in this study:

- *Objective 1:* To develop and optimize a cellular assay for measuring ROS/RNS production as a result of PM exposure and to determine an appropriate parameter to represent ROS/RNS production for comparison with other assays, as well as between different PM samples.
- *Objective 2:* To elucidate PM constituents associated with ROS/RNS production, investigate seasonal trends (summer vs. winter), and determine whether results from chemical assays were representative of cellular responses.

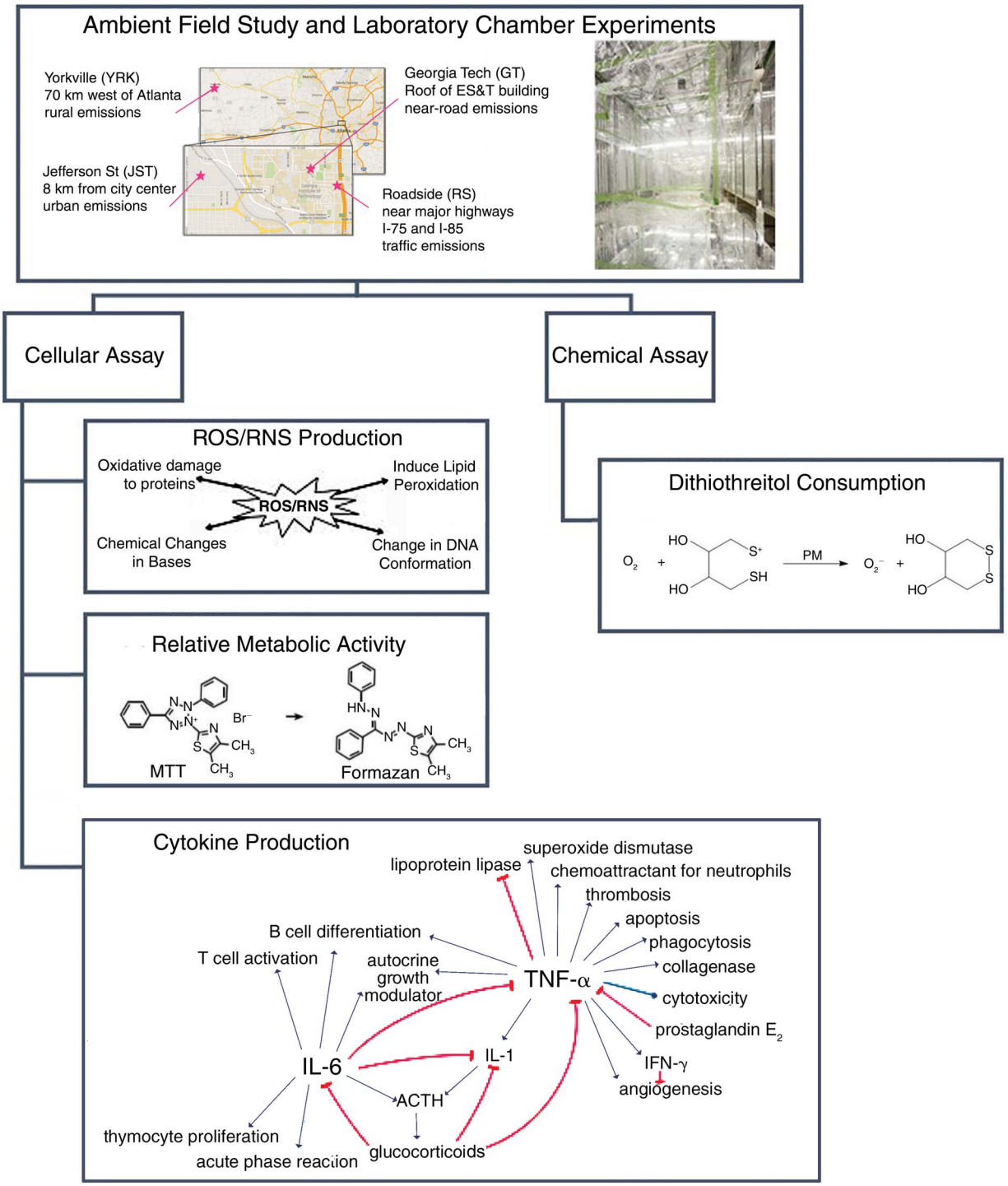

Figure 1. Overview of methodologies taken to assess the oxidative properties of different types of PM mixtures through laboratory chamber experiments and ambient field studies and to determine whether chemical oxidative potential results represent cellular responses.

- *Objective 3:* To provide perspective on the relative toxicities of SOA generated from a variety of biogenic and anthropogenic precursors formed under multiple formation conditions and determine whether correlations exist between chemical composition and ROS/RNS production.
- *Objective 4:* To investigate the effects of photochemical aging processes on aerosol toxicity.

METHODS AND STUDY DESIGN

AMBIENT FIELD STUDY

Southern Center for Air Pollution and Epidemiology

Ambient $PM_{2.5}$ samples were collected from multiple sites (Figure A.1 in Additional Materials 1: Appendix A, available on the HEI website) around the greater Atlanta region as part of the Southeastern Center for Air Pollution and Epidemiology (SCAPE) study (Bates et al. 2015; Fang et al. 2015a, 2015c, 2016; Verma et al. 2014, 2015a; Xu et al. 2015a, 2015b). Filter samples were collected from urban and rural sites between June 2012 and October 2013 using high-volume samplers (ThermoAndersen). The volume of air collected was the same for all samples. Urban sites included Jefferson Street, located 8 km from the city center; Roadside, located near major highways I-75 and I-85; and Georgia Tech, located at the roof of the Ford Environmental Science and Technology building. The rural site (Yorkville) was located 70 km west of Atlanta. Particles were collected over 23 hours onto pre-baked quartz filters (Pallflex Tissuquartz). Collected filter samples were wrapped in pre-baked aluminum foil and stored at −20°C until extraction and analysis (Fang et al. 2015c). The DTT activities of all filters collected during this field campaign had been determined previously and source apportionment regressions had been applied to these results to identify PM sources that may contribute significantly to health effects (Bates et al. 2015; Fang et al. 2015a; Verma et al. 2014, 2015a). In this study, ambient samples were selected for cellular analysis based on the observed DTT activity ranges reported in a previous study (Verma et al. 2014).

Filter Characterization

The concentrations of water-soluble species were characterized and reported in previous studies (Fang et al. 2015a, 2015b). Specifics on filter characterization methods are described elsewhere (Fang et al. 2015a). Briefly, WSOC concentrations and BrC absorptions were determined using an automated system consisting of an autosampler, a liquid waveguide capillary cell, a spectrophotometer, and a total organic carbon analyzer, whereas elemental and organic carbon were determined using a thermal/optical transmittance analyzer (Verma et al. 2014). Water-soluble metal concentrations were also determined using a Xact 625 automated multi-metals monitor (Fang et al. 2015a).

Filter Extraction

Collected ambient particles were extracted following the procedure described in Fang and colleagues (2015a), with modifications for cellular exposure. The mass in each extract was determined based on the PM mass collected on the filter and the fraction of the filter extracted. Briefly, sectioned filter samples were submerged in extraction medium (cell culture medium for cellular exposure and deionized water for oxidative potential measurement) and sonicated for 30 minutes using an Ultrasonic Cleanser (VWR). Extracts were then filtered using 0.45-μm polytetrafluoroethylene syringe filters (Fisherbrand) to remove quartz fibers, which are known to elicit inflammatory responses (Fubini and Hubbard 2003; Knaapen et al. 2002). Extracts for cellular exposure were also supplemented with 10% fetal bovine serum (FBS) prior to exposure and diluted over ten dilutions (from $1x$–$0.00125x$, with $1x$ being the undiluted extract). Although these filter extracts differ from real-world aerosol exposures, a previous study on the health effects of isoprene SOA found similar cellular responses for both filter resuspension extracts (those utilized in this study) and direct air–liquid deposition, which more closely represent real-world aerosol exposures (Arashiro et al. 2016).

LABORATORY CHAMBER EXPERIMENTS

Chamber Facility and Measurements of Aerosol and Gas Phase Composition

SOA was generated in the Georgia Tech Environmental Chamber (GTEC) facility, which consists of two 12-m^3 Teflon chambers suspended inside a 21-ft × 12-ft temperature-controlled (4–40°C) room (Boyd et al. 2015). The chambers are surrounded by black lights (Sylvania 24922) with an output in the ultraviolet range (300–400 nm) and natural sunshine fluorescent lamps (Sylvania 24477) with an output between 300 and 900 nm. To further maximize reflectivity, the chamber interior is constructed using aluminum sheets.

Each chamber has three Teflon manifolds with multiple sampling ports that allow for injection of reagents and continuous monitoring and gas- and particle-phase species. Gas-phase measurements include nitrogen dioxide (NO_2), NO_x, and ozone concentrations as monitored using a cavity attenuated phase shift NO_2 monitor (Aerodyne), a

chemiluminescence NO_x analyzer (Teledyne 200EU), and a ultraviolet absorption ozone analyzer (Teledyne T400), respectively. A gas chromatograph flame ionization detector (Agilent 7890A) was also used to monitor gas-phase hydrocarbon concentrations over the course of the experiment. Particle-phase measurements include aerosol volume concentrations and distributions, as measured using a scanning mobility particle sizer (TSI), and bulk aerosol composition, as determined using a high-resolution time-of-flight aerosol mass spectrometer (AMS, Aerodyne) (DeCarlo et al. 2006). AMS data were analyzed using two data analysis toolkits, SQUIRREL (v. 1.57) and PIKA (v. 1.16G). Bulk aerosol elemental composition (expressed as O:C, H:C, and N:C ratios) were obtained using the method outlined by Canagaratna and colleagues (2015); these ratios were also used to calculate the average carbon oxidation state $\overline{OS}_c$, as described by Kroll and colleagues (2011).

Secondary Organic Aerosol Generation Systems

The laboratory chamber experiments were designed to probe the effects of humidity, peroxy radical (RO_2•) fate, precursor identity, and presence of metal-containing seed particles on SOA formation and toxicity (Table 1). Precursors of biogenic and anthropogenic origins were chosen to include major classes of compounds known to produce SOA upon atmospheric oxidation. Biogenic precursors include: isoprene, the most abundant non-methane hydrocarbon emission with estimated global emissions around 500 Tg/yr (Guenther et al. 2006); α-pinene, the most well-studied monoterpene and a hydrocarbon with emissions on the order of total global anthropogenic emissions (Guenther et al. 1993; Piccot et al. 1992); and β-caryophyllene, a representative sesquiterpene (Hoffmann et al. 1997; Tasoglou and Pandis 2015). Likewise, anthropogenic precursors include: pentadecane, a long-chain alkane; *m*-xylene, a single-ring aromatic; and naphthalene, a polyaromatic. These anthropogenic compounds are emitted as products of incomplete combustion (Bruns et al. 2016; Jia and Batterman 2010; Robinson et al. 2007) and have considerable SOA yields (Chan et al. 2009; Hildebrandt et al. 2009; Lambe et al. 2011; Ng et al. 2007b). SOA precursor concentrations were chosen to strike a balance between typical ambient concentrations and adequate SOA mass for cellular exposure experiments. The SOA mass concentrations generated in all chamber experiments ranged from 6–400 μg/m^3, a range that represents aerosol mass concentration in relatively clean to highly polluted ambient environments.

In addition to precursor identity, different formation conditions were investigated as well. These conditions include the effects of humidity (dry vs. humid); low and high NO_x levels, which influence RO_2• fate (RO_2• + hydroperoxyl radical [HO_2•] vs. RO_2• + nitrogen oxide [NO] at low and high NO_x, respectively); and the presence of metal-containing seed particles (ammonium sulfate vs. iron sulfate). These conditions are known to affect SOA chemical composition and mass loading (Boyd et al. 2015; Chan et al. 2009; Chhabra et al. 2010, 2011; Chu et al. 2012, 2014; Cocker III et al. 2001a, 2001b; Daumit et al. 2016; Eddingsaas et al. 2012; Healy et al. 2009; Loza et al. 2014; Ng et al. 2007a, 2007b; Song et al. 2005; Stirnweis et al. 2017).

All experiments were conducted at approximately 25°C under either dry (relative humidity < 5%) or humid (relative humidity ~ 45%–50%) chamber conditions. Before the start of each experiment, chambers were flushed with pure air for ~24 hours. During this time, a bubbler filled with deionized water was added in-line to humidify chambers for humid experiments. Seed particles were then atomized into the chamber and the seed concentration was allowed to stabilize. The experimental conditions are listed in Table 1. For experiment 7 (i.e., isoprene SOA formed under low NO_x and humid conditions), it should be noted that experimental conditions deviated due to low mass yields in experiment 1. Instead, the SOA was formed via the isoprene epoxydiol uptake pathway by means of an acidic seed and dry chamber. This pathway produces more SOA mass compared with the isoprene epoxydiol + hydroxyl radical (•OH) pathway (experiment 1) and has been shown to contribute significantly to ambient organic aerosols (Budisulistiorini et al. 2013; Chen et al. 2015; Hu et al. 2015; Liao et al. 2015; Lin et al. 2012; Robinson et al. 2011; Slowik et al. 2011; Surratt et al. 2010; Xu et al. 2015a).

After seed injection, hydrocarbon (isoprene, 99%; α-pinene, ≥ 99%; β-caryophyllene, > 98.5%; pentadecane, ≥ 99%; *m*-xylene, ≥ 99%; and naphthalene, 99% [Sigma Aldrich]) was introduced into the chamber by injecting hydrocarbon solution into a glass bulb and passing pure air over the solution. Several hydrocarbons required slightly modified injecting methods: for pentadecane and β-caryophyllene, gentle heat was applied to the glass bulb (Tasoglou and Pandis 2015); for naphthalene, naphthalene was injected by passing pure air over solid naphthalene (Chan et al. 2009). Upon completion of hydrocarbon injection, OH precursor (either hydrogen peroxide [H_2O_2, for low NO_x condition] or nitrous acid [HONO, for high NO_x condition]) was introduced into the chambers. H_2O_2 (50% aqueous solution, Sigma Aldrich) was injected using the same method as that described for hydrocarbon injections, whereas HONO was first prepared (10 mL of 1% wt aqueous sodium nitrite [$NaNO_2$] dropwise into 20 mL of 10% wt sulfuric acid [H_2SO_4]) followed by passing pure air over the

Table 1. Experimental Conditions for Secondary Organic Aerosol Generation Systems

Experiment	SOA precursor	Seed Particle[a,b,c]	OH Precursor	RH (%)	Initial Concentration (ppb)		
					HC	NO_x	NO_2
1	Isoprene	AS	H_2O_2	<5	97	<1	<1
2	α-Pinene	AS	H_2O_2	<5	191	<1	<1
3	β-Caryophyllene	AS	H_2O_2	<5	36	<1	<1
4	Pentadecane	AS	H_2O_2	<5	106	<1	<1
5	*m*-Xylene	AS	H_2O_2	<5	450	<1	<1
6	Naphthalene	AS	H_2O_2	<5	178	<1	<1
7	Isoprene	MS + SA	H_2O_2	<5	97	<1	<1
8	α-Pinene	AS	H_2O_2	40	334	<1	<1
9	β-Caryophyllene	AS	H_2O_2	42	63	<1	<1
10	Pentadecane	AS	H_2O_2	45	106	<1	<1
11	*m*-Xylene	AS	H_2O_2	45	450	<1	<1
12	Naphthalene	AS	H_2O_2	44	431	<1	<1
13	Isoprene	AS	HONO	<5	970	306	276
14	α-Pinene	AS	HONO	<5	174	240	260
15	β-Caryophyllene	AS	HONO	<5	21	260	180
16	Pentadecane	AS	HONO	<5	74	330	250
17	*m*-Xylene	AS	HONO	<5	431	400	270
18	Naphthalene	AS	HONO	<5	145	291	300
19	Naphthalene	AS	H_2O_2	51	32	315	—
20	Naphthalene	AS	H_2O_2	49	92	368	—
21[d]	Naphthalene	AS	H_2O_2	54	186	344	—
22	Naphthalene	AS	H_2O_2	53	342	320	—
23	Naphthalene	FS	H_2O_2	50	32	303	—
24	Naphthalene	FS	H_2O_2	48	84	314	—
25	Naphthalene	FS	H_2O_2	52	182	321	—
26	Naphthalene	FS	H_2O_2	51	331	295	—

Note: HC = hydrocarbon; •OH = hydroxyl radical; RH = relative humidity; SOA = secondary organic aerosol.

[a] AS: Ammonium sulfate seed (15 mM $(NH_4)_2SO_4$).

[b] MS + SA: acidic seed (8 mM $MgSO_4$ and 16 mM H_2SO_4) was used instead of 15 mM $(NH_4)_2SO_4$.

[c] FS: Iron sulfate seed (15 mM $FeSO_4$).

[d] Experiment was repeated, and multiple filters were collected to investigate the effects of aging.

solution (Chan et al. 2009; Kroll et al. 2005). Finally, ultraviolet lights were switched on to initiate photooxidation. An example of a time series for a photooxidation experiment conducted under dry, NO_x dominant conditions is shown in Figure 2.

Aerosol Collection and Extraction

SOA samples were collected onto 47-mm Teflon filters (0.45-μm pore size, Pall Laboratory). The aerosol mass collected on each filter was determined by integrating the volume concentration obtained from the scanning mobility particle sizer (assuming density of 1 g/cm^3) as a function of time over the filter collection period and using the total volume of air collected, as determined by a flow meter placed in-line with the sampling line (Table C.2 in Additional Materials 3: Appendix C, available on the HEI website). Aerosol mass concentrations were determined using SMPS volume concentrations assuming an aerosol density of 1 g/cm^3. While typical SOA density is approximately 1.4 g/cm^3, there is much variation depending on precursor identity and formation condition, and aerosol densities between 1 and 1.6 g/cm^3 have been reported in previous

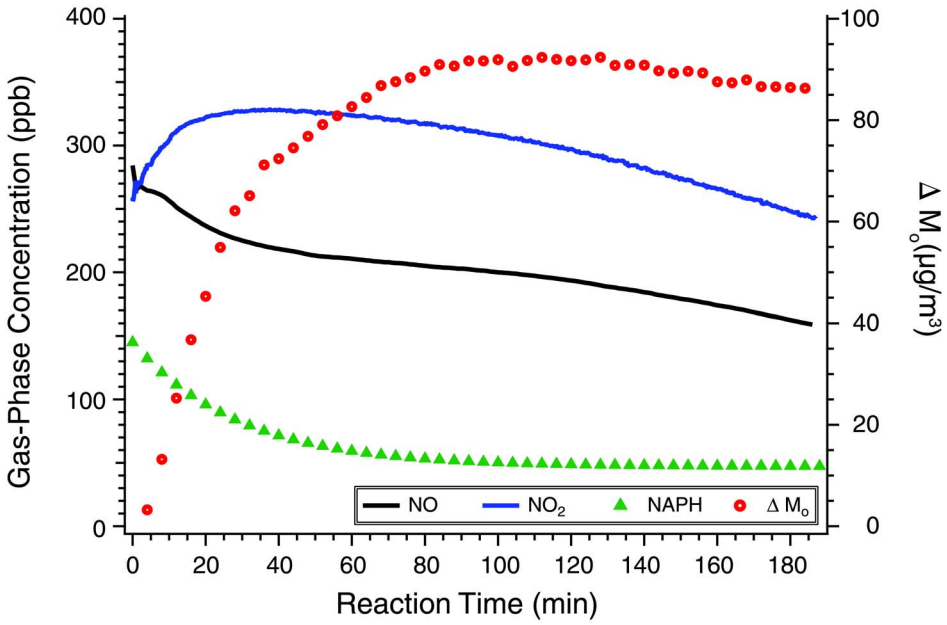

Figure 2. Reaction profile for chamber experiment conducted under dry, high NO_x (RO_2• + NO dominant) conditions. ΔM_o corresponds to aerosol mass concentration. Initial naphthalene concentrations were determined using the chamber volume and mass of naphthalene injected. See Methods for details. Mass concentrations have been corrected for particle wall loss (Nah et al. 2017). (Source: Tuet et al. 2017c. Creative Commons Attribution 3.0 License.)

studies (Bahreini et al. 2005; Chan et al. 2009; Ng et al. 2007a; 2007b; Tasoglou and Pandis, 2015). The use of a density of 1 g/cm^3 is to facilitate easier comparisons with past and future studies. Results from future studies can be scaled accordingly for comparison with the current work. After collection, filter samples were placed in sterile petri dishes, sealed with plastic paraffin film (Parafilm M, Bemis), and stored at −20°C until extraction and analysis (Fang et al. 2015c). The extraction procedure differs slightly for Teflon filters compared to quartz filters (discussed previously for ambient samples). Sectioned filters were submerged in deionized water or cell culture medium and sonicated for 1 hour using an ultrasonic cleaner (VWR). Sonication steps were performed in 30-minute intervals and the bath water was replaced after each interval to reduce the bath temperature. After sonication, extracts were filtered using syringe filters, as described for quartz filters.

CHEMICAL OXIDATIVE POTENTIAL

A semi-automated DTT assay system was used to measure the oxidative potential of PM samples. Details of the high-throughput system are described elsewhere (Fang et al. 2015c). Although various cell-free assays have been developed to measure oxidative potential, the DTT assay is ideal for the purposes of this study. Prior studies have proven that the DTT assay is sensitive to organic constituents and reported correlations between DTT activity and organic carbon (Janssen et al. 2014; Visentin et al. 2016). Additionally, the DTT activities of various types of laboratory-generated SOA and ambient samples have been reported in previous studies for comparison purposes (Bates et al. 2015; Fang et al. 2015c; Kramer et al. 2016; Lu et al. 2014; McWhinney et al. 2013a, 2013b; Verma et al. 2015a; Xu et al. 2015a, 2015b). Like all assays, the DTT assay also has certain limitations. For instance, prior studies have shown that DTT does not respond significantly to iron (Charrier and Anastasio 2012). Furthermore, as a chemical assay, it is unclear whether its results are representative of cellular responses and the use of filter extracts is subject to extraction efficiencies and choice of extraction medium.

In this assay, DTT (Sigma Aldrich) acted as a surrogate antioxidant and PM catalyzed the transfer of electrons from DTT to oxygen. The reaction was carried out in a potassium phosphate buffer (VWR) and incubated at 37°C to mimic the cellular environment. Briefly, the method consisted of three main steps: (1) oxidation of DTT by redox-active species present in the PM sample, (2) reaction of residual, unoxidized DTT with 5,5′-dithiobis-(2-nitrobenzoic acid) (Sigma Aldrich) to form 2-nitro-5-mercaptobenzoic acid, repeated at specific time intervals, and

(3) measurement of 2-nitro-5-mercaptobenzoic acid at 412 nm to determine DTT consumption. After each time interval and between samples, the system was programmed to perform a self-clean, in which all lines and reaction vials were flushed with deionized water. The rate of DTT consumption was then obtained using the measured absorbance of 2-nitro-5-mercaptobenzoic acid over time. This rate of DTT consumption, or DTT activity, was blank-corrected by subtracting the rate of DTT decay obtained from a blank filter extract from that of the PM sample. For comparison purposes, the DTT activity was also normalized by the total volume of air sample (per m^3, extrinsic) or the total mass of PM (per μg, intrinsic). The extrinsic and intrinsic terminology was adapted from previous studies on DTT activity, where both bases were considered to evaluate health effects (e.g., Fang et al. 2015c; Verma et al. 2014). The two bases can be interconverted using the PM concentration of the sample according to the following equations (units are given in brackets):

$$AUC_{extrinsic}\left[\frac{1}{m^3}\right] = AUC_{intrinsic}\left[\frac{1}{\mu g}\right] \times PM\ \ concentration\left[\frac{\mu g}{m^3}\right]$$

and

$$AUC_{intrinsic}\left[\frac{1}{\mu g}\right] = AUC_{extrinsic}\left[\frac{1}{m^3}\right] \times \frac{1}{PM\ \ concentration}\left[\frac{m^3}{\mu g}\right].$$

A detailed example of interconverting between the two metrics can be found in Additional Materials 2: Appendix B, available on the HEI website. Both metrics serve a purpose for health effects investigations. The intrinsic metric provides information on the toxicity of the specific PM source, whereas the extrinsic metric provides information on exposure-related toxicity.

AEROSOL EXPOSURE

For all cellular measurements (i.e., ROS/RNS, metabolic activity, and cytokine production), cells were exposed to ambient PM and SOA samples extracted in cell culture medium supplemented with 10% FBS (Quality Biological). Optimal sample incubation times were considered for each endpoint. Details on optimization and selection of specific time points are given in sections pertaining to each measurement.

INTRACELLULAR REACTIVE OXYGEN/NITROGEN SPECIES PRODUCTION

Alveolar Macrophage Cell Line

Alveolar macrophages are involved in the clearance of foreign material as well as in the inflammatory signaling pathways that may be induced as a result of exposure to foreign material (Oberdörster et al. 1992; Oberdörster 1993). As such, they were chosen to represent an essential line of defense against environmental insults, such as PM exposure. Immortalized murine alveolar macrophages from the MH-S cell line (ATCC CRL-2019) were cultured in RPMI-1640 medium (ATCC) supplemented with 10% FBS, 1% penicillin-streptomycin, and 50 μM β-mercaptoethanol at 37°C and 5% carbon dioxide (CO_2). Details regarding the establishment of this cell line are described in Mbawuike and Herscowitz (1989). The medium formulation used for cell culture will hereon be referred to as complete medium. Cells were grown to confluency, upon which they were seeded at a density of 2×10^4 cells/well onto 96-well plates pretreated with 10% FBS in phosphate-buffered saline (PBS, Cellgro). For seeding and subsequent steps, β-mercaptoethanol addition was removed from the complete medium formulation because it is a reducing agent that may interfere with ROS/RNS measurement. For consistency, the same procedure was followed for other measurements as well (i.e., cytokine production and cellular metabolic activity). Seeded plates were incubated at 37°C and 5% CO_2 for 24 hours prior to PM exposure. This incubation period allows cells to adhere and acclimate to the well plate.

Ventricular Myocyte Isolation and Culture

Selected ambient filter samples were also analyzed using cardiomyocytes. Primary ventricular myocytes are the active cell type in cardiac tissue and were chosen for investigation because cardiac health is known to be affected by air pollution (e.g., increased incidences of ischemic heart disease and cardiac failure) (Brook et al. 2010; Pope and Dockery 2006). Neonatal rat ventricular myocytes (NRVM) were harvested from 2-day-old neonatal Sprague-Dawley rats (Charles River Laboratories) according to preestablished protocol (Grosberg et al. 2012). All animal use followed the guidelines of Institutional Animal Care and Use Committee of University of California, Irvine. Isolated heart tissue cells were resuspended in M199 medium supplemented with 10% FBS, 10 mM 4-(2-hydroxyethyl)-1-piperazineethanesulfonic acid, 0.1 mM minimum essential

medium nonessential amino acids, 3.5 g/L glucose, 2 mM L-glutamine, 2 mg/L vitamin B12, and 50 U/mL penicillin (complete medium for cardiomyocytes). Several iterations of pre-plating were then performed to increase the cardiomyocyte purity to 90–98%. Briefly, the resuspended cell solution was transferred to a tissue-culture flask and incubated for 40–50 minutes. Afterwards, the cell solution was removed and transferred to another flask. This procedure increases the purity of cardiomyocytes, which adhere more slowly than other heart cells, such as fibroblasts. Once the desired purity was reached, cells were seeded onto 96-well plates pre-coated with polydimethylsiloxane (Dow Corning Sylgard 184) and fibronectin (Fisher Scientific) at a density of 3.33×10^4 cells/well. Seeded plates were incubated at 37°C and 5% CO_2 and cultured for 48 hours prior to PM exposure. At 24 hours post-seeding, cells were washed with PBS to remove dead or non-adherent cells and the medium was replaced. From 48 hours on, the FBS concentration in the medium formulation was reduced to 2% to slow the growth of any residual fibroblasts.

Reactive Oxygen/Nitrogen Species Assay

Carboxy-2′,7′-dichlorodihydrofluorescein diacetate (carboxy-H_2DCFDA, Fisher Scientific C-400) was used to detect intracellular ROS/RNS production. The small molecule, cell-permeable probe diffuses across the cell membrane and is subsequently deacetylated by cellular esterases. This yields carboxy-2′,7′-dichlorodihydrofluorescein (carboxy-DCFH), which is impermeable to the cell membrane and therefore remains inside the cell. Although the process is not perfect and there may be some outward diffusion, carboxy-DCFH is better retained than the commonly used 2′,7′-dichlorofluorescein diacetate (DCFH-DA) due to its additional negative charges (Chen et al. 2010; Uchida et al. 2004). Upon reaction with ROS/RNS, carboxy-DCFH is transformed into carboxy-2′,7′-dichlorofluorescein (carboxy-DCF), which fluoresces in the green fluorescent protein range. The measured fluorescence is then proportional to the ROS/RNS produced. It should be noted that although these fluorescent probes are widely used, there have been recent studies on their limitations (e.g., Kalyanaraman et al. 2012) that will require further investigation.

The optimized assay is shown in Figure 3 and consisted of the following main steps: (1) pretreatment of 96-well plates, (2) seeding of cells at desired cell density, (3) incubation of cells with ROS/RNS probe, (4) exposure of probe-treated cells to samples or controls, and (5) measurement of ROS/RNS using a microplate reader (BioTek Synergy H4). Various assay parameters were optimized, including cell density, probe concentration, and sample incubation time. Optimized parameters will be given in the following description of the assay; details on the optimization process are described later (see Macrophage Assay Development and Optimization section).

Prior to seeding cells, 96-well plates were first pretreated to reduce the aggregation of cells near hydrophobic well walls and to ensure a uniform cell density throughout the well. Cells were then seeded at 2×10^4 cells/well for MH-S and 3.33×10^4 cells/well for neonatal rat ventricular myocytes. Seeded plates were returned to the incubator for 24 hours, during which the cells were allowed to adhere and acclimate. Afterwards, the cell culture medium was removed, and cells were washed with PBS. 120 μL of ROS/RNS probe diluted to a final concentration of 10 μM was added to each well and incubated for 40 minutes at 37°C and 5% CO_2. After this incubation period, any probe remaining outside the cell was removed. The cells were then exposed to 120 μL of PM extract of control solution for 24 hours. All controls were prepared using cell culture medium supplemented with 10% FBS. Positive controls included: bacterial cell wall component, lipopolysaccharide (LPS, 1 μg/mL), H_2O_2 (100 μM), and ambient reference filter extract (10 filter punches per mL, one filter punch per filter sample from various ambient filters collected at Georgia Tech). LPS and H_2O_2 are known to induce oxidative stress and inflammation in macrophages (Chen et al. 2007; Tang et al. 2007). On the other hand, the ambient reference filter extract should elicit similar cellular pathways as filter samples of interest. Negative controls include: blank filter extract (two filter punches per mL) and control cells (defined as probe-treated cells exposed to stimulant-free media). After the sample incubation period, samples and controls were removed and replaced with a balanced salt solution (PBS or Tyrode's) for fluorescence measurement (ex: 485 nm, em: 525 nm) using a microplate reader (BioTek Synergy H4).

For each sample, a wide dose range ($0.00125x$–$1x$) was investigated to fully capture the dose–response relationship. The dose ranges investigated are relevant exposure doses based on the average dose delivered to alveolar macrophages assuming 100% deposition and a full day of exposure, based on the optimized sample incubation time (see Macrophage Assay Development and Optimization section). Details of this calculation are given in Table B.5 in Appendix B, available on the HEI website).

The Hill equation was then applied to obtain dose–response metrics (Goutelle et al. 2008; Hill 1910):

$$y = base + \frac{\max - base}{1 + \left(\frac{EC_{50}}{x}\right)^{Hill\ slope}}$$

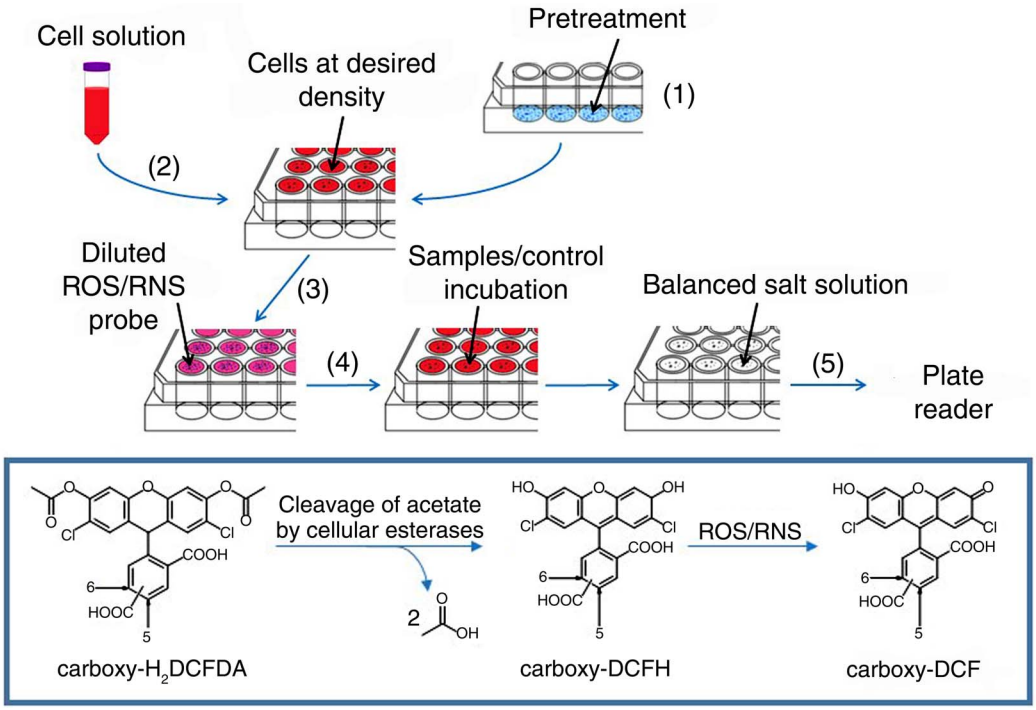

Figure 3. Cellular assay optimized for measuring intracellular reactive oxygen and nitrogen species (ROS/RNS) production as a result of exposure to PM samples. Major steps include (1) pretreatment of 96-well plates, (2) seeding of cells onto wells at desired cell density, (3) incubation of cells with ROS/RNS probe (carboxy-H_2DCFDA), (4) exposure of probe-treated cells to samples or controls, and (5) measurement of ROS/RNS using a microplate reader. The ROS/RNS probe structure, as well as the reaction involved in transforming the probe into a fluorescent compound, is given in the boxed insert. (Adapted from Tuet et al. 2016 with permission from Elsevier.)

where *y* represents ROS/RNS response and *x* represents the PM dose. These parameters include the maximum response attained as a result of PM exposure (max), the dose at which response is 10% above the fitted baseline (threshold), the dose at which 50% of the maximum response is attained (EC_{50}), the rate at which the maximum response is attained once a response is observed (Hill slope), and the area under the dose–response curve (AUC), which may be used to represent the overall effect of PM exposure across the dose range investigated. AUCs were mathematically calculated using the fitted dose–response curve and the same dose range to properly compare different samples. Detailed calculations for AUC determination are given in Appendix B, available on the HEI website. AUCs were expressed in units of fold over control × dose, where dose can be expressed in either units of m^3 or μg. A base of one was used to calculate AUCs because the probe-treated control ROS/RNS response is one after normalization (i.e., all ROS and/or RNS levels were normalized to the ROS/RNS produced from probe-treated cells exposed to stimulant-free media). Therefore, for flat dose–response behaviors, where all responses did not differ from that measured for probe-treated control cells, the calculated AUC was zero and the maximum response was one. To aid interpretation of AUC values, a sample with a higher AUC value induced more ROS/RNS production than a sample with a lower AUC value over the same dose range. When comparing responses from two different samples, although the ROS/RNS levels at specific doses may be higher or lower for a sample, the sample with a higher AUC has an overall higher toxicity over the entire dose range. For comparison purposes, the AUC value for ambient samples was normalized by the total volume of air sampled (per m^3, extrinsic) or the total mass of PM (per μg, intrinsic); the AUC value for laboratory SOA was normalized by total mass of SOA (per μg, intrinsic). We also reported the AUC value for laboratory SOA normalized by total volume of air sampled (per m^3, extrinsic) (in Additional Materials 4.1: Appendix D.1, available on the HEI website) for reference. However, we note that it is not meaningful to compare extrinsic values for laboratory SOA since the volume of air sampled differed in the SOA experiments. Thus, only intrinsic values are compared for SOA systems.

CELLULAR METABOLIC ACTIVITY

For each ROS/RNS measurement of chamber SOA samples and subset of PM samples (data not provided), cellular metabolic activity was also measured to correct for changes in ROS/RNS levels that may result from changes in relative metabolic activity (Zhang et al. 2016). Cellular metabolic activity was assessed using MTT (Biotium) and the data are included in Appendix D, available on the HEI website. Briefly, supernatants were removed post-exposure (24 hours, chosen to be the same time point as that of ROS/RNS) and replaced with medium containing MTT, after which the cells were incubated for 4 hours. During this incubation period, the tetrazolium dye was reduced by cellular NADPH-dependent oxidoreductases to form formazan, an insoluble purple salt. Dimethyl sulfoxide was then added to solubilize the salt. Absorbance at 570 nm was measured using a microplate reader (BioTek Synergy H4).

CELLULAR CYTOKINE PRODUCTION

For selected laboratory SOA samples, an ELISA was used to measure post-exposure secreted levels of TNF-α and IL-6 following manufacturer's specifications (ThermoFisher KMC3011C and KMC0061C). All cytokine measurements were carried out using undiluted cell-culture supernatants collected after 24 hours of PM exposure. This time point was chosen to maximize the signal strength of both cytokines, as the peak production of different cytokines occurs at different times. The chosen time point corresponds to peak IL-6 production and relatively high TNF-α production (Matsunaga et al. 2001). For each sample, secreted cytokine levels were measured over seven dilutions. Each measurement was represented as a fold increase over control and the AUC was used to represent each endpoint for comparison.

STATISTICAL ANALYSIS

Linear regressions between oxidative properties (cellular responses or DTT activity) and aerosol composition (metals, elemental ratios, etc.) were evaluated using Pearson correlation coefficient, where the significance was determined using Monte Carlo simulations. Briefly, oxidative properties were assumed to follow a normal distribution. Ten "estimates" were randomly generated for each oxidative property using the average and standard deviation obtained from Hill equation fits experimentally. The estimates were then plotted against the aerosol composition of interest. This process yielded ten fits, each with a slope and variance. From these values, the between and within variances were calculated and a Student *t*-test was used to calculate and evaluate the associated *P* values (95% confidence interval). The method considers both the within variance and the between variance. The between variance accounts for differences between each slope and the average of all slopes (Iversen and Norpoth 1987). The within variance, also often termed unexplained variance, accounts for variation that cannot be explained by the between variance (Iversen and Norpoth 1987). Both variances are used to calculate the total variance, which is then used to determine the *P* value.

QUALITY CONTROL

All cellular exposure experiments were conducted in triplicate to ensure quality data. Experiments involving cardiomyocytes were also repeated over two harvests to ensure reproducibility. Additionally, multiple positive (LPS, H_2O_2, and ambient filter samples) and negative (blank filters and probe-treated cells exposed to stimulant-free media) controls were assessed with each filter sample to confirm ROS/RNS probe functionality. Furthermore, the responses measured for these controls were compared between different experiments to gauge the variability of the assay (Table B.1 in Appendix B, available on the HEI website). The within-plate standard error (calculated for each triplicate) for positive and negative controls averaged around 11%. Overall standard errors (calculated for all runs, across multiple plates) were much lower and averaged around 5%. These calculations confirm that the response for controls was reproducible and did not differ significantly between experiments.

Selected chamber experiments (Table 1, Experiments 1–6) were repeated to ensure reproducibility in SOA generation and collection. DTT activities and ROS/RNS production were measured for each repeat experiment and compared with the reproducibility of sample treatment for each assay (e.g., filter extraction and sample dilution). All repeat experiments yielded comparable results within experimental error (Figure C.1 in Appendix C, available on the HEI website). For comparison purposes, the different values obtained for response metrics (DTT activity and ROS/RNS production) for each repeat chamber experiment were averaged and the uncertainty propagated to obtain a single response metric value for the given SOA formed under the given formation condition (Table 1, Experiments 1–6). Finally, background filters containing only seed particles and OH precursor (H_2O_2 or HONO) (both at experimental concentrations) were collected to account for potential OH precursor uptake, which may influence oxidative properties. With the exception of the metal seed background filter (discussed later in the section on effect of redox-active metals on oxidative potentials and inflammatory responses), the oxidative potential and ROS/RNS

production for all background filters were within the uncertainty of that measured for blank Teflon filters, indicating no significant OH precursor uptake (Figure C.2 and Table C.1 in Appendix C.) Furthermore, this confirmed that the presence of ammonium sulfate seed particles alone did not contribute appreciably to either oxidative property.

RESULTS

MACROPHAGE ASSAY DEVELOPMENT AND OPTIMIZATION

Alveolar macrophages were exposed to water-soluble ambient PM extracts and the ROS/RNS produced as a result of exposure was measured using an optimized assay. Multiple parameters were optimized first using the MH-S cell line and later adapted for use with primary neonatal rat ventricular myocytes. These parameters include: the cell density seeded onto each well, the ROS/RNS probe concentration, and the sample incubation time. Several considerations were given to identify an appropriate cell density. A low cell density could result in an easily saturated assay, whereas a high cell density could cause oxidative stress due to crowding (Murray et al. 2004; Sung et al. 2006). Optimization experiments comparing the ROS/RNS levels produced as a result of exposure with stimulant-free medium (negative control) and LPS and H_2O_2 (positive controls) showed that higher cell densities (i.e., 1×10^5cells/well produced a higher and more variable ROS/RNS baseline. At a lower cell density, 2×10^4 cells/well, a low baseline was attained, and microscopic images were visually consistent with low-density reference images (ATCC). Multiple concentrations of the ROS/RNS probe were also investigated for optimization. It was observed that probe concentrations greater than 30 μM resulted in enlarged cells and cell membrane irregularities, suggesting that cells under these conditions may be basally stressed. Finally, different sample incubation times (between 1 minute and 24 hours) were tested to maximize the signal separation between positive and negative responses. Short time points were included because ROS/RNS may decay after production; long time points were included because inflammatory assays involving LPS have shown that responses generally peaked around 8–24 hours (Haddad 2001). From the time series obtained for positive and negative controls, the largest signal separation was observed after a sample incubation time of 24 hours (Figure B.1 in Appendix B, available on the HEI website). The final assay parameters are given in Table 2.

CARDIOMYOCYTE ASSAY ADAPTATION

The optimized macrophage assay was adapted for analysis with cardiomyocytes using a similar approach that investigated several assay parameters. Cell density did not require optimization as cardiomyocytes form a confluent tissue and the seeding density to achieve this has been previously optimized (Grosberg et al. 2012). Several other changes based on cell culture requirements were also implemented (e.g, all incubation solutions contained calcium, which is necessary for cardiomyocytes). Each change was systematically introduced and tested using positive and negative controls to ensure that they did not interfere with the assay. The same ROS/RNS probe was utilized for the cardiomyocyte assay. For probe concentration optimization, the optimal concentration obtained for macrophage analysis was evaluated for cardiomyocyte toxicity. As cardiomyocytes were observed to be healthy and maintained a similar beating frequency to that of control cells post-incubation, the same probe concentration could be utilized for both cellular assays. Finally, a time-series experiment was conducted in which it was determined that 24 hours was the optimal sample incubation time because it produced the largest signal separation between positive and negative controls (Figure B.1 in Appendix B, available on the HEI website). The final assay parameters are given in Table 2.

MACROPHAGE METABOLIC ACTIVITY

For each SOA dose, cellular metabolic activity was measured to correct for changes in ROS/RNS levels that may result from changes in relative metabolic activity (Zhang et al. 2016). That is, PM exposure may induce cell death, resulting in a lower ROS/RNS measurement. To correct for this, levels of ROS/RNS production were divided by relative cellular metabolic activity to obtain corrected ROS/RNS levels in accordance with previous studies (Zhang et al. 2016). Over the dose range investigated for AUC determination, decreased cellular metabolic activities were only observed for naphthalene SOA generated under humid conditions in the presence of NO (Experiments 19–26, Table 1).

CELLULAR ASSAY DOSE–RESPONSE METRICS

Cellular assays utilizing macrophages and cardiomyocytes were optimized for measuring ROS/RNS produced as a result of PM exposure. Various assay parameters were optimized to ensure low basal ROS/RNS production and high signal separation between positive and negative responses. Each parameter was also systematically investigated to ensure general cellular health (e.g., no membrane

Table 2. Final, Optimized Cellular Assay Parameters

Parameter	MH-S	NRVM
Cell number	2×10^4 cells/well	3.33×10^4 cells/well
Probe concentration	10 µM	10 µM
Sample incubation time	24 hr	24 hr

irregularities and functional cardiomyocytes). Besides parameter optimization, a dose–response approach was utilized for sample analysis because inflammatory studies have shown that endpoints (e.g., IL-6, TNF-α, and NF-κB) generally followed a sigmoidal dose–response relationship (Haddad 2001; Hardin et al. 2008; Yoo et al. 2013). We demonstrate clearly in this study that ROS/RNS produced as a result of PM exposure was highly dose-dependent and nonlinear with respect to PM dose. Moreover, the dose–response region captured for each sample was strongly influenced by the dilution range chosen, for example, a narrow dilution range may only fully represent the response behavior of a limited number of samples.

To characterize the dose–response relationship for each filter sample, the Hill equation was applied to obtain dose–response metrics (Goutelle et al. 2008; Hill 1910). These parameters are labeled in Figure 4 and include the maximum response attained as a result of PM exposure, the dose at which response is 10% above the fitted baseline (threshold), the dose at which 50% of the maximum response is attained (EC_{50}), the rate at which the maximum response is attained once a response is observed (Hill slope), and the area under the dose–response curve (AUC), which may be used to represent the overall effect of PM exposure across the dose range investigated. In addition to the classic dose–response shown in Figure 4, several other dose–response behaviors were observed, including samples where the maximum response was not attained, a decreased response was observed at higher doses, and no response above the baseline was observed at all doses investigated (Figure B.2 in Appendix B, available on the HEI website). For the majority of samples analyzed, the maximum response was not attained. A decreased response at higher doses was uncommon and only observed for a few samples (2% of ambient samples and 3% of chamber samples). Negligible responses above the baseline, or flat dose–response curves, were more prevalent (15% of ambient samples, 6% of chamber samples). These behaviors introduced large uncertainties in several dose–response metrics, including the EC_{50} and Hill slope. Previous studies have shown that these two metrics are often more unstable and less reliable because of their high sensitivity to dose range, especially in cases where either the maximum response or baseline were not observed (Beam and Motsinger-Reif 2014). Conversely, the uncertainties associated with AUC were low across all samples, including those with non-classic dose–response behaviors. This is especially valuable as it is not always feasible to attain the maximum response, and in many cases, the dose range may be limited because of low mass loadings. As such, the AUC parameter can be utilized for a variety of filter samples, regardless of many limitations that may impede the usefulness of other response metrics.

AMBIENT AEROSOL STUDY

Correlation Between Reactive Oxygen/Nitrogen Species Production and Oxidative Potential

Ambient PM samples collected from rural and urban sites in the greater Atlanta area throughout the year (2012–2013) were analyzed using the optimized cellular assay ($n = 104$; 10 spring, 47 summer, 15 autumn, and 32 winter filter samples). Oxidative potentials have been previously measured and are reported by Verma and colleagues (2014). We investigated the correlations between all metrics of ROS/RNS production and oxidative potentials to determine whether results from chemical assays are representative of cellular responses. The correlations between extrinsic (per volume of air sampled) and intrinsic (per mass of PM) AUCs and oxidative potentials are shown in Figure 5. Data points represent a single filter sample and are colored by season for both cell types. For summer samples, a significant correlation between extrinsic AUC and oxidative potential was observed ($n = 47$, $R = 0.63$, $P < 0.05$), whereas a relatively constant AUC was observed for all winter samples ($n = 32$) regardless of the corresponding measured

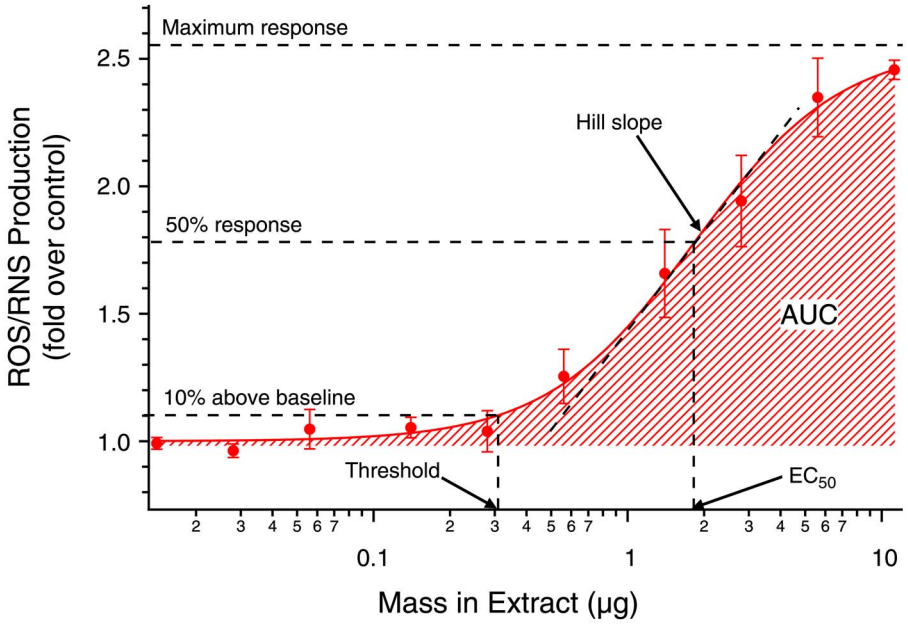

Figure 4. Dose–response curve of reactive oxygen and nitrogen species (ROS/RNS) produced as a result of an aerosol exposure. ROS/RNS production is expressed as the fold increase over control cells (probe-treated cells exposed to stimulant-free media); dose is expressed as the mass in the extract (given in μg). Data shown were obtained from Experiment 18 (Table 1) and are means ± standard error of triplicate exposure experiments. The Hill equation was used to fit the dose–response curve and obtain dose–response parameters, which include maximum response, threshold (the dose at which the response is 10% above the baseline), EC_{50} (the dose at which 50% of the response is attained), the Hill slope (the rate at which the maximum response is attained once there is response), and the area under the dose–response curve (AUC). (Adapted from Tuet et al. 2017a. Creative Commons Attribution 3.0 License.)

oxidative potential. Similar behaviors were observed for the intrinsic counterparts. Other dose–response metrics were not significantly correlated with oxidative potentials and no spatial trends were observed (Table B.2 in Appendix B, available on the HEI website).

Correlations with PM Components

To elucidate PM components associated with ROS/RNS production, extrinsic and intrinsic metrics representing ROS/RNS produced as a result of PM exposure were correlated with absolute mass concentrations and relative mass fractions of water-soluble constituents, respectively. Similar analyses have been performed for oxidative potentials and are reported by Fang and colleagues (2015a). Seasonal trends for correlations observed in this study are shown in Figure 6. For several constituents (WSOC, BrC, iron, and titanium), a significant correlation existed between extrinsic AUCs and constituent mass concentrations for summer samples ($R = 0.66$, 0.62, 0.65, and 0.71, respectively). Similarly, the mass fraction of titanium was found to be significantly correlated with intrinsic AUCs in summer ($R = 0.66$). Correlations between all dose–response metrics and all PM constituents are given in Tables B.3 and B.4 for all samples (in all seasons: spring, summer, autumn, winter). No other statistically significant correlations were observed (Tables B.3 and B.4 in Appendix B, available on the HEI website), including metals grouped by source apportionment results (Fang et al. 2015a).

Correlation Between Macrophage and Cardiomyocyte Assay Results

Of the ambient filter samples investigated in this study, 18 were analyzed using both assays (macrophage and cardiomyocyte). Correlations between dose–response metrics from both cell types were evaluated to determine whether ROS/RNS production induced by PM exposure differed between cell types that directly participate in defending the body against foreign materials (macrophages) and other cell types that are affected by PM less directly (e.g., via translocation of constituents into the bloodstream or systemic oxidative stress spill-over) (Brook et al. 2010). A statistically significant positive correlation ($R = 0.80$) was observed

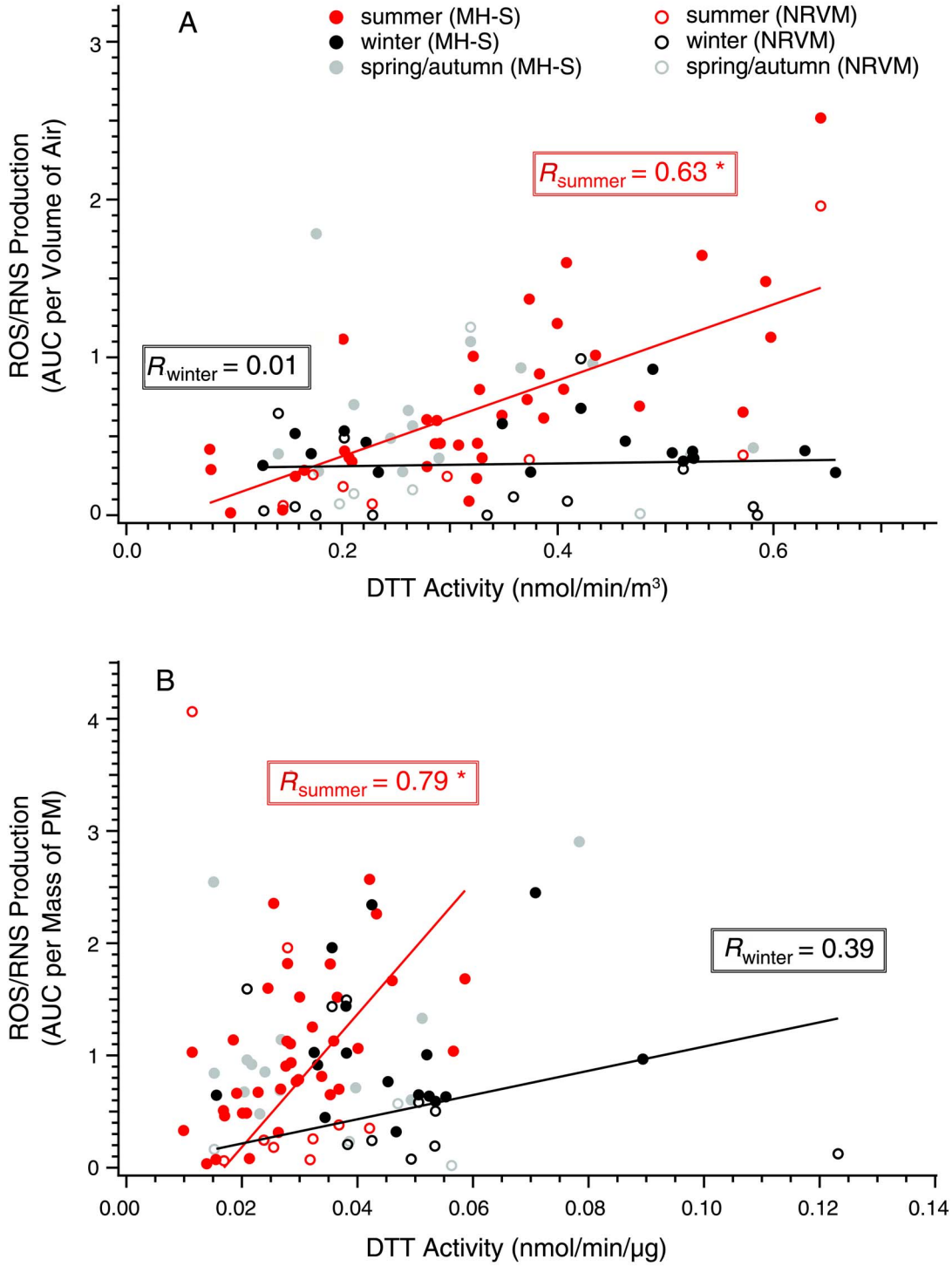

Figure 5. Correlation between reactive oxygen and nitrogen species (ROS/RNS) production and DTT activity induced by ambient PM by season. ROS/RNS production is expressed as (**A**) extrinsic (per volume of air sampled) and (**B**) intrinsic (per mass of PM) AUC. DTT activity is expressed per mass of PM. Data are grouped by summer and winter samples (spring/autumn data in gray shown for reference). Each data point represents the AUC of an individual filter tested using either alveolar macrophages (MH-S, closed circles) or ventricular myocytes (NRVM, open circles) and the corresponding DTT activity. Linear regressions and Pearson correlation coefficients are shown. * indicates significance between the cellular and the DTT assays ($P < 0.05$). (Source: Tuet et al. 2016 with permission from Elsevier.)

between the intrinsic AUCs obtained from both cell types (Figure 7). The strong correlation suggests that the ROS/RNS response may be similar for active cell types, such as macrophages, which participate in the immune response, and cardiomyocytes, which contract and pump blood.

LABORATORY-GENERATED AEROSOL STUDY

Oxidative Potentials

The water-soluble DTT activity, a measure of the concentration of redox-active species present in the water-soluble

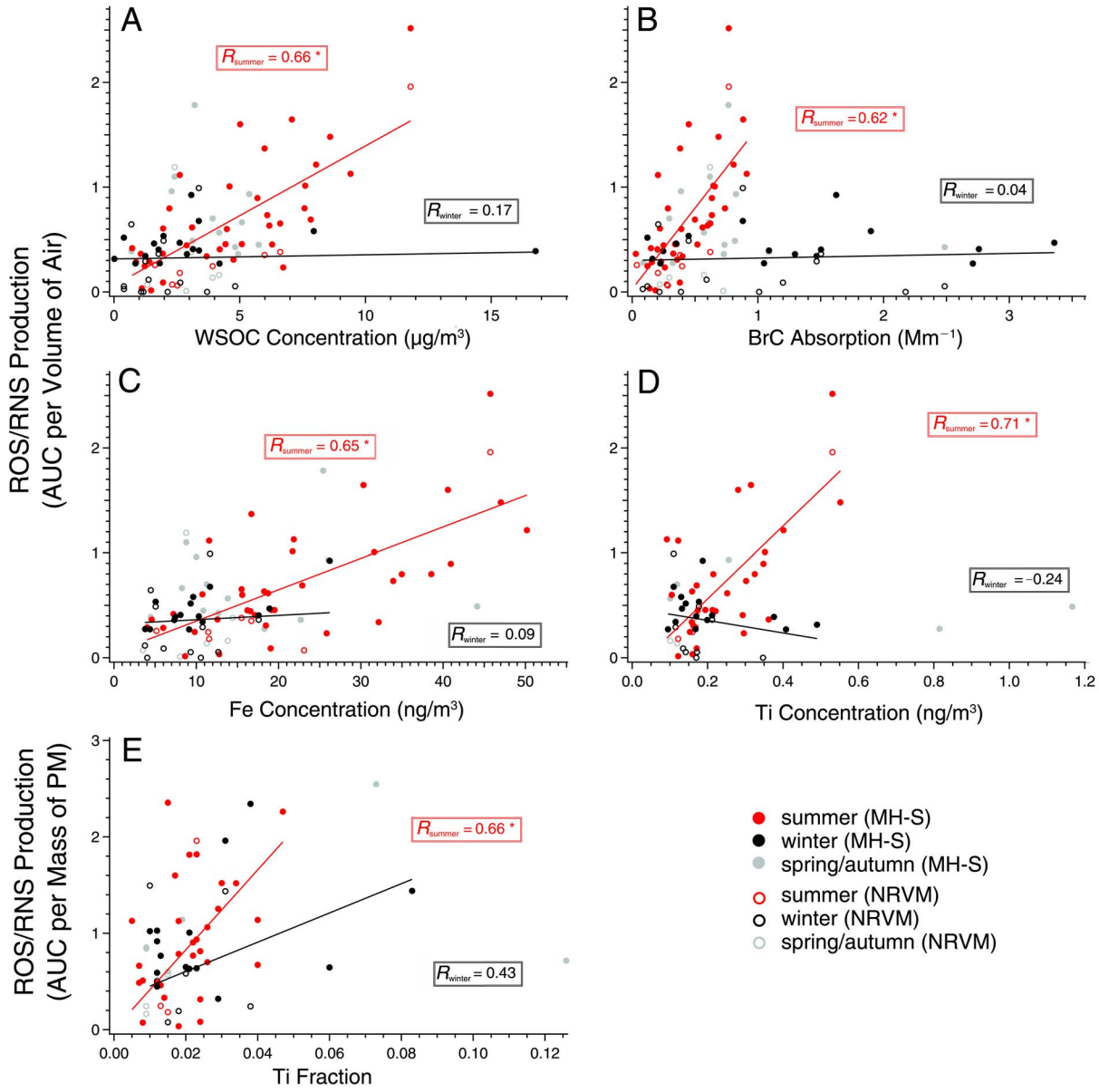

Figure 6. Correlation between reactive oxygen and nitrogen species (ROS/RNS) production and extrinsic and intrinsic AUC and PM components. Production expressed as extrinsic (per volume of air sampled) AUC in (**A**) through (**D**) and as intrinsic (per mass of PM) AUC in (**E**) with PM components for summer and winter (spring/autumn data in gray shown for reference). PM components are (**A**) water-soluble organic carbon concentration (WSOC); (**B**) brown carbon concentration (BrC) (Mm = megameter); (**C**) iron concentration (Fe); (**D**) titanium concentration (Ti); and (**E**) titanium fraction. Data points represent individual filters tested using either alveolar macrophages (MH-S, closed circles) or ventricular myocytes (NRVM, open circles). Linear regressions and Pearson correlation coefficients are shown. * indicates significance ($P < 0.05$). (Adapted from Tuet et al. 2016 with permission from Elsevier.)

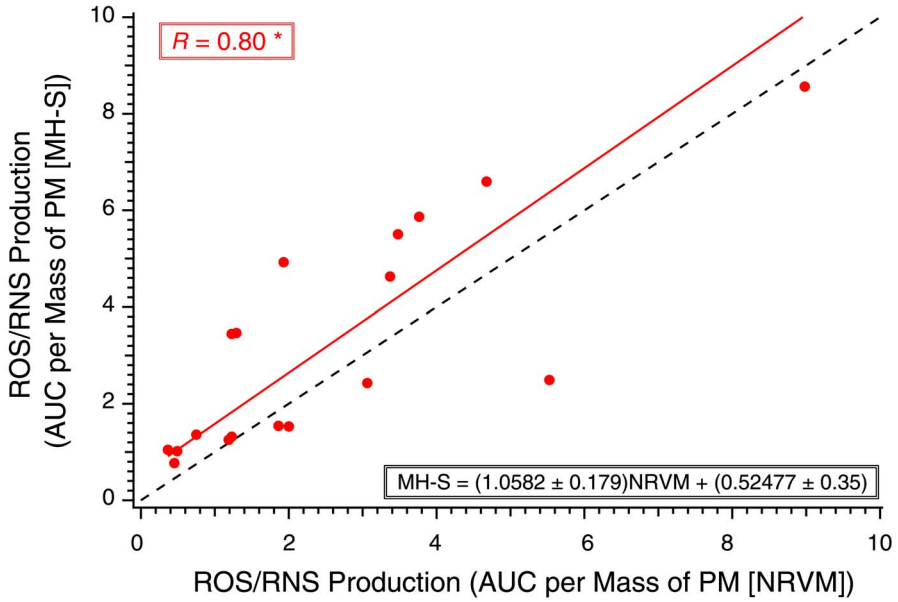

Figure 7. Correlation between reactive oxygen and nitrogen species (ROS/RNS) production, expressed as intrinsic AUCs, by macrophages (MH-S) and cardiomyocytes (NRVM). Data points represent individual filter samples tested using both cell types. An orthogonal regression, the corresponding Pearson coefficient, and a 1:1 line for reference are shown. The equation represents the correlation between the two assays (MH-S and NRVM). * indicates significance, $P < 0.05$. (Source: Tuet et al. 2016 with permission from Elsevier.)

extract, was determined for SOA generated under various conditions to probe whether different types of aerosol differ in toxicity. Intrinsic, blank-corrected DTT activities are presented in Figure 8. Isoprene SOA and naphthalene SOA had the lowest and highest intrinsic DTT activities, respectively. For the majority of SOA systems (isoprene, α-pinene, β-caryophyllene, and pentadecane), a low oxidative potential was measured across all formation conditions. The oxidative potential of *m*-xylene SOA was not affected by the NO_x level, but was altered by humidity. Both low NO_x and high NO_x conditions and humidity affected naphthalene SOA oxidative potential.

Previously reported DTT activities for other sources and subtypes of PM are also given for comparison (Bates et al. 2015; Fang et al. 2015c; Kramer et al. 2016; Lu et al. 2014; McWhinney et al. 2013a, 2013b; Verma et al. 2015a; Xu et al. 2015a, 2015b). The intrinsic DTT activities measured for isoprene SOA are in agreement with previously reported DTT activities for isoprene SOA and for the isoprene-OA factor resolved from positive matrix factorization (PMF) analysis of AMS data (Verma et al. 2015a; Xu et al. 2015a, 2015b). Similarly, the oxidative potentials measured for naphthalene SOA were in agreement with prior studies (McWhinney et al. 2013b). Naphthalene SOA was also the only SOA system whose oxidative potential was on par or higher than that of traffic-related aerosols (generated by light-duty gasoline vehicles, heavy-duty diesel vehicles, and diesel exhaust particles).

Cellular Reactive Oxygen/Nitrogen Species Production and Inflammatory Responses

Cellular responses induced as a result of exposure to SOA generated under various conditions were measured to investigate whether different types of SOA induced different cellular responses. Levels of ROS/RSN, IL-6, and TNF-α are shown in Figure 9. All data points are reported as intrinsic AUC over the same dose range for comparison purposes. Both precursor identity and formation condition influenced SOA-induced ROS/RNS and inflammatory responses. Isoprene SOA induced low levels of all cellular responses across all formation conditions. Moderate ranges of IL-6 and TNF-α responses were observed for α-pinene, β-caryophyllene, and *m*-xylene. Pentadecane SOA induced a wide range of IL-6 levels depending on the formation condition under which the SOA was generated. Naphthalene SOA induced wide ranges of both inflammatory cytokines (TNF-α and IL-6), both of which were also strongly influenced by formation condition.

Although there were no apparent trends for individual inflammatory responses, several response patterns were

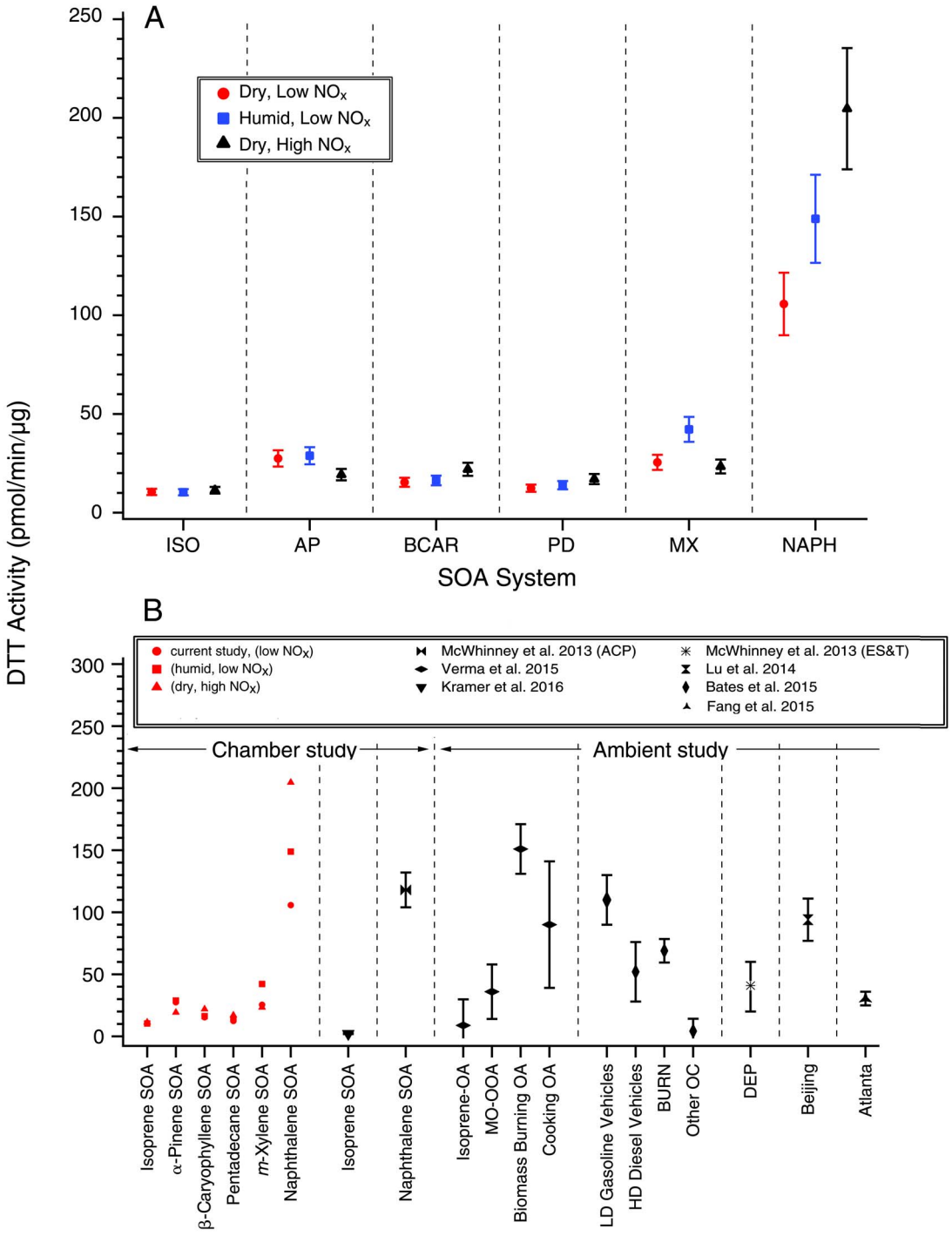

Figure 8. Intrinsic DTT activities for (A) chamber SOA formed under different formation conditions and (B) the same SOA DTT activities in the context of other types of PM. With the exception of the study by Kramer and colleagues (2016), all studies utilized the DTT method described by Cho and colleagues (2005). (**A**) SOA was generated from various precursors: isoprene (ISO), α-pinene (AP), β-caryophyllene (BCAR), pentadecane (PD), *m*-xylene (MX), and naphthalene (NAPH) under different formation conditions: dry, low NO_x (RO_2• + HO_2•) [circles]; humid, low NO_x (RO_2• + HO_2•) [squares]; and dry, high NO_x (RO_2• + NO) [triangles]). (**B**) Specifics on factor resolution methods and site locations are described elsewhere: isoprene SOA (Kramer et al. 2016); naphthalene SOA (McWhinney et al. 2013b); isoprene-OA, more-oxidized oxygenated OA (MO-OOA), biomass burning OA, and cooking OA (Verma et al. 2015a; Xu et al. 2015a; Xu et al. 2015b); light-duty (LD) gasoline vehicles, heavy-duty (HD) diesel vehicles, biomass burning (BURN), and other organic carbon (OC) (Bates et al. 2015); and diesel exhaust particles (DEP) (McWhinney et al. 2013a). DTT activities shown for Beijing (Lu et al. 2014) and Atlanta (Fang et al. 2015c) were averaged across multiple seasons. (Source: Tuet et al. 2017c. Creative Commons Attribution 3.0 License.)

observed for the SOA systems investigated. These response patterns are shown in Figure 10. Levels of TNF-α, and IL-6 are represented as AUC for comparison purposes and shaded regions are shown to highlight the extent of clustering. Data points are sized according to ROS/RNS levels. Overall, isoprene SOA induced a low inflammatory response. SOA formed from the photooxidation of α-pinene and *m*-xylene induced similar inflammatory responses, as shown by the overlap between the two shaded regions. Pentadecane and β-caryophyllene SOA induced a wide range of IL-6 levels, and naphthalene SOA induced wide ranges of both inflammatory cytokines and ROS/RNS.

Effect of Iron Sulfate Seed on Oxidative Potential and Reactive Oxygen/Nitrogen Species

The presence of iron sulfate seed did not have an obvious effect on oxidative potentials (i.e., SOA formed in the presence of iron sulfate seed did not always have a higher oxidative potential than that formed in the presence of ammonium sulfate seed) using naphthalene as the SOA precursor (Figure 11).

In terms of the effect on cellular ROS/RNS production, an SOA formed in the presence of iron sulfate induced higher ROS/RNS levels than an SOA formed in the presence of ammonium sulfate (Figure 11).

Correlation Between Bulk Elemental Composition and Oxidative Properties

Aerosol bulk elemental ratios (O:C, H:C, and N:C) were determined for each SOA system investigated, and correlations between these ratios and oxidative properties (i.e., DTT activity and ROS/RNS production) were evaluated to determine whether there exists a good predictor for SOA oxidative properties. The correlations between ROS/RNS production and $\overline{OS}_c$ (determined from O:C and H:C) are shown in Figure 12. For all SOA systems investigated, a positive, significant (R = 0.64) correlation exists between ROS/RNS production and $\overline{OS}_c$ regardless of formation condition and precursor identity (Figure 12A).

For the seed effects (iron sulfate vs. ammonium sulfate) and photochemical aging experiments, a positive relationship is also observed between ROS/RNS production and $\overline{OS}_c$ (Figure 13) for naphthalene SOA. The types of seeds do not affect the ROS/RNS response as all data follow the same trend.

A van Krevelen diagram is also shown to visualize changes in O:C and H:C ratios (Figure 12B). Changes in the slope of data points within the van Krevelen space provide information on the chemical functionalization of the SOA formed (Heald et al. 2010; Ng et al. 2011; van Krevelen 1950). Beginning with the SOA precursor, a slope of 0 indicates the

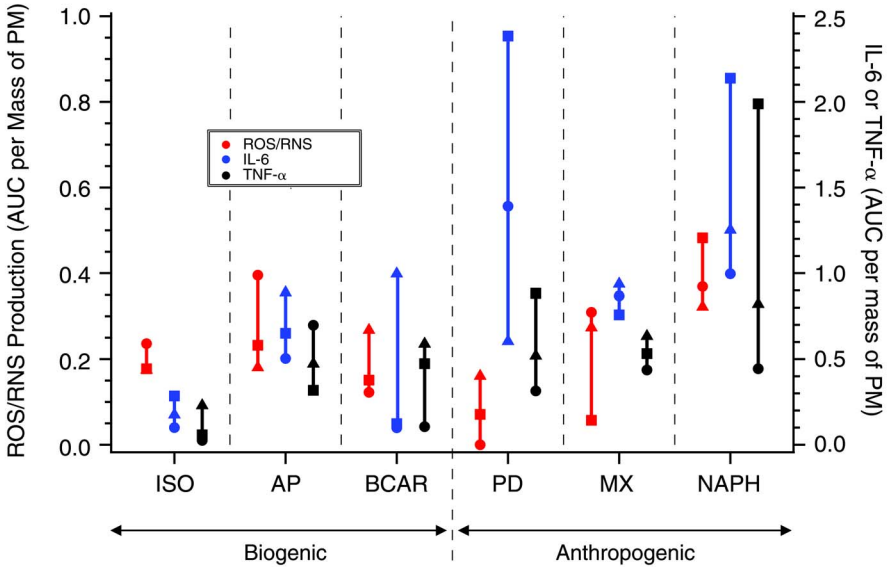

Figure 9. Reactive oxygen and nitrogen species (ROS/RNS) production and inflammatory responses (IL-6 and TNF-α), expressed as intrinsic AUC, induced as a result of exposure to SOA generated from various precursors. Precursors studied are isoprene (ISO), α-pinene (AP), β-caryophyllene (BCAR), pentadecane (PD), *m*-xylene (MX), and naphthalene (NAPH) under different formation conditions: dry, low NO_x (RO_2• + HO_2•) [circles]; humid, low NO_x (RO_2• + HO_2•) [squares]; and dry, high NO_x (RO_2• + NO) [triangles]. The lines connect the same inflammatory response for aerosol generated from the same precursor under different reaction conditions. (Adapted from: Tuet et al. 2017a. Creative Commons Attribution 3.0 License.)

addition of alcohol groups, a slope of −1 indicates the addition of carbonyl and alcohol groups on separate carbons of the carbon backbone or the addition of carboxylic acids, and a slope of −2 indicates the addition of ketones or aldehydes. ROS/RNS induced as a result of SOA exposure were not associated with either O:C or H:C ratios. That is, a higher O:C or H:C did not correspond to a higher ROS/RNS level. Furthermore, the van Krevelen diagram shows that the aerosol compositional changes between different precursors (different colored markers in Figure 12) were generally more substantial than those arising between different formation conditions of the same precursor (different shapes in Figure 12).

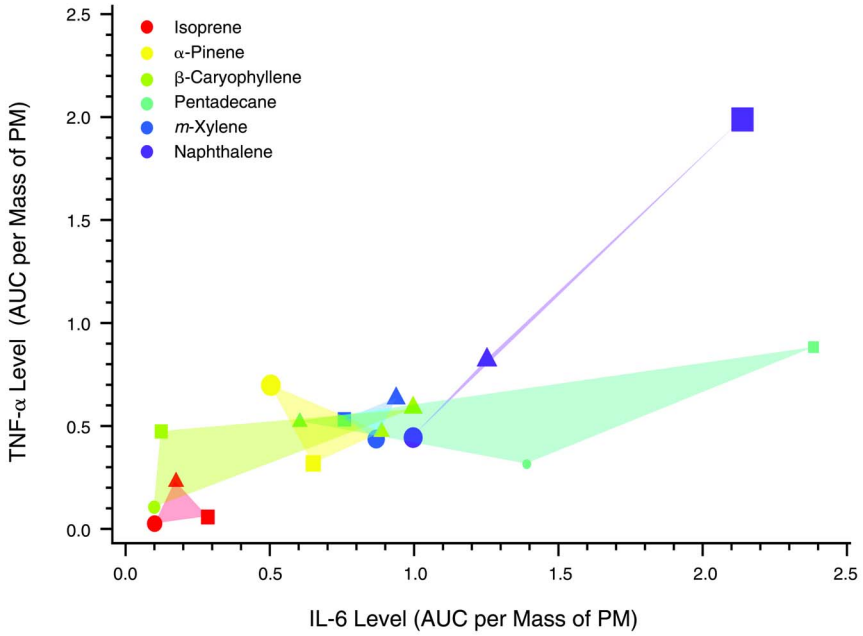

Figure 10. Inflammatory (TNF-α and IL-6) responses, induced as a result of exposure to SOA generated from various precursors sized according to reactive oxygen and nitrogen species (ROS/RNS) production. All endpoints are expressed as the intrinsic AUC. Precursors studied are isoprene, α-pinene, β-caryophyllene, pentadecane, *m*-xylene, and naphthalene under different formation conditions: dry, low NO_x (RO_2• + HO_2•) [circles]; humid, low NO_x (RO_2• + HO_2•) [squares]; and dry, high NO_x (RO_2• + NO) [triangles]. Shaded regions are shown for each SOA system to highlight the extent of clustering and provide visualization for the different response patterns observed. The size of the symbols indicates the level of ROS/RNS. (Source: Tuet et al. 2017a. Creative Commons Attribution 3.0 License.)

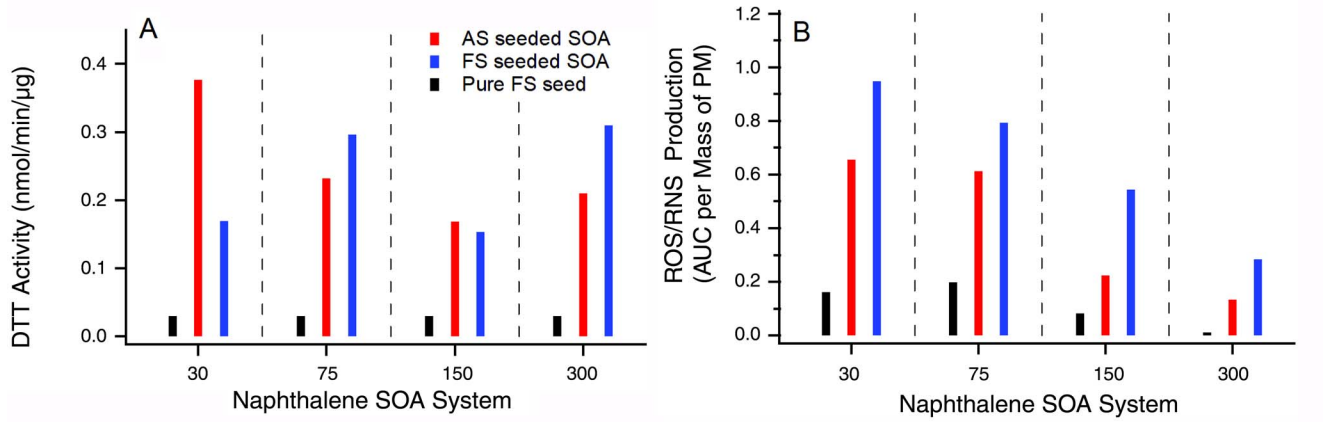

Figure 11. Oxidative potentials (A) and reactive oxygen and nitrogen species (ROS/RNS) levels (B) for naphthalene SOA generated in the presence of ammonium sulfate or iron sulfate as seed. All experiments were conducted using H_2O_2 as OH precursor and in the presence of NO.

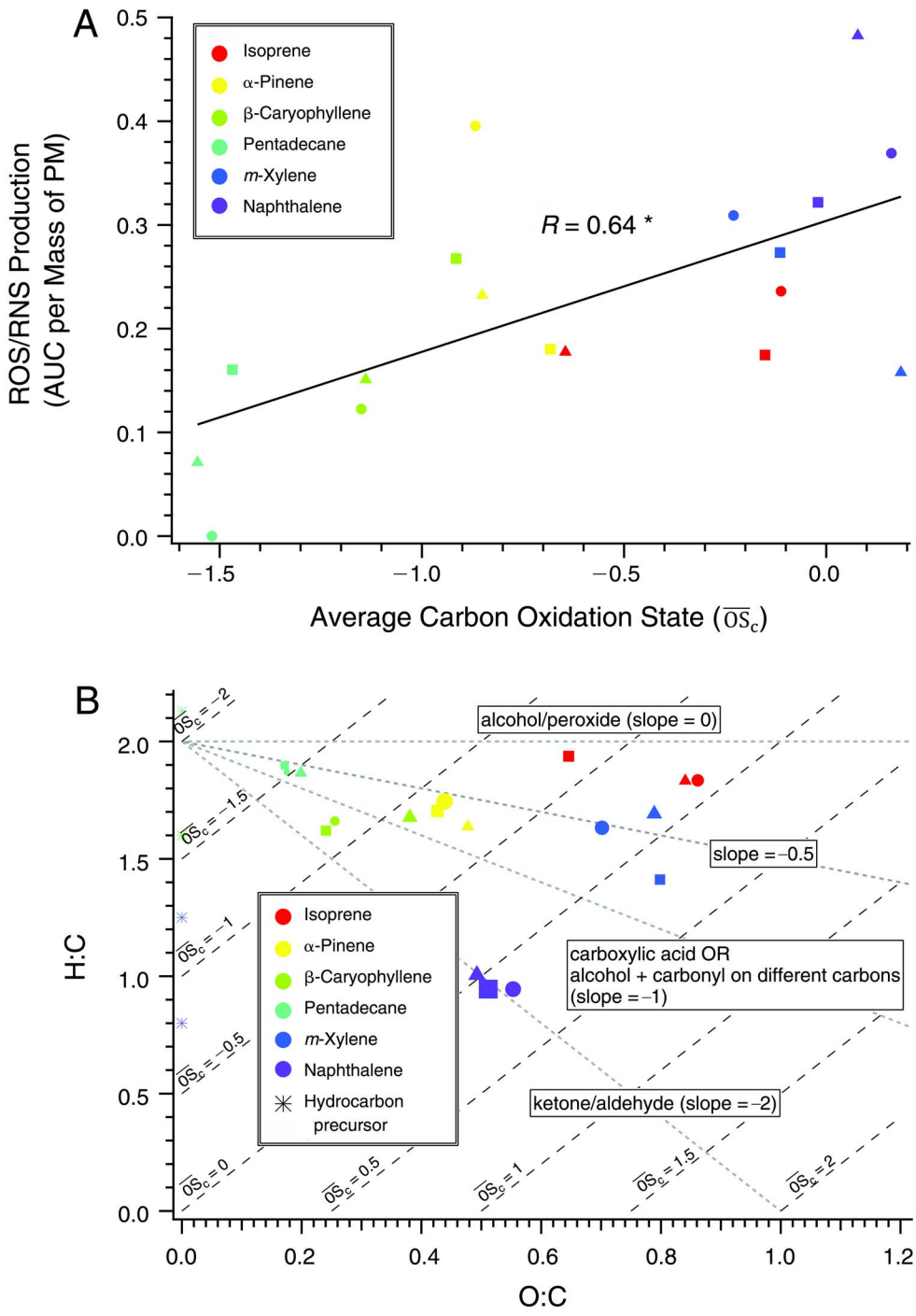

Figure 12. Correlations between aerosol average carbon oxidation state ($\overline{OS}_c$) and reactive oxygen and nitrogen species (ROS/RNS) production for different types of SOA: (A) ROS/RNS are given as the AUC per mass of PM and (**B**) the same data shown as a van Krevelen diagram to visualize changes in oxidation. SOA was generated from various precursors (isoprene, α-pinene, β-caryophyllene, pentadecane, *m*-xylene, and naphthalene) under different formation conditions: dry, low NO_x ($RO_2\bullet + HO_2\bullet$); humid, low NO_x ($RO_2\bullet + HO_2\bullet$); dry, high NO_x ($RO_2\bullet + NO$). Linear fits and corresponding Pearson correlation coefficient are given. * indicates significance, $P < 0.05$. (Adapted from: Tuet et al. 2017a. Creative Commons Attribution 3.0 License.)

Correlation Between Laboratory-Generated Aerosol Response and Ambient Samples Responses

Oxidative potentials and cellular ROS/RNS production measured for laboratory-generated aerosol samples were compared in the context of that measured for ambient samples to evaluate the relative toxicity of pure SOA. This comparison is shown in Figure 14 for all laboratory-generated SOA and summer and winter ambient samples collected from the greater Atlanta region. With the exception of naphthalene SOA (purple markers), the oxidative potentials of all SOA systems investigated were comparable to those observed in the ambient aerosol samples. In contrast, for ROS/RNS production, SOA systems induced comparable or higher levels of ROS/RNS compared with the levels induced by ambient aerosol samples.

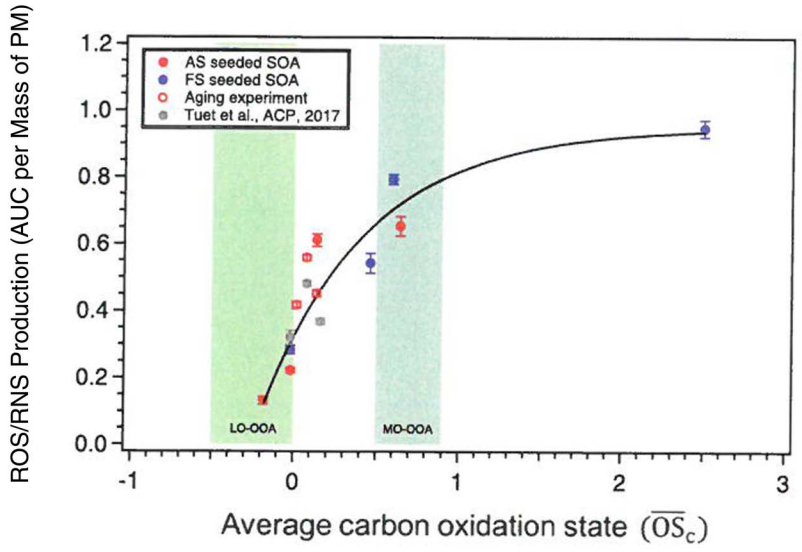

Figure 13. Correlations between aerosol average carbon oxidation state ($\overline{OS}_c$) and reactive oxygen and nitrogen species (ROS/RNS) production for naphthalene SOA generated in the presence of different seeds types (ammonium sulfate [AS] and iron sulfate [FS]) and aging experiments. The shaded regions correspond to two common ambient organic aerosols subtypes: less oxidized oxygenated organic aerosols (LO-OOA) and more oxidized oxygenated organic aerosols (MO-OOA). The oxidation state ($\overline{OS}_c$) values of laboratory SOA span the range of these two ambient organic aerosol subtypes. (Tuet et al. 2017b. Creative Commons Attribution 4.0 License.)

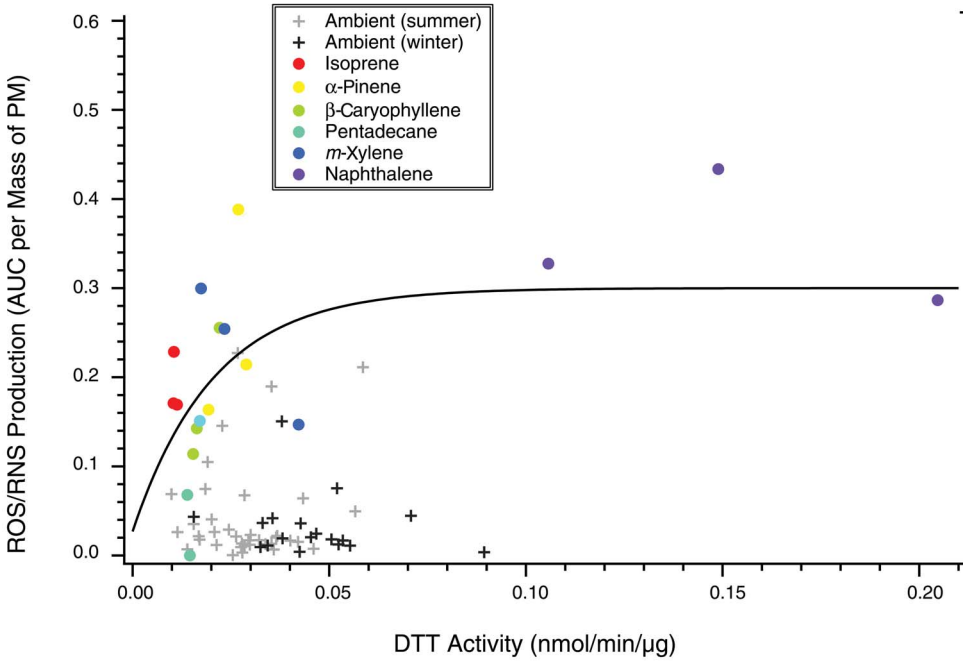

Figure 14. Oxidative potentials and reactive oxygen and nitrogen species (ROS/RNS) production for laboratory-generated SOA and ambient samples collected around the greater Atlanta region. Oxidative potentials are given as DTT activities per PM mass, whereas ROS/RNS production is given as the AUC per PM mass. SOA was generated from various precursors (isoprene, α-pinene, β-caryophyllene, pentadecane, *m*-xylene, and naphthalene) under different formation conditions: dry, low NO_x, (RO_2• + HO_2•); humid, low NO_x (RO_2• + HO_2•); and dry, high NO_x (RO_2• + NO). Ambient samples were collected in summer and winter, as determined by solstice and equinox dates between June 2012 and October 2013. An exponential fit is shown as a guide for laboratory-generated aerosol samples. (Adapted from Tuet et al. 2017a. Creative Commons Attribution 3.0 License.)

DISCUSSION AND CONCLUSION

The key findings of this study are summarized in Table 3 and discussed in greater detail in the following sections.

ASSOCIATIONS BETWEEN CELLULAR AND CHEMICAL ASSAYS

Correlations between all ROS/RNS response metrics (maximum response, Hill slope, EC_{50}, threshold, and AUC) and oxidative potentials were evaluated to determine whether results from chemical assays were representative of cellular responses. For ambient PM samples, a distinct seasonal trend was observed for extrinsic AUC and DTT activity, where the two were significantly correlated for summer filter samples (Figure 5a). On the other hand, winter samples exhibited a different trend, where a relatively constant AUC was observed regardless of DTT activity. Several spring and autumn filter samples were also analyzed as part of this study; however, the sample size was too small for statistical significance and the samples did not span the entire DTT activity range observed in the ambient field campaign. Nevertheless, it is interesting to note that the majority of spring and autumn samples induced ROS/RNS production (as represented by extrinsic AUC) within the range observed for summer and winter filter samples. This suggests that spring and autumn trends may be an intermediate between those observed for summer and winter samples. Similar behaviors were observed for intrinsic AUCs and DTT activities, although no obvious trend was noted for winter samples (Figure 5b).

Table 3. Summary of Key Findings

Objective / Main results
Cellular Assay Development
• Various parameters (cell density, probe concentration, and sample incubation time) optimized for measuring ROS/RNS produced as a result of aerosol exposure
• ROS/RNS was highly dose-dependent and non-linear with respect to PM concentration, demonstrating that cellular responses should not be reported using a single PM concentration
• AUC was most robust dose–response parameter capable of describing classical and non-classical dose–response behaviors
PM Constituents Associated with ROS/RNS Production
• Correlations evaluated between all dose–response metrics and all PM constituents
• Positive, significant correlations observed between AUC and various PM constituents (water-soluble organic carbon, brown carbon, iron, and titanium) for summer ambient samples
• Significant summer correlations with organic constituents may highlight the importance of SOA to PM-induced toxicity
• Other dose–response metrics and PM constituents did not yield significant correlations
Applicability of Chemical Assays to Cellular Responses
• Positive, significant correlation observed between AUC and DTT activity for summer ambient samples
• No simple correlation between ROS/RNS and DTT activity
• DTT assay may serve as a screening tool to identify samples for further cellular analysis
Relative Toxicities of Different SOA Systems
• SOA precursor identity influenced oxidative potentials notably
• Cellular response patterns observed for SOA precursors whose photooxidation products share similar carbon chain length and functionalities
• Results highlight importance of chemical structure and may lead the way for rough cellular response predictions given known SOA products
Effects of Photochemical Aging on Aerosol Toxicity
• SOA formed in the presence of iron induced higher levels of ROS/RNS
• Positive, significant correlation observed between ROS/RNS and average carbon oxidation state
• Observed correlation has significant implications as aerosols have an atmospheric lifetime of a week, over which aging can occur leading to more oxidized species
• Observed correlation may also pave the way to real-time ROS/RNS predictions due to the fine resolution of average carbon oxidation state measurements

For laboratory-generated samples, an exponential trend was observed between intrinsic ROS/RNS production and DTT activity (Figure 12). This trend, along with the seasonal trends observed for ambient samples, suggest that there is not a simple correlation between oxidative potentials as measured by chemical assays such as DTT and cellular ROS/RNS responses. Nevertheless, the DTT assay may serve as a valuable tool to screen samples for cellular analysis, as it has been automated for high-throughput analysis and a low DTT activity will likely correspond to a low cellular ROS/RNS response for both ambient and laboratory-generated aerosol.

Besides extrinsic and intrinsic AUC, no other ROS/RNS response parameter was significantly correlated with oxidative potential as measured by means of DTT. For these parameters (e.g., EC_{50} and Hill slope), the lack of correlation may be attributable to the large uncertainties associated with parameter determination. Uncertainties were especially large for filter samples where a maximum response was not attained over the dose range investigated.

Nonetheless, because each dose–response metric may serve as a different measure of toxicity, the lack of correlation with other parameters suggests that oxidative potentials may not fully capture all aspects of the cellular ROS/RNS response. Furthermore, the significant correlation between DTT and AUC, a measure of the overall effect of PM over a specified dose range, suggests that DTT, too, may be considered an indicator of the overall effect of PM.

It is also interesting to note that although both maximum response and EC_{50} were not significantly correlated with PM oxidative potential or composition, a significant positive correlation was observed between the two for all filter samples studied (Figure B.3 in Appendix B, available on the HEI website). This is intriguing because one would expect an anti-correlation between these parameters, where a more potent sample (with a lower EC_{50}) would induce more ROS/RNS production (hence, a higher maximum response). However, previous studies have found that EC_{50} is often positively correlated with antioxidant concentrations (Chiang et al. 2015; Zhang et al. 2006), suggesting several possibilities for the correlation observed in this study. For instance, there may be constituents present in more potent samples that induce antioxidant production pathways. The presence of antioxidants would neutralize ROS/RNS and result in a lower measured maximum response. Alternatively, constituents may also induce cellular protective pathways to counter oxidative damages; the reduced cellular damage results in longer-lived cells and may increase ROS/RNS accumulation.

AMBIENT PM COMPONENTS ASSOCIATED WITH CELLULAR RESPONSES

Similarly, correlations between all dose–response metrics and water-soluble mass concentrations and mass fractions of ambient PM constituents were evaluated to determine whether there exists a good predictor for cellular responses to PM toxicity. For ambient summer PM samples, a significant correlation was observed between ROS/RNS production as represented by extrinsic AUC and the mass concentrations of WSOC, BrC, iron, and titanium (Figure 6A–D), as well as between intrinsic AUC and the mass fraction of titanium (Figure 6E).

Furthermore, a relatively flat ROS/RNS response was observed for winter samples regardless of WSOC or BrC concentrations. These seasonal differences suggest that responses may be dependent on PM composition, as previous studies have shown that PM collected during different seasons differs in both mass concentration and chemical composition (Fang et al. 2015a; Verma et al. 2014, 2015a; Xu et al. 2015a, 2015b). In particular, PMF analysis of AMS data collected as part of the SCAPE study showed that the organic aerosols at these sites are dominated by SOA (Xu et al. 2015b). The positive correlation between AUC and WSOC observed for summer samples may therefore reflect contributions from photochemical and/or aged SOA, as photochemistry is more intense during summertime (Xu et al. 2015b). In addition to stronger photooxidation, biogenic emissions are also higher in summer. As a result, contributions from less-oxidized and more-oxidized oxygenated organic aerosols (LO-OOA and MO-OOA) to total organic aerosols may be significant as well (Xu et al. 2015b). These observations further highlight the importance of studying the contributions of SOA, in particular those arising from photochemical oxidation, to PM-induced adverse effects.

Likewise, different sources of BrC may induce different cellular pathways and result in the observed seasonal variability of ROS/RNS responses. Although biomass burning is the predominant source of BrC, there may be non-negligible contributions to BrC from aged SOA as well (Hecobian et al. 2010). Moreover, BrC was observed in both summer and winter filter samples (Verma et al. 2014), whereas biomass burning organic aerosols (BBOAs) were only identified in the winter samples (Xu et al. 2015b). Together, these observations suggest there may be an unknown source of BrC, other than biomass burning, in the summer. It is possible that the cellular ROS/RNS assay is only sensitive to BrC from the unknown source and relatively insensitive to BrC from BBOAs, as supported by the relatively low ROS/RNS production (low AUCs) observed for winter samples even though BBOAs were previously found to be highly redox active (Verma et al. 2015a). Furthermore, the cell membrane may be impermeable to larger species of BrC, such as humic-like substances (Sullivan and Weber 2006); size-dependent hindrance has been observed for the cellular transport of macromolecules and nanoparticles (Matsukawa et al. 1997; Sheng-Hann et al. 2010). Alternatively, transport through the cell membrane may be impeded once a certain intracellular concentration is reached. In both scenarios, a relatively constant response may be observed regardless of the sample's BrC concentration.

Both metal species correlated with ROS/RNS production (iron and titanium) are transition metals with positive oxidation states that have been shown to correlate with oxidative potential and participate in reactions that produce ROS/RNS (Charrier and Anastasio 2012; Fang et al. 2015a; Halliwell and Gutteridge 1984; Saffari et al. 2013; Verma et al. 2009). Titanium(IV) may also interfere with protein structures by interacting with cysteine amino acids (Conroy and Park 1968; Tinoco and Valentine 2005), and titanium dioxide is known to induce pulmonary inflammation (Bermudez et al. 2004). Similarly, iron(II) may

participate in Fenton-like reactions and produce ROS/RNS (Sutton and Winterbourn 1989). Other metals were not correlated with any metric of ROS/RNS production. This is in contrast with previous health studies investigating the ROS production from filter samples collected in California, where correlations between ROS production and multiple metals (arsenic, chromium, copper, iron, manganese, nickel, lead, vanadium, and zinc) were observed (Daher et al. 2014; Hu et al. 2008; Saffari et al. 2014a; Wang et al. 2013). Nevertheless, the discrepancy is not surprising because different metrics were utilized to represent ROS production in previous studies (e.g., the linear slope obtained over a few doses); and although the Hill slope investigated in this study is similar to the linear slope metric used in previous studies, pharmacology studies have found that the Hill slope is heavily influenced by dose range and is a less reliable metric compared to AUC in general (Beam and Motsinger-Reif 2014).

The lack of correlation with other metals, however, did not reflect a lack of response, as exposure to pure metal salt solutions at concentrations observed in SCAPE induced ROS/RNS production (Figure B.4 in Appendix B, available on the HEI website). These observed responses demonstrate that complex interactions may occur in mixture exposures such that a simple sum of individual responses may not recapitulate the observed response. For instance, individual metals clearly induce cellular ROS/RNS production; however, complex interactions may occur in the mixture such that metal–cell interactions are hindered. Previous studies using high performance liquid chromatography have shown that certain metals (e.g., iron, vanadium, and zinc) are retained on a C-18 column, which largely removes hydrophobic compounds. It is therefore possible that metal–organic complexes may form, and the resulting complexes may be too large to diffuse freely across the cellular membrane. This process may effectively prevent certain metals from interacting with cellular components that then promote ROS/RNS production. The relative WSOC:metal ratio may be a potential indicator of this effect, where enhanced metal–organic complex formation, and hence greater metal–cell hindrance, may occur for samples with a higher WSOC:metal ratio. The WSOC:metal ratio was vastly higher in this study (range: 18–23) compared with that of ambient samples collected in California (range: 0.98–3) (Daher et al. 2014; Hu et al. 2008; Saffari et al. 2014a), suggesting that the lack of correlations between ROS/RNS production and metals observed in this study may be attributable to significant metal–organic complex formation. Another explanation for the lack of correlation observed may be attributable to the simplistic correlation-model assumption. Only simple linear correlations were investigated in the study. It is possible that the "true" model between ROS/RNS response and these species is nonlinear, thus resulting in the lack of observed correlations. Additional studies are warranted to investigate and confirm an accurate effect model for aerosol exposure responses.

EFFECT OF PRECURSOR AND FORMATION CONDITION ON OXIDATIVE POTENTIALS AND INFLAMMATORY RESPONSES

Oxidative Potentials

Results from laboratory chamber experiments showed that precursor identity influenced oxidative potentials significantly, with isoprene and naphthalene SOA having the lowest and highest intrinsic DTT activities, respectively. Although the isoprene SOA investigated in this study was formed via a wide range of reaction pathways known to yield different aerosol compositions (Chan et al. 2010; Kroll et al. 2005; Surratt et al. 2010; Xu et al. 2014), the measured intrinsic DTT activities were similar across all formation conditions. Furthermore, these intrinsic DTT activities are in agreement with the isoprene-derived organic aerosols factor resolved from PMF analysis of AMS data collected as part of the SCAPE study (Verma et al. 2015a; Xu et al. 2015a, 2015b). Although this factor is largely attributed to aerosols formed via isoprene epoxydiol uptake, contributions from other isoprene oxidation pathways are also possible (Xu et al. 2015a, 2015b). The agreement between ambient and laboratory-generated isoprene SOA suggests that isoprene SOA may have a low oxidative potential regardless of formation condition, which is in contrast with a previous study where isoprene SOA formed in the presence of "high-NO_x" was found to be more DTT active than that formed in the presence of "low-NO_x" (Kramer et al. 2016). However, these studies may not be directly comparable as the isoprene SOA investigated in Kramer and colleagues (2016) was formed under different conditions (i.e., reaction regimes defined by the ratio of volatile organic compound to NO_x) and a different DTT method was utilized (i.e., different initial DTT concentration, different extraction solvent, and different method for quantifying DTT activity).

Photooxidation of α-pinene, β-caryophyllene, and pentadecane under all formation conditions produced SOA with low oxidative potential, even though the different conditions investigated are known to affect SOA loading and composition because of competing RO_2• pathways (Chan et al. 2009; Eddingsaas et al. 2012; Loza et al. 2014; Ng et al. 2007a). For instance, high NO_x (RO_2• + NO dominant) conditions favor the formation of organic nitrates,

whereas low NO_x (RO_2• + HO_2• dominant) conditions favor organic peroxide production. The relatively low and similar oxidative potentials measured for these SOA systems therefore suggest that organic peroxides and organic nitrates formed from these precursors are not highly redox active. As such, the overall oxidative potential may be similar even though different products are present.

Likewise, the intrinsic DTT activities for *m*-xylene SOA formed under different RO_2• pathways were not significantly different and were in fact similar to that measured for α-pinene, β-caryophyllene, and pentadecane SOA. This similarity may largely be explained by the large portion of ring-opening *m*-xylene oxidation products formed under both low NO_x and high NO_x conditions (Jenkin et al. 2003; Vivanco and Santiago 2010). Because DTT activity is a measure of the concentration of redox-active species present in a sample, the ability of constituent species to participate in electron transfer may be related. As such, it is not surprising that *m*-xylene oxidation yielded SOA with comparably low oxidative potential because the majority of products lack conjugated systems, similar to those of α-pinene, β-caryophyllene, and pentadecane oxidation. Aerosols formed from *m*-xylene under humid conditions were more DTT-active compared with those formed under dry conditions. Previous studies involving the effect of humidity on SOA composition yielded mixed results, with some studies finding significant changes in SOA composition and yields (Healy et al. 2009; Nguyen et al. 2011; Stirnweis et al. 2017; Wong et al. 2015) and others reporting little difference (Boyd et al. 2015; Cocker et al. 2001b; Edney et al. 2000)**.** Humidity effects are therefore highly hydrocarbon-dependent, and further studies into specific oxidation products in the photooxidation of aromatic hydrocarbon under dry and humid conditions may be warranted to understand the difference in DTT activity.

The SOA formed from the photooxidation of naphthalene was the most DTT-active among the aerosol systems investigated. The intrinsic DTT activity measured for naphthalene SOA formed under dry, low NO_x conditions is also in agreement with that measured by McWhinney and colleagues (2013b), where naphthalene SOA was generated under similar conditions using the same •OH radical. Moreover, the same DTT method was used to obtain oxidative potentials in both McWhinney's study and the current study (Cho et al. 2005), and as such, these values should be directly comparable. A strong formation condition effect was also noted for naphthalene SOA. The difference observed between aerosols formed under different NO_x conditions, that is, different RO_2• pathways, may be largely attributable to the different products known to form along each pathway. Many products are formed under both conditions (e.g., naphthoquinones and all ring-opening derivatives of 2-formylcinnamaldehyde), however, under high NO_x dominant conditions, nitroaromatics (e.g., nitronaphthols and nitronaphthalenes) are also formed (Kautzman et al. 2010). The nitrite group next to the aromatic ring in nitroaromatics may promote electron transfer and result in higher DTT consumption, and hence, higher measured oxidative potential. As mentioned previously, this effect was not observed for *m*-xylene because of the formation of predominantly ring-opening oxidation products (Jenkin et al. 2003; Vivanco and Santiago 2010). Together, these observations suggest that the presence of an aromatic ring in oxidation products may be a significant indicator of oxidative potential; comparison of AMS mass spectra further supports this conclusion. Significant peaks at *m/z* 77 and 91 (indicative of aromatic phenyl and benzyl ions) were observed in the AMS mass spectra for naphthalene SOA, whereas these peaks were not strong in that of *m*-xylene SOA (Figure C.3 in Appendix C, available on the HEI website).

Reactive Oxygen/Nitrogen Species and Inflammatory Responses

Both precursor identity and formation condition influenced the responses induced by SOA exposure, as demonstrated by the range of responses observed for SOA formed from different precursors and under different formation conditions (Figure 9). However, no clear trends were observed for either variable (precursor identity or formation condition), in contrast to that observed for oxidative potentials, where only precursor identity influenced DTT activity substantially. This dissimilarity may be a reflection of the differences between chemical and cellular assays, which may be further highlighted as a result of the considerably different classes of compounds chosen as SOA precursors. In this study, the aerosol compositional changes between different precursors were generally more substantial than those arising between different formation conditions of the same precursor (Figure 12). The DTT chemical assay may only be sensitive to larger differences, such as those arising from different SOA precursors, whereas cellular assays may also be sensitive to differences arising from SOA formed from the same precursor but under different formation conditions. These differences may also result from the different oxidants measured by each assay. The DTT assay measures the concentration of redox-active species in a sample. These redox-active species may induce cellular ROS/RNS production, which is measured by the cellular assay. Some of these species may also diffuse across the cell membrane and interact with the ROS/RNS probe. Therefore, although the assays measure different oxidants, there may be some overlap.

Although the effects of SOA precursor and formation condition did not yield an apparent trend in individual inflammatory responses, several patterns can be distinguished for SOA precursors whose photooxidation products have similar carbon-chain length and chemical functionality. Exposure to isoprene SOA generated under different formation conditions induced comparable responses for the inflammatory endpoints. Furthermore, these responses were the lowest among all aerosol systems investigated (Figure 10). This result suggests that different isoprene oxidation products (Chan et al. 2010; Surratt et al. 2010; Xu et al. 2014) may induce similarly low inflammatory responses, which is consistent with that observed for the oxidative potentials of ambient isoprene SOA (Figure 8). However, this finding is different from that observed in a previous study, where methacrylic acid epoxide–derived SOA was found to be significantly more potent than isoprene epoxydiol-derived SOA in inducing the upregulation of genes related to oxidative stress (Lin et al. 2016). Nevertheless, the fold change of several genes reported in the previous study are actually comparable. It is therefore possible that the inflammatory endpoints chosen in this study may correspond to genes whose expression was comparable regardless of SOA formation condition.

Likewise, inflammatory responses induced as a result of exposure to α-pinene and *m*-xylene SOA were similar regardless of formation condition (Figures 9 and 10). In addition, the levels of all three endpoints induced by these aerosol systems are fairly comparable, suggesting that oxidation products of both precursors participate in similar cellular pathways. Indeed, photooxidation products of both α-pinene and *m*-xylene share similarities, such as a large portion of ring-breaking products with a similar carbon chain length (Eddingsaas et al. 2012; Jenkin et al. 2003; Vivanco and Santiago 2010). It is possible that products that bear a certain level of resemblance may interact with the same cellular targets and participate in the same cellular pathways, resulting in a comparable response.

Another response pattern was observed for β-caryophyllene and pentadecane SOA, where the IL-6 response spanned a much larger range than that of TNF-α (Figure 10). This pattern is unlike that observed for oxidative potential, where the DTT activity was comparable regardless of formation condition for these aerosol systems (Figure 8), and further supports that certain changes in aerosol composition may not be captured by redox potential measurements. The response pattern observed here also appears to reflect oxidation product structure. No prior studies have investigated the oxidation products of pentadecane, however, these products are expected to resemble those of dodecane (i.e., products with the same functionalities, but a longer carbon chain) because both are long-chain alkanes (Loza et al. 2014). As such, pentadecane oxidation products are likely to bear a resemblance to long-chain fatty acids. These compounds may therefore be able to insert into the cell membrane and alter membrane fluidity; downstream effects of this alteration vary depending on the specific modification and cell type, however, all effects are known to affect cell function substantially (Baritaki et al. 2007; Spector and Yorek 1985). For instance, certain changes in membrane fluidity may induce apoptosis, which involves pathways leading to the production of TNF-α; TNF-α may then in turn induce IL-6 production, which is involved in a feedback loop that inhibits the TNF-α production (Baritaki et al. 2007; Kishimoto 2003; Wang et al. 2003). The combination of these cellular events is consistent with the observed levels of inflammatory endpoints (high IL-6 and lower TNF-α), as well as the lower ROS/RNS levels because IL-6 exhibits anti-inflammatory functions. Responses are likely less pronounced for β-caryophyllene because of the shorter carbon-chain length observed in known oxidation products; even though both precursors have the same number of carbons (15), β-caryophyllene is bicyclic and many oxidation products retain the four-membered ring, resulting in a shorter carbon backbone (Chan et al. 2011). As such, there may be fewer products capable of inserting into the cell membrane, resulting in a less pronounced response in comparison to pentadecane aerosol.

Exposure to naphthalene aerosol resulted in a different response pattern, where a large response range was observed for both cytokines and levels of ROS/RNS (Figure 10). These results complement those obtained from oxidative potential measurements, where naphthalene aerosol was also an outlier with a DTT activity at least twice that of the next highest aerosol system (Figure 8). As previously discussed, these responses are likely a reflection of specific oxidation products, such as naphthoquinones, which are known to induce redox-cycling and may therefore induce higher levels of inflammatory endpoints (Henkler et al. 2010; Kautzman et al. 2010; Lorentzen et al. 1979). Furthermore, the presence of aromatic ring–retaining products differentiates naphthalene aerosol from other SOA systems, where the majority of products do not contain aromatic rings and may therefore result in outlier response levels. A clear increasing trend also exists between levels of TNF-α and IL-6, suggesting that naphthalene SOA may also induce anti-inflammatory pathways not captured by oxidative potential measurements. Additionally, many naphthalene oxidation products bear resemblance to dinitrophenol, a compound known to

decouple phosphorylation from electron transfer (Terada 1990), whereas others (such as nitroaromatics and polyaromatics) have known mutagenic effects, including the formation of DNA adducts (Baird et al. 2005; Helmig et al. 1992). Together, these results suggest that the aromatic functionality may result in the involvement of very different cellular pathways and yield health effects beyond redox imbalance and oxidative stress.

EFFECT OF REDOX-ACTIVE METALS ON OXIDATIVE POTENTIALS AND INFLAMMATORY RESPONSES

The use of iron sulfate as seed for naphthalene-derived SOA did not have an effect on oxidative potential relative to ammonium sulfate, but induced higher ROS/RNS. The observed lack of effect of iron sulfate seed relative to ammonium sulfate seed on oxidative potential is interesting, as it suggests that the presence of iron may not always induce an additive effect in the case of aerosol oxidative potentials. Future studies should investigate whether concentration addition (a model used to predict the effect of combinations of chemicals) is an applicable effect model for oxidative potential measurements. The contribution of seed to oxidative potential was evaluated and found to be relatively low (<20%) for all experiments, suggesting that organic constituents contribute significantly to oxidative potential.

In terms of the effect of metallic seed on cellular ROS/RNS production, all SOA formed in the presence of iron sulfate induced higher ROS/RNS levels than that formed in the presence of ammonium sulfate (Figure 11). The observed difference was attributed to both a seed effect and an organic aerosol effect. To further explore the seed effect, the seed mass collected onto each filter was estimated by characterizing the seed particle wall loss (i.e., fitting a double exponential to seed concentrations as a function of time) and integrating over the filter collection period (Figure C.4, in Appendix C, available on the HEI website). The ROS/RNS response attributable to the presence of iron seed (ROS/RNS_{FS}, where FS indicates iron[II] sulfate) was then calculated using a pure iron sulfate dose–response curve (Figure C.5, in Appendix C) and found to be a relatively low percentage (2–12%) of the total response ($ROS/RNS_{FS + SOA}$). Similar results were observed for oxidative potentials. It should be noted that these are simple estimations performed to provide relative perspective. The absolute contributions of iron sulfate may differ as concentration addition may not apply for cellular responses. However, similar to oxidative potentials, the validity of this effect model for cellular response is beyond the scope of this study. Nevertheless, the results are interesting as they suggest that the measured ROS/RNS response may be predominantly attributable to organic constituents.

CORRELATION BETWEEN AEROSOL OXIDATION STATE AND OXIDATIVE PROPERTIES

The laboratory-generated aerosol spanned a wide range of $\overline{OS}_c$ values and a significant positive correlation was observed between ROS/RNS production and $\overline{OS}_c$ (Figure 12). This correlation is not surprising, as aerosol with higher degrees of oxidation (higher $\overline{OS}_c$) are likely to be better oxidizing agents, which in turn may induce ROS/RNS production. The observed correlation may also provide insight into the differences observed for SOA generated in the presence of different seed types, where, for example, aerosols generated in the presence of iron sulfate induced higher levels of ROS/RNS than those formed in the presence of ammonium sulfate. In these cases, the presence of iron serves as a catalyst to increase the oxidation of organic species via Fenton-like reactions (Chevion 1988; Frei 1994). Furthermore, since the correlation applies for all laboratory-generated aerosols, including those formed from different precursors under different formation conditions, it is plausible that all the other effects (i.e., precursor identity and seed type) are ultimately an effect of the degree of oxidation of aerosols. This has notable implications for future studies because atmospheric photochemical aging leads to increases in aerosol oxidation (Jimenez et al. 2009; Ng et al. 2011) and aerosols have an atmospheric lifetime of approximately a week, during which these processes can occur. Finally, the observed correlation suggests that $\overline{OS}_c$ values may be utilized to estimate ROS/RNS levels. $\overline{OS}_c$ values are easily obtained with no additional processing, such as filter collection and extraction, required. They can be readily calculated from H:C and O:C ratios, which are measured by the AMS, an online instrument. Together, these results may lead to real-time ROS/RNS levels, which could provide valuable information and insight on the aerosol health effects.

No significant correlations were observed between aerosol oxidation state and cytokine levels induced as a result of aerosol exposure (Figure C.6 in Appendix C, available on the HEI website). It is likely that the pathways involved in cytokine production involve many complex feedback and feedforward loops that may convolute any obvious effects. Likewise, oxidative potentials were not obviously affected by the degree of oxidation. This is consistent with ambient results, where more-oxidized organic aerosol subtypes did not necessarily have a higher oxidative potential (Verma et al. 2015a; Xu et al. 2015a, 2015b).

COMPARISON WITH AMBIENT DATA

With the exception of naphthalene SOA, the oxidative potentials of all laboratory-generated aerosols were comparable with those observed in ambient samples collected around the greater Atlanta region. Naphthalene aerosol was likely an outlier because of its aromatic ring–retaining products (Kautzman et al. 2010), which other SOA systems lack. In terms of cellular ROS/RNS responses, laboratory-generated SOA induced comparable or higher levels of ROS/RNS compared with that induced by ambient samples. Several possibilities exist for the observed higher ROS/RNS response obtained for some SOA systems. For one, aerosol systems considered in this study were single precursor, pure SOA systems. Ambient aerosol comprises SOA from multiple precursors, which may interact with each other and result in a different response level. Interactions between SOA and other species present in ambient aerosol (e.g., metals and other organic species) are also likely to alter the response level. Although the influence of iron was investigated in this study, there are multiple other metal species present in the ambient aerosols that were not explored. Additionally, certain species present in the ambient aerosols may contribute to PM mass, but induce little to no ROS/RNS production, resulting in a lower overall intrinsic ROS/RNS production level.

LIMITATIONS OF STUDY

Several limitations must be noted for this study. For instance, an immortalized murine cell line was utilized for exposure experiments. To our knowledge, immortalized human alveolar macrophages do not exist. As a result, we chose to use a non-human cell line. In choosing this specific cell line, we considered that mice have been widely used as a model organism for studying human response (e.g., Rosenthal and Brown 2007; Takao and Miyakawa 2015) and chose a murine alveolar macrophage cell line for exposure experiments. Furthermore, we did not choose primary cells as primary cells are harvested from multiple animals, which may increase the response variability and less reproducible results compared to cell lines. The particular cell line chosen for this study also retains many properties of primary alveolar macrophages, such as phagocytosis and production of ROS/RNS and cytokines (Mbawuike and Herscowitz 1989; Sankaran and Herscowitz 1995).

Additional limitations that warrant further study include the use of only one cell type, whereas an organism consists of multiple tissues, and the lungs alone consist of multiple cell types. Interactions between tissue systems and different cell types were not explored in this study and may produce very different results. These interactions would be important to consider when extrapolating results from this study to in vivo exposures. Furthermore, the doses investigated in this study may not accurately represent real-world exposures as a result of different exposure routes and potential recovery effects related to clearance. Resuspension extracts (used in this study) also differ from real-world exposures. However, a recent study on the health effects of isoprene SOA found similar cellular responses for both filter-resuspension extracts and direct air–liquid deposition, which more closely represent real-world aerosol exposures (Arashiro et al. 2016). These results may be a positive indication for the extrapolation of in vitro results, although more aerosol systems and cell types must be investigated first to confirm these conclusions. Finally, water-insoluble material was also not considered in this study. Inclusion of water-insoluble material may induce different cellular responses, as previous studies have shown that insoluble particles have substantial oxidative potential that may translate into cellular responses (Fang et al. 2017; McWhinney et al. 2013a; Verma et al. 2012; Yang et al. 2014). Nevertheless, despite these limitations, this study provides a perspective on which future studies can be built. For instance, this study demonstrates that cellular responses resulting from PM exposure cannot be expressed using a single PM dose, which aids the design of future exposure studies. Additionally, the perspective gained on the relative toxicities of different SOA systems can be used to focus future studies. Specifically, the more toxic SOA systems may warrant additional in-depth investigations. Finally, results from this study suggest that aerosols may become more toxic as they age. These results can provide inspiration for future studies to focus on changes that occur throughout atmospheric aging and determine whether those changes result in more toxic aerosols.

IMPLICATIONS OF FINDINGS

Intracellular ROS/RNS produced as a result of exposure to ambient aerosol collected around the greater Atlanta region and to laboratory-generated aerosol were measured using an optimized alveolar macrophage cellular assay. Results from 104 ambient filter samples and multiple laboratory-generated SOA systems demonstrate that a wide dose range was necessary to fully capture the dose–response relationship. Multiple dose–response parameters, including maximum response, threshold, EC_{50}, Hill slope, and AUC, were also evaluated because different metrics may provide different measures of toxicity. AUC was found to be the most robust metric, whereas other metrics varied in informativeness, depending on the dose

range investigated and whether a baseline or maximum response was observed.

Results from ambient samples highlighted the importance of summertime organic species, as significant correlations were observed between organic species (i.e., WSOC and BrC) and cellular ROS/RNS responses for filter samples collected during the summer months. The significance of photochemically driven summertime SOA was further established by results from laboratory-generated aerosols, as organic aerosol alone (in the absence of metallic species) were capable of inducing oxidative responses as measured by oxidative potential and cellular inflammatory measurements. Our comprehensive laboratory-chamber study allowed for evaluation of a wide variety of SOA systems under different formation conditions for the first time. We found that precursor identity influenced the oxidative potential and cellular responses of laboratory-generated organic aerosols substantially, further demonstrating the importance of PM sources. The oxidative potentials spanned a wide range, with isoprene SOA and naphthalene SOA having the lowest and highest DTT activities, respectively. In general, the oxidative potential for biogenic SOA was lower than that of anthropogenic SOA. These bounds were less clear for cellular responses. Although isoprene and naphthalene SOA still generated the lowest and highest inflammatory responses, respectively, in general, a few exceptions were noted for other SOA systems (e.g., the ROS/RNS levels induced by pentadecane SOA were lower than that of isoprene SOA). Collectively, these results suggest that to evaluate overall oxidative properties of ambient aerosols, precursor emissions and their corresponding SOA formation potential must be considered. The high response of naphthalene SOA also suggests that the presence of conjugated systems may be important for PM-induced health effects. Detailed studies exploring the cellular effects of known naphthalene SOA products may be worthwhile given its high response among different aerosol systems. Patterns noted for cellular responses also highlighted the importance of chemical structure (i.e., carbon-chain length and functionality), as products with similar chemical structure may participate in similar cellular pathways, leading to similar cellular responses. It may therefore be possible to roughly predict cellular responses given known SOA products. These findings can guide future health effects studies to explore whether certain hypothesized cellular pathways are indeed induced post-exposure. Although the aerosol-formation condition also affected oxidative properties, further studies exploring the aerosol chemistry under different conditions is required to fully interpret these results.

As demonstrated by the correlation between aerosol oxidation state and ROS/RNS production observed for all laboratory-generated aerosol (e.g., different precursor, formation condition, and photochemical age), the degree of oxidation may serve as a useful tool to estimate roughly ROS/RNS levels. The observed correlation has significant implications for future health studies because bulk measures of aerosol oxidation are easily accessible and do not require the additional processing that cellular ROS/RNS measurements entail. Moreover, aerosols have a lifetime of approximately one week, during which photochemical aging occurs, thus yielding more oxidized species and aerosols with higher degrees of oxidation. As such, aerosols may potentially become more toxic over their lifetime, which may inspire further studies. Finally, these measurements have a finer time resolution and may pave the way for real-time ROS/RNS predictions should further studies find that the relationship holds for other aerosol systems as well. The observed correlation also suggests that there may be a negligible seed effect with respect to ROS/RNS production, as all laboratory-generated aerosols follow the correlation regardless of seed type. As such, differences observed between different seed types are likely an effect of differences in aerosol oxidation.

Although no simple trend was observed between chemical and cellular assay results for both ambient and laboratory-generated aerosol, chemical assays such as DTT may serve as a useful screening tool because samples with low DTT activity are likely to induce low levels of ROS/RNS production (based on ambient data, Figure 5). However, the cellular inflammatory responses induced as a result of exposure to laboratory-generated aerosol also demonstrate that a low ROS/RNS response may not necessarily indicate a lack of cellular response. Although ROS/RNS levels were generally associated with inflammatory cytokine production, there were aerosol systems in which a low ROS/RNS response was accompanied by levels of cytokine production that were higher than expected given the ROS/RNS level detected. Taken together, these results suggest that chemical assays may serve as a useful screening tool in terms of general oxidative stress, as measured by ROS/RNS production. However, additional measures, such as inflammatory cytokine production, may be required to interpret cellular responses fully.

Finally, results from this study demonstrate that PM species cannot be treated as individual components in a mixture. That is, complex interactions may occur between PM species such that the overall response cannot be approximated by a simple sum of individual effects. Although mixture effects were not explored in this study, their importance is apparent given the results obtained

from both ambient and laboratory-generated aerosol cellular exposures. For instance, although few metal species were correlated with ROS/RNS response for ambient samples, exposure to individual metals induced measurable ROS/RNS production. Although the assumed correlation model may also be too simplistic and warrants further investigation, mixture effects are also important given that ambient PM contains SOA formed from multiple precursors, as well as multiple metallic species emitted as a result of mechanical processes and combustion. It may therefore be worthwhile to test the validity of various mixture models because it is not feasible to explore every possible combination of PM components and their relevant interactions.

ACKNOWLEDGMENTS

This work was supported by the Health Effects Institute under research agreement No. 4943-RFA13-2/14-4. Wing Y. Tuet acknowledges support by the National Science Foundation Graduate Research Fellowship under Grant No. DGE-1650044.

REFERENCES

Akhtar US, McWhinney RD, Rastogi N, Abbatt JPD, Evans GJ, Scott JA. 2010. Cytotoxic and proinflammatory effects of ambient and source-related particulate matter (PM) in relation to the production of reactive oxygen species (ROS) and cytokine adsorption by particles. Inhal Toxicol 22:37–47.

Anderson JO, Thundiyil JG, Stolbach A. 2011. Clearing the air: A review of the effects of particulate matter air pollution on human health. J Med Tox 8:166–175.

Antinolo M, Willis MD, Zhou S, Abbatt JPD. 2015. Connecting the oxidation of soot to its redox cycling abilities. Nat Commun 6:8612.

Arashiro M, Lin YH, Sexton KG, Zhang Z, Jaspers I, Fry RC, et al. 2016. In vitro exposure to isoprene-derived secondary organic aerosol by direct deposition and its effects on *COX-2* and *IL-8* gene expression. Atmos Chem Phys 16:14079–14090; https://doi.org/10.5194/acp-16-14079-2016.

Bahreini R, Keywood MD, Ng NL, Varutbangkul V, Gao S, Flagan RC, et al. 2005. Measurements of secondary organic aerosol from oxidation of cycloalkenes, terpenes, and *m*-xylene using an aerodyne aerosol mass spectrometer. Environ Sci Technol 39:5674–5688; doi:10.1021/es048061a.

Bai Y, Suzuki AK, Sagai M. 2001. The cytotoxic effects of diesel exhaust particles on human pulmonary artery endothelial cells in vitro: Role of active oxygen species. Free Rad Biol Med 30:555–562.

Baird WM, Hooven LA, Mahadevan B. 2005. Carcinogenic polycyclic aromatic hydrocarbon-DNA adducts and mechanism of action. Environ Mol Mutagen 45:106–114.

Baltensperger U, Dommen J, Alfarra R, Duplissy J, Gaeggeler K, Metzger A, et al. 2008. Combined determination of the chemical composition and of health effects of secondary organic aerosols: The POLYSOA Project. J Aerosol Med Pulm Drug Deliv 21:145–154.

Baritaki S, Apostolakis S, Kanellou P, Dimanche-Boitrel MT, Spandidos DA, Bonavida B. 2007. Reversal of tumor resistance to apoptotic stimuli by alteration of membrane fluidity: Therapeutic implications. Adv Cancer Research 98:149–190.

Bates JT, Weber RJ, Abrams J, Verma V, Fang T, Klein M, et al. 2015. Reactive oxygen species generation linked to sources of atmospheric particulate matter and cardiorespiratory effects. Environ Sci Tech 49:13605–13612.

Beam A, Motsinger-Reif A. 2014. Beyond IC50s: Towards robust statistical methods for in vitro association studies. J Pharmacogenomics Pharmacoproteomics 5:1000121.

Bermudez E, Mangum JB, Wong BA, Asgharian B, Hext PM, Warheit DB, et al. 2004. Pulmonary responses of mice, rats, and hamsters to subchronic inhalation of ultrafine titanium dioxide particles. Toxicol Sci 77:347–357.

Boyd CM, Sanchez J, Xu L, Eugene AJ, Nah T, Tuet WY, et al. 2015. Secondary organic aerosol formation from the β-pinene+NO_3 system: Effect of humidity and peroxy radical fate. Atmos Chem Phys 15:7497–7522.

Brook RD, Rajagopalan S, Pope CA, Brook JR, Bhatnagar A, Diez-Roux AV, et al. 2010. Particulate matter air pollution and cardiovascular disease an update to the scientific statement from the American Heart Association. Circulation 121:2331–2378.

Brunekreef B, Holgate ST. 2002. Air pollution and health. Lancet 360:1233–1242.

Bruns EA, El Haddad I, Slowik JG, Kilic D, Klein F, Baltensperger U, et al. 2016. Identification of significant precursor gases of secondary organic aerosols from residential wood combustion. Sci Rep 6:27881.

Budisulistiorini SH, Canagaratna MR, Croteau PL, Marth WJ, Baumann K, Edgerton ES, et al. 2013. Real-time

continuous characterization of secondary organic aerosol derived from isoprene epoxydiols in downtown Atlanta, Georgia, using the aerodyne aerosol chemical speciation monitor. Enviro Sci Technology 47:5686–5694.

Burnett R, Brook J, Dann T, Delocla C, Philips O, Cakmak S, et al. 2001. Association between particulate- and gas-phase components of urban air pollution and daily mortality in eight Canadian cities. Inhal Toxicol 12S4:15–39.

Canagaratna MR, Jimenez JL, Kroll JH, Chen Q, Kessler SH, Massoli P, et al. 2015. Elemental ratio measurements of organic compounds using aerosol mass spectrometry: Characterization, improved calibration, and implications. Atmos Chem Phys 15:253–272.

Castro L, Freeman BA. 2001. Reactive oxygen species in human health and disease. Nutrition 17:161–165.

Chan AWH, Chan MN, Surratt JD, Chhabra PS, Loza CL, Crounse JD, et al. 2010. Role of aldehyde chemistry and NO_x concentrations in secondary organic aerosol formation. Atmos Chem Phys 10:7169–7188.

Chan AWH, Kautzman KE, Chhabra PS, Surratt JD, Chan MN, Crounse JD, et al. 2009. Secondary organic aerosol formation from photooxidation of naphthalene and alkylnaphthalenes: Implications for oxidation of intermediate volatility organic compounds (IVOCs). Atmos Chem Phys 9:3049–3060.

Chan MN, Surratt JD, Chan AWH, Schilling K, Offenberg JH, Lewandowski M, et al. 2011. Influence of aerosol acidity on the chemical composition of secondary organic aerosol from β-caryophyllene. Atmos Chem Phys 11:1735–1751.

Charrier JG, Anastasio C. 2012. On dithiothreitol (DTT) as a measure of oxidative potential for ambient particles: Evidence for the importance of soluble transition metals. Atmos Chem Phys 12:9321–9333.

Charrier JG, Richards-Henderson NK, Bein KJ, McFall AS, Wexler AS, Anastasio C. 2015. Oxidant production from source-oriented particulate matter – Part 1: Oxidative potential using the dithiothreitol (DTT) assay. Atmos Chem Phys 15:2327–2340.

Chen CY, Peng WH, Tsai KD, Hsu SL. 2007. Luteolin suppresses inflammation-associated gene expression by blocking NF-κB and AP-1 activation pathway in mouse alveolar macrophages. Life Sci 81:1602–1614.

Chen Q, Farmer D, Rizzo L, Pauliquevis T, Kuwata M, Karl TG, et al. 2015. Submicron particle mass concentrations and sources in the Amazonian wet season (AMAZE-08). Atmos Chem Phys 15:3687–3701.

Chen XP, Zhong ZF, Xu ZT, Chen LD, Wang YT. 2010. 2′,7′-Dichlorodihydrofluorescein as a fluorescent probe for reactive oxygen species measurement: Forty years of application and controversy. Free Radic Res 44:587–604.

Chevion M. 1988. A site-specific mechanism for free radical induced biological damage: The essential role of redox-active transition metals. Free Rad Bio Med 5:27–37.

Chhabra PS, Flagan RC, Seinfeld JH. 2010. Elemental analysis of chamber organic aerosol using an aerodyne high-resolution aerosol mass spectrometer. Atmos Chem Phys 10:4111–4131.

Chhabra PS, Ng NL, Canagaratna MR, Corrigan AL, Russell LM, Worsnop DR, et al. 2011. Elemental composition and oxidation of chamber organic aerosol. Atmos Chem Phys 11:8827–8845.

Chiang SS, Ulziijargal E, Chien RC, Mau JL. 2015. Antioxidant and anti-inflammatory properties of solid-state fermented products from a medicinal mushroom, Taiwanofungus salmoneus (higher Basidiomycetes) from Taiwan. Int J Med Mushrooms 17:21–32.

Cho AK, Sioutas C, Miguel AH, Kumagai Y, Schmitz DA, Singh M, et al. 2005. Redox activity of airborne particulate matter at different sites in the Los Angeles basin. Environ Res 99:40–47.

Chu B, Hao J, Takekawa H, Li J, Wang K, Jiang J. 2012. The remarkable effect of $FeSO_4$ seed aerosols on secondary organic aerosol formation from photooxidation of α-pinene/NO_x and toluene/NO_x. Atmos Environ 55:26–34.

Chu B, Liu Y, Li J, Takekawa H, Liggio J, Li SM, et al. 2014. Decreasing effect and mechanism of $FeSO_4$ seed particles on secondary organic aerosol in α-pinene photooxidation. Environ Pollut 193:88–93.

Cocker DR III, Clegg SL, Flagan RC, Seinfeld JH. 2001a. The effect of water on gas–particle partitioning of secondary organic aerosol. Part I: α-Pinene/ozone system. Atmos Environ 35:6049–6072.

Cocker DR III, Mader BT, Kalberer M, Flagan RC, Seinfeld JH. 2001b. The effect of water on gas–particle partitioning of secondary organic aerosol: II. *M*-xylene and 1,3,5-trimethylbenzene photooxidation systems. Atmos Environ 35:6073–6085.

Conroy LE, Park KC. 1968. Electrical properties of the Group IV disulfides, titanium disulfide, zirconium disulfide, hafnium disulfide and tin disulfide. Inorg Chem 7:459–463.

Daher N, Saliba NA, Shihadeh AL, Jaafar M, Baalbaki R, Shafer MM, et al. 2014. Oxidative potential and chemical speciation of size-resolved particulate matter (PM) at near-freeway and urban background sites in the greater Beirut area. Sci Total Environ 470:417–426.

Daumit KE, Carrasquillo AJ, Sugrue RA, Kroll JH. 2016. Effects of condensed-phase oxidants on secondary organic aerosol formation. J Phys Chem A 120:1386–1394.

DeCarlo PF, Kimmel JR, Trimborn A, Northway MJ, Jayne JT, Aiken AC, et al. 2006. Field-deployable, high-resolution, time-of-flight aerosol mass spectrometer. Anal Chem 78:8281–8289.

Dockery DW, Pope CA, Xu X, Spengler JD, Ware JH, Fay ME, et al. 1993. An association between air pollution and mortality in six U.S. Cities. N Eng J Med 329:1753–1759.

Dou J, Lin P, Kuang BY, Yu JZ. 2015. Reactive oxygen species production mediated by humic-like substances in atmospheric aerosols: Enhancement effects by pyridine, imidazole, and their derivatives. Environ Sci Tech 49:6457–6465.

Eddingsaas NC, Loza CL, Yee LD, Chan M, Schilling KA, Chhabra PS, et al. 2012. α-Pinene photooxidation under controlled chemical conditions – Part 2: SOA yield and composition in low- and high-NO_x environments. Atmos Chem Phys 12:7413–7427.

Edney EO, Driscoll DJ, Speer RE, Weathers WS, Kleindienst TE, Li W, et al. 2000. Impact of aerosol liquid water on secondary organic aerosol yields of irradiated toluene/propylene/NO_x/$(NH_4)_2SO_4$/air mixtures. Atmos Environ 34:3907–3919.

Fang T, Guo H, Verma V, Peltier RE, Weber RJ. 2015a. $PM_{2.5}$ water-soluble elements in the southeastern United States: Automated analytical method development, spatiotemporal distributions, source apportionment, and implications for heath studies. Atmos Chem Phys 15:11667–11682.

Fang T, Verma V, Bates J, Abrams J, Klein M, Strickland M, et al. 2015b. Oxidative potential of ambient water-soluble $PM_{2.5}$ measured by dithiothreitol (DTT) and ascorbic acid (AA) assays in the southeastern United States: Contrasts in sources and health associations. Atmos Chem Phys 15:30609–30644.

Fang T, Verma V, Bates JT, Abrams J, Klein M, Strickland MJ, et al. 2016. Oxidative potential of ambient water-soluble $PM_{2.5}$ in the southeastern United States: Contrasts in sources and health associations between ascorbic acid (AA) and dithiothreitol (DTT) assays. Atmos Chem Phys 16:3865–3879.

Fang T, Verma V, Guo H, King LE, Edgerton ES, Weber RJ. 2015c. A semi-automated system for quantifying the oxidative potential of ambient particles in aqueous extracts using the dithiothreitol (DTT) assay: Results from the Southeastern Center for Air Pollution and Epidemiology (SCAPE). Atmos Meas Tech 8:471–482.

Fang T, Zeng L, Gao D, Verma V, Stefaniak AB, Weber RJ. 2017. Ambient size distributions and lung deposition of aerosol dithiothreitol-measured oxidative potential: Contrast between soluble and insoluble particles. Environ Sci Tech 51:6802–6811.

Frei B. 1994. Reactive oxygen species and antioxidant vitamins: Mechanisms of action. Amer J Med 97:S5–S13.

Fubini B, Hubbard A. 2003. Reactive oxygen species (ROS) and reactive nitrogen species (RNS) generation by silica in inflammation and fibrosis. Free Rad Biol Med 34:1507–1516.

Goutelle S, Maurin M, Rougier F, Barbaut X, Bourguignon L, Ducher M, et al. 2008. The Hill equation: A review of its capabilities in pharmacological modelling. Fundam Clin Pharma 22:633–648.

Grosberg A, Nesmith AP, Goss JA, Brigham MD, McCain ML, Parker KK. 2012. Muscle on a chip: In vitro contractility assays for smooth and striated muscle. J Pharma Toxicol Meth 65:126–135.

Guenther A, Karl T, Harley P, Wiedinmyer C, Palmer PI, Geron C. 2006. Estimates of global terrestrial isoprene emissions using MEGAN (Model of Emissions of Gases and Aerosols from Nature). Atmos Chem Phys 6:3181–3210.

Guenther AB, Zimmerman PR, Harley PC, Monson RK, Fall R. 1993. Isoprene and monoterpene emission rate variability: Model evaluations and sensitivity analyses. J Geophys Res–Atmos 98:12609–12617.

Gurgueira SA, Lawrence J, Coull B, Murthy GGK, Gonzalez-Flecha B. 2002. Rapid increases in the steady-state concentration of reactive oxygen species in the lungs and heart after particulate air pollution inhalation. Environ Health Perspect 110:749–755.

Haddad JJ. 2001. L-Buthionine-(S,R)-sulfoximine, an irreversible inhibitor of gamma-glutamylcysteine synthetase, augments LPS-mediated pro-inflammatory cytokine biosynthesis: Evidence for the implication of an IκB-α/NFκB insensitive pathway. Eur Cytokine Netw 12:614–624.

Halliwell B, Gutteridge JM. 1984. Oxygen toxicity, oxygen radicals, transition metals and disease. Biochem J 219:1–14.

Hallquist M, Wenger JC, Baltensperger U, Rudich Y, Simpson D, Claeys M, et al. 2009. The formation, properties and impact of secondary organic aerosol: Current and emerging issues. Atmos Chem Phys 9:5155–5236.

Hamad SH, Shafer MM, Kadhim AKH, Al-Omran SM, Schauer JJ. 2015. Seasonal trends in the composition and ROS activity of fine particulate matter in Baghdad, Iraq. Atmos Environ 100:102–110.

Hardin BJ, Campbell KS, Smith JD, Arbogast S, Smith J, Moylan JS, et al. 2008. TNF-α acts via TNFR1 and muscle-derived oxidants to depress myofibrillar force in murine skeletal muscle. J Appl Physio 104:694–699.

Heald CL, Kroll JH, Jimenez JL, Docherty KS, DeCarlo PF, Aiken AC, et al. 2010. A simplified description of the evolution of organic aerosol composition in the atmosphere. Geophys Res Lett 37(8).

Healy RM, Temime B, Kuprovskyte K, Wenger JC. 2009. Effect of relative humidity on gas/particle partitioning and aerosol mass yield in the photooxidation of *p*-xylene. Environ Sci Tech 43:1884–1889.

Hecobian A, Zhang X, Zheng M, Frank N, Edgerton ES, Weber RJ. 2010. Water-soluble organic aerosol material and the light-absorption characteristics of aqueous extracts measured over the southeastern United States. Atmos Chem Phys 10:5965–5977.

Helmig D, Arey J, Harger WP, Atkinson R, Lopez-Cancio J. 1992. Formation of mutagenic nitrodibenzopyranones and their occurrence in ambient air. Environ Sci Tech 26:622–624.

Henkler F, Brinkmann J, Luch A. 2010. The role of oxidative stress in carcinogenesis induced by metals and xenobiotics. Cancers 2:376.

Hensley K, Robinson KA, Gabbita SP, Salsman S, Floyd RA. 2000. Reactive oxygen species, cell signaling, and cell injury. Free Radic Biol Med 28:1456–1462.

Hildebrandt L, Donahue NM, Pandis SN. 2009. High formation of secondary organic aerosol from the photo-oxidation of toluene. Atmos Chem Phys 9:2973–2986.

Hill AV. 1910. The possible effects of the aggregation of the molecules of haemoglobin on its dissociation curves. J Physiol (London) 40:4–7.

Hoek G, Krishnan RM, Beelen R, Peters A, Ostro B, Brunekreef B, et al. 2013. Long-term air pollution exposure and cardio-respiratory mortality: A review. Environ Health 12:43.

Hoffmann T, Odum J, Bowman F, Collins D, Klockow D, Flagan R, et al. 1997. Formation of organic aerosols from the oxidation of biogenic hydrocarbons. J Atmos Chem 26:189–222.

Hu S, Polidori A, Arhami M, Shafer MM, Schauer JJ, Cho A, et al. 2008. Redox activity and chemical speciation of size fractioned PM in the communities of the Los Angeles-Long Beach harbor. Atmos Chem Phys 8:6439–6451.

Hu WW, Campuzano-Jost P, Palm BB, Day DA, Ortega AM, Hayes PL, et al. 2015. Characterization of a real-time tracer for isoprene epoxydiols-derived secondary organic aerosol (IEPOX-SOA) from aerosol mass spectrometer measurements. Atmos Chem Phys 15:11807–11833.

Huang YCT, Ghio AJ, Stonehuerner J, McGee J, Carter JD, Grambow SC, et al. 2003. The role of soluble components in ambient fine particles-induced changes in human lungs and blood. Inhal Toxicol 15:327–342.

Iversen GR, Norpoth H. 1987. Analysis of Variance. Thousand Oaks, CA:Sage Publishing.

Janssen NAH, Yang A, Strak M, Steenhof M, Hellack B, Gerlofs-Nijland ME, et al. 2014. Oxidative potential of particulate matter collected at sites with different source characteristics. Sci Total Environ 472:572–581.

Jenkin ME, Saunders SM, Wagner V, Pilling MJ. 2003. Protocol for the development of the master chemical mechanism, MCM V3 (Part B): Tropospheric degradation of aromatic volatile organic compounds. Atmos Chem Phys 3:181–193.

Jia C, Batterman S. 2010. A critical review of naphthalene sources and exposures relevant to indoor and outdoor air. Int J Environ Res Pub Health 7:2903–2939.

Jimenez JL, Canagaratna MR, Donahue NM, Prevot ASH, Zhang Q, Kroll JH, et al. 2009. Evolution of organic aerosols in the atmosphere. Science 326:1525–1529.

Kalyanaraman B, Darley-Usmar V, Davies KJA, Dennery PA, Forman HJ, Grisham MB, et al. 2012. Measuring reactive oxygen and nitrogen species with fluorescent probes: Challenges and limitations. Free Radic Biol Med 52:1–6.

Kanakidou M, Seinfeld JH, Pandis SN, Barnes I, Dentener FJ, Facchini MC, et al. 2005. Organic aerosol and global

climate modelling: A review. Atmos Chem Phys 5:1053–1123.

Kautzman KE, Surratt JD, Chan MN, Chan AWH, Hersey SP, Chhabra PS, et al. 2010. Chemical composition of gas- and aerosol-phase products from the photooxidation of naphthalene. J Phys Chem A 114:913–934.

Kishimoto T. 2003. Interleukin-6. In: The Cytokine Handbook, Chapter 12, fourth ed. (Thomson AW and Lotze MT, eds). London:Academic Press, 281–304.

Kleinman MT, Hamade A, Meacher D, Oldham M, Sioutas C, Chakrabarti B, et al. 2005. Inhalation of concentrated ambient particulate matter near a heavily trafficked road stimulates antigen-induced airway responses in mice. J Air Waste Manage Assoc 55:1277–1288.

Knaapen AM, Albrecht C, Becker A, Höhr D, Winzer A, Haenen GR, et al. 2002. DNA damage in lung epithelial cells isolated from rats exposed to quartz: Role of surface reactivity and neutrophilic inflammation. Carcinogenesis 23:1111–1120.

Koike E, Kobayashi T. 2006. Chemical and biological oxidative effects of carbon black nanoparticles. Chemosphere 65:946–951.

Kramer AJ, Rattanavaraha W, Zhang Z, Gold A, Surratt JD, Lin Y-H. 2016. Assessing the oxidative potential of isoprene-derived epoxides and secondary organic aerosol. Atmos Environ 130:211–218.

Kroll JH, Donahue NM, Jimenez JL, Kessler SH, Canagaratna MR, Wilson KR, et al. 2011. Carbon oxidation state as a metric for describing the chemistry of atmospheric organic aerosol. Nat Chem 3:133–139.

Kroll JH, Ng NL, Murphy SM, Flagan RC, Seinfeld JH. 2005. Secondary organic aerosol formation from isoprene photooxidation under high-NO_x conditions. Geophys Res Lett 32:18.

Kroll JH, Seinfeld JH. 2008. Chemistry of secondary organic aerosol: Formation and evolution of low-volatility organics in the atmosphere. Atmos Environ 42:3593–3624.

Kumagai Y, Koide S, Taguchi K, Endo A, Nakai Y, Yoshikawa T, et al. 2002. Oxidation of proximal protein sulfhydryls by phenanthraquinone, a component of diesel exhaust particles. Chem Res Toxicol 15:483–489.

Lambe AT, Onasch TB, Massoli P, Croasdale DR, Wright JP, Ahern AT, et al. 2011. Laboratory studies of the chemical composition and cloud condensation nuclei (CCN) activity of secondary organic aerosol (SOA) and oxidized primary organic aerosol (OPOA). Atmos Chem Phys 11:8913–8928.

Landreman AP, Shafer MM, Hemming JC, Hannigan MP, Schauer JJ. 2008. A macrophage-based method for the assessment of the reactive oxygen species (ROS) activity of atmospheric particulate matter (PM) and application to routine (daily-24 h) aerosol monitoring studies. Aerosol Sci Technol 42:946–957.

Li N, Hao MQ, Phalen RF, Hinds WC, Nel AE. 2003a. Particulate air pollutants and asthma — A paradigm for the role of oxidative stress in PM-induced adverse health effects. Clin Immunol 109:250–265.

Li N, Sioutas C, Cho A, Schmitz D, Misra C, Sempf J, et al. 2003b. Ultrafine particulate pollutants induce oxidative stress and mitochondrial damage. Environ Health Perspect 111:455–460.

Li N, Xia T, Nel AE. 2008. The role of oxidative stress in ambient particulate matter-induced lung diseases and its implications in the toxicity of engineered nanoparticles. Free Radic Biol Med 44:1689–1699.

Liao J, Froyd KD, Murphy DM, Keutsch FN, Yu G, Wennberg PO, et al. 2015. Airborne measurements of organosulfates over the continental US. J Geophys Res–Atmos 120:2990–3005.

Lim SS, Vos T, Flaxman AD, Danaei G, Shibuya K, Adair-Rohani H, et al. 2012. A comparative risk assessment of burden of disease and injury attributable to 67 risk factors and risk factor clusters in 21 regions, 1990–2010: A systematic analysis for the Global Burden of Disease Study 2010. Lancet 380:2224–2260.

Lin P, Yu JZ. 2011. Generation of reactive oxygen species mediated by humic-like substances in atmospheric aerosols. Environ Sci Tech 45:10362–10368.

Lin YH, Arashiro M, Martin E, Chen Y, Zhang Z, Sexton KG, et al. 2016. Isoprene-derived secondary organic aerosol induces the expression of oxidative stress response genes in human lung cells. Environ Sci Tech Lett 3:250–254.

Lin YH, Zhang Z, Docherty KS, Zhang H, Budisulistiorini SH, Rubitschun CL, et al. 2012. Isoprene epoxydiols as precursors to secondary organic aerosol formation: Acid-catalyzed reactive uptake studies with authentic compounds. Environ Sci Tech 46:250–258.

Lorentzen RJ, Lesko SA, McDonald K, Ts'o POP. 1979. Toxicity of metabolic benzo(a)pyrenediones to cultured cells

and the dependence upon molecular oxygen. Cancer Res 39:3194–3198.

Loza CL, Craven JS, Yee LD, Coggon MM, Schwantes RH, Shiraiwa M, et al. 2014. Secondary organic aerosol yields of 12-carbon alkanes. Atmos Chem Phys 14:1423–1439.

Lu Y, Su S, Jin W, Wang B, Li N, Shen H, et al. 2014. Characteristics and cellular effects of ambient particulate matter from Beijing. Environ Pollut 191:63–69.

Lund AK, Doyle-Eisele M, Lin YH, Arashiro M, Surratt JD, Holmes T, et al. 2013. The effects of alpha-pinene versus toluene-derived secondary organic aerosol exposure on the expression of markers associated with vascular disease. Inhal Toxicol 25:309–324.

Matsukawa Y, Lee VHL, Crandall ED, Kim K-J. 1997. Size-dependent dextran transport across rat alveolar epithelial cell monolayers. J Pharm Sci 86:305–309.

Matsunaga K, Klein TW, Friedman H, Yamamoto Y. 2001. Involvement of nicotinic acetylcholine receptors in suppression of antimicrobial activity and cytokine responses of alveolar macrophages to Legionella pneumophilainfection by nicotine. J Immunol 167:6518–6524.

Mbawuike IN, Herscowitz HB. 1989. MH-S, a murine alveolar macrophage cell line: Morphological, cytochemical, and functional characteristics. J Leukocyte Biol 46:119–127.

McDonald JD, Doyle-Eisele M, Campen MJ, Seagrave J, Holmes T, Lund A, et al. 2010. Cardiopulmonary response to inhalation of biogenic secondary organic aerosol. Inhal Toxicol 22:253–265.

McDonald JD, Doyle-Eisele M, Kracko D, Lund A, Surratt JD, Hersey SP, et al. 2012. Cardiopulmonary response to inhalation of secondary organic aerosol derived from gas-phase oxidation of toluene. Inhal Toxicol 24:689–697.

McWhinney RD, Badali K, Liggio J, Li S-M, Abbatt JPD. 2013a. Filterable redox cycling activity: A comparison between diesel exhaust particles and secondary organic aerosol constituents. Environ Sci Tech 47:3362–3369.

McWhinney RD, Zhou S, Abbatt JPD. 2013b. Naphthalene SOA: Redox activity and naphthoquinone gas-particle partitioning. Atmos Chem Phys 13:9731–9744.

Møller P, Jacobsen NR, Folkmann JK, Danielsen PH, Mikkelsen L, Hemmingsen JG, et al. 2009. Role of oxidative damage in toxicity of particulates. Free Radic Res 44:1–46.

Murray JI, Whitfield ML, Trinklein ND, Myers RM, Brown PO, Botstein D. 2004. Diverse and specific gene expression responses to stresses in cultured human cells. Molec Biol Cell 15:2361–2374.

Nah T, McVay RC, Pierce JR, Seinfeld JH, Ng NL. 2017. Constraining uncertainties in particle-wall deposition correction during SOA formation in chamber experiments, Atmos Chem Phys 17:2297–2310; https://doi.org/10.5194/acp-17-2297-2017.

Ng NL, Canagaratna MR, Jimenez JL, Chhabra PS, Seinfeld JH, Worsnop DR. 2011. Changes in organic aerosol composition with aging inferred from aerosol mass spectra. Atmos Chem Phys 11:6465–6474.

Ng NL, Canagaratna MR, Zhang Q, Jimenez JL, Tian J, Ulbrich IM, et al. 2010. Organic aerosol components observed in northern hemispheric datasets from aerosol mass spectrometry. Atmos Chem Phys 10:4625–4641.

Ng NL, Chhabra PS, Chan AWH, Surratt JD, Kroll JH, Kwan AJ, et al. 2007a. Effect of NO_x level on secondary organic aerosol (SOA) formation from the photooxidation of terpenes. Atmos Chem Phys 7:5159–5174.

Ng NL, Kroll JH, Chan AWH, Chhabra PS, Flagan RC, Seinfeld JH. 2007b. Secondary organic aerosol formation from *m*-xylene, toluene, and benzene. Atmos Chem Phys 7:3909–3922.

Nguyen TB, Roach PJ, Laskin J, Laskin A, Nizkorodov SA. 2011. Effect of humidity on the composition of isoprene photooxidation secondary organic aerosol. Atmos Chem Phys 11:6931–6944.

Oberdörster G. 1993. Lung dosimetry: Pulmonary clearance of inhaled particles. Aerosol Sci Technol 18:279–289.

Oberdörster G, Ferin J, Gelein R, Soderholm SC, Finkelstein J. 1992. Role of the alveolar macrophage in lung injury: Studies with ultrafine particles. Environ Health Perspect 97:193–199.

Pardo M, Shafer MM, Rudich A, Schauer JJ, Rudich Y. 2015. Single exposure to near roadway particulate matter leads to confined inflammatory and defense responses: Possible role of metals. Environ Sci Tech 49:8777–8785.

Philip M, Rowley DA, Schreiber H. 2004. Inflammation as a tumor promoter in cancer induction. Semin Cancer Biol 14:433–439.

Piccot SD, Watson JJ, Jones JW. 1992. A global inventory of volatile organic compound emissions from anthropogenic sources. J Geophys Res–Atmos 97:9897–9912.

Platt SM, Haddad IE, Pieber SM, Huang RJ, Zardini AA, Clairotte M, et al. 2014. Two-stroke scooters are a

dominant source of air pollution in many cities. Nature Comm 5:3749.

Pope CA III, Burnett RT, Thun MJ, Calle EE, Krewski D, Ito K, et al. 2002. Lung cancer, cardiopulmonary mortality, and long-term exposure to fine particulate air pollution. JAMA 287:1132–1141.

Pope CA III, Dockery DW. 2006. Health effects of fine particulate air pollution: Lines that connect. J Air Waste Manage Assoc 56:709–742.

Rattanavaraha W, Rosen E, Zhang H, Li Q, Pantong K, Kamens RM. 2011. The reactive oxidant potential of different types of aged atmospheric particles: An outdoor chamber study. Atmos Environ 45:3848–3855.

Robinson AL, Donahue NM, Shrivastava MK, Weitkamp EA, Sage AM, Grieshop AP, et al. 2007. Rethinking organic aerosols: Semivolatile emissions and photochemical aging. Science 315:1259–1262.

Robinson N, Hamilton J, Allan J, Langford B, Oram D, Chen Q, et al. 2011. Evidence for a significant proportion of secondary organic aerosol from isoprene above a maritime tropical forest. Atmos Chem Phys 11:1039–1050.

Rosenthal N, Brown S. 2007. The mouse ascending: Perspectives for human-disease models. Nat Cell Biol 9:993–999.

Saffari A, Daher N, Shafer MM, Schauer JJ, Sioutas C. 2013. Seasonal and spatial variation in reactive oxygen species activity of quasi-ultrafine particles ($PM_{0.25}$) in the Los Angeles metropolitan area and its association with chemical composition. Atmos Environ 79:566–575.

Saffari A, Daher N, Shafer MM, Schauer JJ, Sioutas C. 2014a. Global perspective on the oxidative potential of airborne particulate matter: A synthesis of research findings. Environ Sci Tech 48:7576–7583.

Saffari A, Daher N, Shafer MM, Schauer JJ, Sioutas C. 2014b. Seasonal and spatial variation in dithiothreitol (DTT) activity of quasi-ultrafine particles in the Los Angeles basin and its association with chemical species. J Environ Sci Health A Tox Hazard Subst Environ Eng 49:441–451.

Sankaran K, Herscowitz HB. 1995. Phenotypic and functional heterogeneity of the murine alveolar macrophage-derived cell line MH-S. J Leukoc Biol 57:562–568.

Sheng-Hann W, Chia-Wei L, Arthur C, Pei-Kuen W. 2010. Size-dependent endocytosis of gold nanoparticles studied by three-dimensional mapping of plasmonic scattering images. J Nanobiotechnology 8:33–45.

Slowik J, Brook J, Chang R-W, Evans G, Hayden K, Jeong C-H, et al. 2011. Photochemical processing of organic aerosol at nearby continental sites: Contrast between urban plumes and regional aerosol. Atmos Chem Phys 11:2991–3006.

Song C, Na K, Cocker DR. 2005. Impact of the hydrocarbon to NO_x ratio on secondary organic aerosol formation. Environ Sci Tech 39:3143–3149.

Spector AA, Yorek MA. 1985. Membrane lipid composition and cellular function. J Lipid Res 26:1015–1035.

Stirnweis L, Marcolli C, Dommen J, Barmet P, Frege C, Platt SM, et al. 2017. Assessing the influence of NO_x concentrations and relative humidity on secondary organic aerosol yields from α-pinene photo-oxidation through smog chamber experiments and modelling calculations, Atmos Chem Phys 17:5035–5061; https://doi.org/10.5194/acp-17-5035-2017.

Sullivan AP, Weber RJ. 2006. Chemical characterization of the ambient organic aerosol soluble in water: 1. Isolation of hydrophobic and hydrophilic fractions with a XAD-8 resin. J Geo Res 111, D05314, doi: 10.1029/2005JD006485.

Sung SY, Kubo H, Shigemura K, Arnold RS, Logani S, Wang R, et al. 2006. Oxidative stress induces ADAM9 protein expression in human prostate cancer cells. Cancer Res 66:9519–9526.

Surratt JD, Chan AWH, Eddingsaas NC, Chan M, Loza CL, Kwan AJ, et al. 2010. Reactive intermediates revealed in secondary organic aerosol formation from isoprene. Proc Natl Acad Sci USA 107:6640–6645.

Sutton HC, Winterbourn CC. 1989. On the participation of higher oxidation states of iron and copper in Fenton reactions. Free Radic Med 6:53–60.

Takao K, Miyakawa T. 2015. Genomic responses in mouse models greatly mimic human inflammatory diseases. Proc Natl Acad Sci USA 112:1167–1172.

Tang D, Shi Y, Kang R, Li T, Xiao W, Wang H, et al. 2007. Hydrogen peroxide stimulates macrophages and monocytes to actively release HMGB1. J Leukoc Biol 81:741–747.

Tao F, Gonzalez-Flecha B, Kobzik L. 2003. Reactive oxygen species in pulmonary inflammation by ambient particulates. Free Radic Biol Med 35:327–340.

Tasoglou A, Pandis SN. 2015. Formation and chemical aging of secondary organic aerosol during the β-caryophyllene oxidation. Atmos Chem Phys 15:6035–6046.

Terada H. 1990. Uncouplers of oxidative phosphorylation. Environ Health Perspect 87:213–218.

Tinoco AD, Valentine AM. 2005. Ti(IV) binds to human serum transferrin more tightly than does Fe(III). J Amer Chem Soc 127:11218–11219.

Tuet WY, Chen Y, Fok S, Champion JA, Ng NL. 2017a. Inflammatory responses to secondary organic aerosols (SOA) generated from biogenic and anthropogenic precursors. Atmos Chem Phys 17:11423–11440; doi.org/10.5194/acp-17-11423-2017.

Tuet WY, Chen Y, Fok S, Gao D, Weber RJ, Champion JA, Ng NL. 2017b. Chemical and cellular oxidant production induced by naphthalene secondary organic aerosol (SOA): Effect of redox-active metals and photochemical aging. Scientific Reports 7:15157; doi.org/10.1038/s41598-017-15071-8.

Tuet WY, Chen Y, Xu L, Fok S, Gao D, Weber RJ, et al. 2017c. Chemical oxidative potential of secondary organic aerosol (SOA) generated from the photooxidation of biogenic and anthropogenic volatile organic compounds. Atmos Chem Phys 17:839–853; doi.org/10.5194/acp-17-839-2017.

Tuet WY, Fok S, Verma V, Tagle Rodriguez MS, Grosberg A, Champion JA, et al. 2016. Dose-dependent intracellular reactive oxygen and nitrogen species (ROS/RNS) production from particulate matter exposure: comparison to oxidative potential and chemical composition. Atmos Environ 144:335–344.

Turner J, Hernandez M, Snawder JE, Handorean A, McCabe KM. 2015. A toxicology suite adapted for comparing parallel toxicity responses of model human lung cells to diesel exhaust particles and their extracts. Aerosol Sci Technol 49:599–610.

Uchida Y, Ohba K-I, Yoshioka T, Irie K, Muraki T, Maru Y. 2004. Cellular carbonyl stress enhances the expression of plasminogen activator inhibitor-1 in rat white adipocytes via reactive oxygen species-dependent pathway. J Biol Chem 279:4075–4083.

Van Krevelen D. 1950. Graphical-statistical method for the study of structure and reaction processes of coal. Fuel 29:269–284.

Verma V, Fang T, Guo H, King L, Bates JT, Peltier RE, et al. 2014. Reactive oxygen species associated with water-soluble $PM_{2.5}$ in the southeastern United States: Spatiotemporal trends and source apportionment. Atmos Chem Phys 14:12915–12930.

Verma V, Fang T, Xu L, Peltier RE, Russell AG, Ng NL, et al. 2015a. Organic aerosols associated with the generation of reactive oxygen species (ROS) by water-soluble $PM_{2.5}$. Environ Sci Tech 49:4646–4656.

Verma V, Ning Z, Cho AK, Schauer JJ, Shafer MM, Sioutas C. 2009. Redox activity of urban quasi-ultrafine particles from primary and secondary sources. Atmos Environ 43:6360–6368.

Verma V, Rico-Martinez R, Kotra N, King L, Liu JM, Snell TW, et al. 2012. Contribution of water-soluble and insoluble components and their hydrophobic/hydrophilic subfractions to the reactive oxygen species-generating potential of fine ambient aerosols. Environ Sci Tech 46:11384–11392.

Verma V, Shafer MM, Schauer JJ, Sioutas C. 2010. Contribution of transition metals in the reactive oxygen species activity of PM emissions from retrofitted heavy-duty vehicles. Atmos Environ 44:5165–5173.

Verma V, Wang Y, El-Afifi R, Fang T, Rowland J, Russell AG, et al. 2015b. Fractionating ambient humic-like substances (HULIS) for their reactive oxygen species activity — Assessing the importance of quinones and atmospheric aging. Atmos Environ 120:351–359.

Visentin M, Pagnoni A, Sarti E, Pietrogrande MC. 2016. Urban $PM_{2.5}$ oxidative potential: Importance of chemical species and comparison of two spectrophotometric cell-free assays. Environ Pollut 219:72–79.

Vivanco MG, Santiago M. 2010. Secondary organic aerosol formation from the oxidation of a mixture of organic gases in a chamber. In: Air Quality (Ashok Kumar, ed.). InTech, doi: 10.5772/9761. Available from: *www.Intechopen.Com/books/air-quality/secondary-organic-aerosols-experiments-in-an-outdoor-chamber-.*

Wang D, Pakbin P, Shafer MM, Antkiewicz D, Schauer JJ, Sioutas C. 2013. Macrophage reactive oxygen species activity of water-soluble and water-insoluble fractions of ambient coarse, $PM_{2.5}$ and ultrafine particulate matter (PM) in Los Angeles. Atmos Environ 77:301–310.

Wang H, Czura C, Tracey K. 2003. Tumor necrosis factor. In: The Cytokine Handbook, Chapter 35. Fourth edit. (Thomson AW and Lotze MT, eds.), pp. 837–860. Academic Press, London. 4:837–860.

Weichenthal SA, Lavigne E, Evans GJ, Godri Pollitt KJ, Burnett RT. 2016. Fine particulate matter and emergency room visits for respiratory illness. Effect modification by oxidative potential. Amer J Respir Crit Care Med 194:577–586.

Wiseman H, Halliwell B. 1996. Damage to DNA by reactive oxygen and nitrogen species: Role in inflammatory disease and progression to cancer. Biochem J 313:17–29.

Wong JPS, Lee AKY, Abbatt JPD. 2015. Impacts of sulfate seed acidity and water content on isoprene secondary organic aerosol formation. Environ Sci Tech 49:13215–13221.

Xu L, Guo H, Boyd CM, Klein M, Bougiatioti A, Cerully KM, et al. 2015a. Effects of anthropogenic emissions on aerosol formation from isoprene and monoterpenes in the southeastern United States. Proc Natl Pr Acad Sciences 112:37–42.

Xu L, Kollman MS, Song C, Shilling JE, Ng NL. 2014. Effects of NO_x on the volatility of secondary organic aerosol from isoprene photooxidation. Environ Sci Tech 48:2253–2262.

Xu L, Suresh S, Guo H, Weber RJ, Ng NL. 2015b. Aerosol characterization over the southeastern United States using high-resolution aerosol mass spectrometry: Spatial and seasonal variation of aerosol composition and sources with a focus on organic nitrates. Atmos Chem Phys 15:7307–7336.

Yang A, Janssen NAH, Brunekreef B, Cassee FR, Hoek G, Gehring U. 2016. Children's respiratory health and oxidative potential of $PM_{2.5}$: The PIAMA birth cohort study. Occup Environ Med 73(3):154–160.

Yang A, Jedynska A, Hellack B, Kooter I, Hoek G, Brunekreef B, et al. 2014. Measurement of the oxidative potential of $PM_{2.5}$ and its constituents: The effect of extraction solvent and filter type. Atmos Environ 83:35–42.

Yoo E, Crall BM, Balakrishna R, Malladi SS, Fox LM, Hermanson AR, et al. 2013. Structure–activity relationships in Toll-like receptor 7 agonistic 1*H*-imidazo [4, 5-*c*] pyridines. Org Biomol Chem 11:6526–6545.

Zhang J, Doshi U, Suzuki A, Chang C-W, Borlak J, Li AP, et al. 2016. Evaluation of multiple mechanism-based toxicity endpoints in primary cultured human hepatocytes for the identification of drugs with clinical hepatotoxicity: Results from 152 marketed drugs with known liver injury profiles. Chem Bio Inter 255:3–11.

Zhang J, Stanley RA, Adaim A, Melton LD, Skinner MA. 2006. Free radical scavenging and cytoprotective activities of phenolic antioxidants. Mol Nut Food Res 50:996–1005.

Zhang Q, Jimenez JL, Canagaratna MR, Allan JD, Coe H, Ulbrich I, et al. 2007. Ubiquity and dominance of oxygenated species in organic aerosols in anthropogenically-influenced northern hemisphere midlatitudes. Geophys Res Lett 34:L13801.

MATERIALS AVAILABLE ON THE HEI WEBSITE

The Additional Materials (Appendices A through F) contain supplemental material not included in the printed report. These can be found on the HEI website at *www.healtheffects.org/publications.*

Additional Materials 1: Appendix A. Ambient Sample Analysis

Additional Materials 2: Appendix B. Cellular Assay Optimization

Additional Materials 3: Appendix C. Chamber Sample Analysis

Additional Materials 4.1: Appendix D.1. Dose–Response Curves and Metrics for Ambient Samples

Additional Materials 4.2: Appendix D.2. Dose–Response Curves and Metrics for SOA Samples

Additional Materials 5: Appendix E. Dithiothreitol Consumption for All Samples

Additional Materials 6: Appendix F. Chamber Reaction Profiles

ABOUT THE AUTHORS

Nga L. Ng received her Ph.D. in chemical engineering from California Institute of Technology in 2007. Ng is currently an associate professor in the School of Chemical and Biomolecular Engineering at Georgia Institute of Technology. She also holds a joint appointment in the School of Earth and Atmospheric Sciences.

Wing Y. Tuet received her B.S. in chemical engineering from the University of Texas–Austin in 2013. Tuet is currently a doctoral candidate in the School of Chemical and Biomolecular Engineering at Georgia Institute of Technology.

Yunle Chen received her B.S. in chemistry from Fudan University in 2014. Chen is currently a graduate student in the School of Materials Science and Engineering at Georgia Institute of Technology.

Shierly Fok was an undergraduate student in the School of Chemical and Biomolecular Engineering at Georgia Institute of Technology. Fok received her B.S. in 2017.

Dong Gao received her B.S. in environmental engineering from Sun Yat-sen University in 2014. Gao is currently a graduate student in the School of Civil and Environmental Engineering at Georgia Institute of Technology.

Marlen S. Tagle Rodriguez received her B.S. in biomedical engineering from the University of California–Irvine in 2017.

Mitchel Klein received his Ph.D. from Emory University in 1998. Klein is currently a research assistant professor in the Rollins School of Public Health at Emory University. He also holds a joint appointment in the Department of Environmental Health and the Department of Epidemiology.

Anna Grosberg received her Ph.D. in bioengineering from California Institute of Technology in 2008. Grosberg is currently an assistant professor in the Department of Biomedical Engineering at the University of California–Irvine. She also holds a joint appointment in the Department of Chemical Engineering and Materials Science

Rodney J. Weber received his Ph.D. in mechanical engineering from the University of Minnesota in 1995. Weber is currently a professor in the School of Earth and Atmospheric Sciences at Georgia Institute of Technology.

Julie A. Champion received her Ph.D. in chemical engineering from the University of California–Santa Barbara in 2007. Champion is currently an associate professor in the School of Chemical and Biomolecular Engineering at Georgia Institute of Technology.

OTHER PUBLICATIONS RESULTING FROM THIS RESEARCH

Tuet WY, Chen Y, Xu L, Fok S, Gao D, Weber RJ, et al. 2017. Chemical and cellular oxidant production induced by naphthalene secondary organic aerosol (SOA): Effect of redox-active metals and photochemical aging. Sci Rep 7:15157.

Tuet WY, Chen Y, Xu L, Fok S, Gao D, Weber RJ, et al. 2017. Chemical oxidative potential of secondary organic aerosol (SOA) generated from the photooxidation of biogenic and anthropogenic volatile organic compounds. Atmos Chem Phys 17:839–853.

Tuet WY, Chen Y, Fok S, Champion JA, Ng NL. 2017. Inflammatory responses to secondary organic aerosols (SOA) generated from biogenic and anthropogenic precursors. Atmos Chem Phys 17:11423–11440.

Tuet WY, Fok S, Verma V, Tagle Rodriguez MS, Grosberg A, Champion JA, et al. 2016. Dose-dependent intracellular reactive oxygen and nitrogen species production from particulate matter exposure: Comparison to oxidative potential and chemical composition. Atmos Environ 144:335–344.

Research Report 197, *Cellular and Acellular Assays for Measuring Oxidative Stress Induced by Ambient and Laboratory-Generated Aerosols*, N.L. Ng et al.

INTRODUCTION

A large number of epidemiological studies have reported associations between increases in exposure to ambient particulate matter (PM*) and higher rates of mortality and hospitalization. It has been hypothesized that the common pathophysiological mechanism underlying the effects of PM is through the enhancement of reactions between reactive oxygen species (ROS) on the particles and lung cells. These reactions could lead to the cellular production of biomarkers of oxidative stress, which in turn could trigger inflammatory responses in both the lung and the circulatory system. ROS are derivatives of oxygen that are more reactive than molecular oxygen and are also referred to as *oxygen radicals*. Research has demonstrated oxidant generation by particles in acellular systems as well as by cellular components in cellular assays (Ghio et al. 2012). However, a clear correlation between in vitro responses and responses in humans has not been established.

Particles in the atmosphere are distinguished based on their source and formation mechanism: primary particles are emitted directly from the source (such as combustion of fossil fuels or biomass burning), and secondary aerosol particles are formed either by gas-to-particle conversion of inorganic gases (for example, SO_2 and NO_2) or from photooxidation of volatile and semivolatile organic compounds (VOCs) in the atmosphere. These reactions form products of low volatility that partition into the condensed phase and are referred to as secondary organic aerosol (SOA) (Hallquist et al. 2009; Kroll and Seinfeld 2008). Although SOA represents an important component of ambient PM, research on its effect on ROS production has been limited.

Dr. Nga Lee (Sally) Ng of the Georgia Institute of Technology submitted a proposal titled "Laboratory chamber and field study characterization of the composition and oxidative properties of particulate matter mixtures: Effects of particle physical state, acidity, and transition metals" in response to HEI Request for Applications 13-2: Walter A. Rosenblith New Investigator Award. In her application to HEI, Ng proposed to explore the link between key chemical and physical properties of particles and their oxidative properties with a focus on SOA using an in vitro approach.

The Rosenblith Award was established to provide support for an outstanding new investigator at the assistant professor level to conduct research in the area of air pollution and health and is unrestricted with respect to the topic of research.

This Critique provides the HEI Review Committee's evaluation of the study. It is intended to aid the sponsors of HEI and the public by highlighting both the strengths and limitations of the study and by placing the Investigators' Report into scientific perspective.

BACKGROUND

SECONDARY ORGANIC AEROSOL FORMATION

Air pollution includes a large number of VOCs emitted from both anthropogenic and biogenic sources. In the atmosphere, they undergo oxidation–reduction (redox) reactions initiated by ozone and various radicals that lead to their transformation and degradation. A radical is a chemical species that has lost an electron (so that it has one unpaired electron) due to oxidation; as such, radicals are very reactive and initiate the transformation of organic compounds either by extracting hydrogen or by adding a double bond.

The hydroxyl radical (•OH) is the most important oxidant in the atmosphere and is involved in a large number of oxidation reactions (Mather et al. 1997). Other important atmospheric oxidants that participate in the degradation of VOCs are the nitrate radical (NO_3•) and ozone (O_3) (Hallquist et al. 2009; Kroll and Seinfeld 2008).

The most studied pathways of VOC degradation in the atmosphere are those initiated by their reaction with •OH and NO_3• radicals and O_3. The initial attack of the radical

Dr. Nga L. Ng's 3-year study, "Laboratory chamber and field study characterization of the composition and oxidative properties of particulate matter mixtures: Effects of particle phase state, acidity and transition metals," began in March 2014. Total expenditures were $437,354. The draft Investigators' Report from Ng and colleagues was received for review in August 2017. A revised report, received in January 2018, was accepted for publication in June 2018. During the review process, the HEI Review Committee and the investigators had the opportunity to exchange comments and to clarify issues in both the Investigators' Report and the Review Committee's Critique.

* A list of abbreviations and other terms appears at the end of this volume.

on R (R indicates the VOC molecule) in the presence of oxygen and sunlight yields the peroxy radical RO_2•, which plays a central role in the production of subsequent products. The SOA yield of this reaction depends on the NO_x level, with yields generally decreasing as NO_x increases (Kroll and Seinfeld 2008). The mechanisms by which NO_x influences the yield of SOA is related to fate of RO_2•. At high NO_x, RO_2• reacts with NO, forming organic nitrate ($RONO_2$) and an alkoxy radical (RO•), which generally fragments or reacts with O_2. At low NO_x, RO_2• reacts with the hydroxyperoxyl radical •OH_2 to produce hydroperoxide (ROOH), which can be quite low in volatility and is a major component of SOA. The chemistry involving the formation of SOA is complex and still not well understood; it depends on many other factors, such as temperature and humidity, seed aerosol composition, and NO_x levels (see Critique Figure).

SOA is an important component of atmospheric particulate matter that influences climate, air quality, and human health (Carslaw et al. 2013; Hallquist et al. 2009). Field and modeling studies suggest that, on a global scale, SOA from biogenic VOCs is more abundant than SOA from anthropogenic VOCs (Henze et al. 2008). Biogenic VOCs, such as isoprene and monoterpenes, are key precursors for global SOA formation owing to their larger emissions and higher reactivity with atmospheric oxidants compared with anthropogenic VOCs (Hodzic et al. 2016). They are also thought to be important precursors in many regions of the United States, especially the Southeast (Xu et al. 2015). Among anthropogenic VOCs, aromatic compounds have been traditionally considered to be the most important SOA precursors (Henze et al. 2008), but there is growing evidence that the photo-oxidation of lower volatility alkanes and other classes of compounds also generates SOA (Robinson et al. 2007).

In many areas of the United States, SOA contributes a substantial fraction of atmospheric fine PM, one of the criteria pollutants whose maximum levels are set through the National Ambient Air Quality Standards for PM with an aerodynamic diameter ≤ 2.5 µm ($PM_{2.5}$). Thus, understanding its possible mechanisms of action is relevant to the broader understanding of the effects of PM.

MEASUREMENT OF PM OXIDATIVE POTENTIAL AND OXIDATIVE STRESS

Several chemical and cellular assays have been developed to measure the production of ROS induced by exposure to particles (for a recent review, see Hedayat et al. 2015). The ability of PM to generate ROS and chemically oxidize target molecules in non-cellular systems is referred to as *oxidative potential*. A commonly used chemical assay to quantify the oxidative potential of PM is the dithiothreitol (DTT) assay, which is based on the oxidation of DTT to its disulfide form. The rate of DTT consumption is used as a measure of the concentration of redox species in the extract but does necessarily reflect the capacity of the extract to induce production of ROS in cells.

The capacity of PM to induce cells to generate ROS intracellularly is generally referred to as *oxidative stress*. Oxidative stress is a biochemical imbalance that occurs when the generation of ROS exceeds the natural antioxidant capacity of the cells (Nel 2005). Ambient aerosols may lead to oxidative stress by transporting ROS on particles into the respiratory system or introducing aerosol components (such as metals and organic compounds [Ghio et al. 2012; Miller et al. 2012]) that are capable of stimulating cellular generation

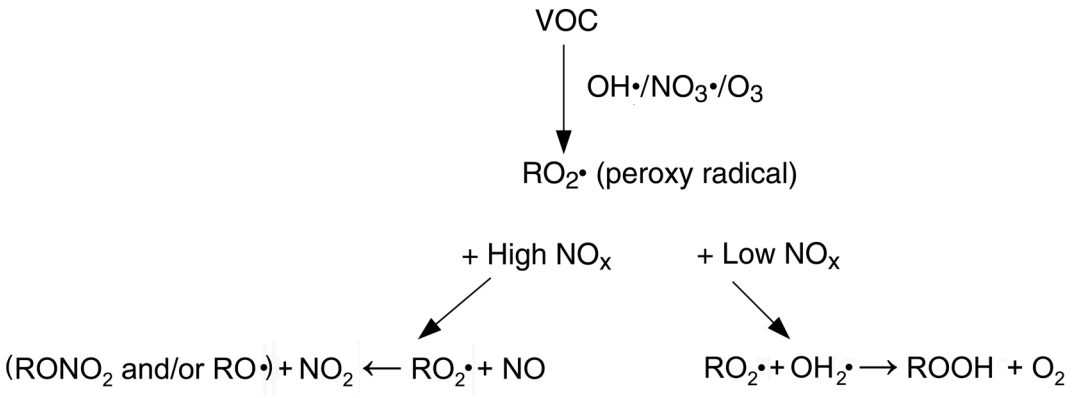

Critique Figure. Simplified schematic showing the chemistry of SOA formation in the presence of high and low NO_x. R represents the molecule from VOC.

of ROS. The resulting oxidative stress is thought to be an important underlying mechanism of action by which exposure to PM may lead to inflammation and adverse health effects (Delfino et al. 2013; Miller et al. 2012).

Cellular assays to measure intracellular production of ROS in response to PM have utilized primarily cell lines of macrophages or epithelial cells derived from humans or rodents. In some studies, cultures of human bronchial epithelial cells obtained from biopsies were used (e.g., Volckens et al. 2009). However, the most common approach for delivering the particles to the cells has been to use soluble extracts of the particles collected on filters. This approach has limitations because the extracts do not include many components present in ambient aerosols and because the method of PM delivery does not reflect human inhalation exposures. On the other hand, it has been widely considered a practical approach to test mechanistic hypotheses. Because the chemical and the cellular assays measure different aspects of oxidative activity, there is no expectation that the assays would be correlated (Hu et al. 2008).

AIMS

The overall objective of Dr. Ng's study was to characterize and compare the oxidative properties of ambient PM and different types of laboratory-generated SOA using in vitro assays.

The specific aims were as follows:

1. Develop a cellular assay for measuring ROS production resulting from PM exposure.
2. Elucidate PM constituents associated with ROS production and determine whether results from chemical assays were representative of the DTT chemical assay.
3. Provide a perspective on the relative toxicities of SOA generated from biogenic and anthropogenic precursors under different conditions (high and low humidity, high and low NO_x, and presence of a redox-active metal), and determine whether there are correlations between chemical composition and cellular responses.
4. Investigate the effects of photochemical aging processes on SOA toxicity.

STUDY DESIGN AND METHODS

Dr. Ng studied the oxidative potential of ambient PM and laboratory-generated SOA and its ability to induce the production of ROS using a chemical assay and a cellular assay. Dr. Ng refers to the oxidant species formed as "reactive oxygen and reactive nitrate species (ROS/RNS)" to include reactive nitrogen species, which can be formed in biological systems from endogenous NO (Patel et al. 1999). In this Critique we will use "ROS" to refer to all oxidant species.

COLLECTION AND PREPARATION OF PARTICLES

Ambient PM samples were collected at different locations on quartz filters between June 2012 and October 2013 as part of the U.S. EPA's Southeastern Center for Air Pollution and Epidemiology (SCAPE) study. All samples were collected during a 24-hour period over multiple days at a constant sampling rate.

SOA was generated from six VOCs (*m*-xylene, naphthalene, pentadecane, isoprene, α-pinene, and β-caryophyllene) in the Georgia Tech environmental chamber in the presence of an OH precursor created by photolyzing either hydrogen peroxide [H_2O_2] for low NO_2 conditions or nitrous acid [HONO] for high NO_2 conditions. The experiments were performed in the presence of ammonium sulfate as a seed aerosol, which acts as substrate onto which the semivolatile products may condense (Ng et al. 2007). In some experiments using naphthalene as the SOA precursor, iron-containing particles were used as seed. Experiments were performed using different concentrations of the six VOCs to strike a balance between typical ambient concentrations and adequate SOA mass for cellular exposure experiments. The air was sampled from the chamber at a constant rate, but the total volume of air sampled from the chamber (and passed through the filter) varied across the different types of SOA (see Appendix Table C.2, available on the HEI website, for details).

The particles were extracted from the filters in water for the chemical assay and in cell culture medium supplemented with 10% fetal bovine serum for the cellular assay. Ambient PM extracts were analyzed for water-soluble organic compounds (WSOCs), brown carbon (BrC), and elements, and used in the assays described below. Bulk SOA composition was measured by mass spectrometry for determination of elemental ratios (O:C, H:C, and N:C).

ENDPOINTS MEASURED

Oxidative Potential (DTT Assay)

For this assay, extracts were added to the DTT solution, and DTT consumption was measured over a period of approximately 1 hour. The DTT activity was reported as pmoles per minute per μg of PM. The PM extract concentrations used in the assays were not reported. These assays

were conducted as part of a previous study (Fang et al. 2015; Verma et al 2014).

ROS Production (C-DCFH Assay)

ROS production was measured in a murine alveolar macrophage cell line using the non-fluorescent carboxy-2′,7′-dichlorohydrofluorescein-diacetate (C-H_2DCFDA) probe. The probe diffuses from the medium into the cells, where it undergoes a de-esterification reaction to carboxy-2′,7′-dichlorohydrofluorescein (C-DCFH) that renders the compound impermeable to cell membranes. Following its reaction with ROS generated in the cells, C-DCFH turns into a fluorescent product, carboxy-2′,7′-dichlorofluorescein (C-DCF). This assay will be referred to as C-DCFH (to distinguish it from the more common assay that uses dichlorodihydrofluorescein [DCFH] [Kalyanaramana et al. 2012]). The probe was added to the cells and incubated for 40 minutes. At the end of this period the probe remaining in solution was removed, and the cells were exposed to the filter extracts for 24 hours. The amount of C-DCF formed was measured using a fluorescence plate reader. Each PM and SOA extract was sequentially added in amounts between 0.01 μg and 10 μg to develop a dose–response curve. Parameters such as the initial cell density, the probe concentration, and the sample incubation times were optimized using positive and negative controls prior to starting the experiments with the ambient PM and SOA extracts.

To account for possible changes in cell viability after exposure, the investigators corrected the fluorescence response by the metabolic activity. Metabolic activity was evaluated at the end of the 24-hour exposure period by spectrophotometrically measuring the reduction of 3-[4,5-dimethylthiazol-2-yl]-2,5-diphenyl tetrazolium bromide (MTT) during an additional 4 hours of culture. MTT is a water-soluble yellow dye that is readily taken up by viable cells and metabolized by mitochondrial enzymes to its blue formazan derivative. The production of the formazan has been shown to be directly proportional to the number of living cells present during the exposure (Sylvester 2011). This assay was added during the course of the study, after the experiments with the ambient PM had been completed, so only the results of the SOA assays were corrected. A subset of the ambient PM samples was also tested for MTT, but these results are not included in the report (see Tuet et al. 2016).

Production of Inflammatory Mediators

In the experiments in which macrophages were exposed to SOA extract, the investigators also measured tumor necrosis factor-α (TNF-α) and interleukin-6 (IL-6) (markers of inflammation) by enzyme-linked immunosorbent assay at the end of the 24-hour exposure period.

DATA ANALYSIS

Dr. Ng analyzed the dose–response curves for the cellular response using the Hill equation, which is generally used to describe the binding of a ligand to a receptor. From the Hill curve, the investigators calculated various dose metrics: the threshold (the concentration at which the response is 10% above the baseline), the EC_{50} (the effective concentration at which the response was 50% of the maximum), the maximum response, the area under the curve (AUC), and the Hill slope (the rate at which the maximum response is attained once a response is observed). Ultimately, only the AUC response was reported because they observed no associations with any of the other response metrics (see below). The results of the assays were normalized to the mass of PM in the extract (intrinsic measure) or to the volume of air that passed through the filter (extrinsic measure). The authors used a linear regression method and calculated Pearson correlation coefficients to determine the strength of the associations. Statistical significance was determined using Monte Carlo simulations.

SUMMARY OF KEY RESULTS

AMBIENT PM SAMPLES

Extracts of ambient PM caused an increase in ROS production relative to controls in the C-DCFH assay. There was a correlation between the extrinsic ROS production (AUC) and the concentrations of WSOC, BrC, iron, and titanium for the samples collected in summer. There was a significant correlation between the DTT activity and intracellular ROS production (based on both the extrinsic and the intrinsic AUC) for the summer samples (R = 0.63 and R = 0.79, respectively), but not for samples collected in winter (R = 0.01 and R = 0.39).

CHAMBER-GENERATED SECONDARY ORGANIC AEROSOLS

The investigators found that extracts of SOA formed from naphthalene had the highest oxidative potential (DTT assay), whereas isoprene had the lowest. SOA formed from the other five precursors also had low activity. The effect of changes in chamber composition (e.g., NO_x concentration, relative humidity, and temperature) was small, with the

exception of naphthalene-derived SOA (see Figure 8A in the Investigators' Report).

As observed in the DTT assay, extract from naphthalene-derived SOA induced the highest ROS production in the C-DCFH assay. The other SOA extracts induced a lower response, with isoprene-derived SOA yielding the lowest response. There was some variation in the effect of chamber condition on ROS production across the types of SOA, but no clear pattern.

Extracts of naphthalene-derived SOA also yielded the largest range in inflammatory responses for most chamber conditions. Extracts of SOA formed from α-pinene and *m*-xylene elicited moderate inflammatory responses, whereas SOA from β-caryophyllene and pentadecane elicited IL-6 responses that spanned a much larger range than the TNF-α and ROS responses. Isoprene induced low levels of inflammatory response across all chamber conditions. The investigators noted that "several patterns can be distinguished for SOA precursors whose photo-oxidation products have similar carbon-chain length and chemical functionality."

The correlation between ROS production and inflammatory response was not investigated.

EFFECT OF NAPHTHALENE-DERIVED SECONDARY ORGANIC AEROSOL GENERATED USING IRON SULFATE SEED

Extracts of SOA generated from naphthalene in the presence of iron sulfate had similar oxidative potential (DTT assay) to extracts of SOA generated in the presence of ammonium sulfate as seed (shown in Figure 11 of the Investigators' Report). However, in the macrophage assay (also shown in Figure 11), extracts of SOA formed in the presence of iron sulfate appeared to induce a slightly higher ROS response than extracts of SOA formed in the presence of ammonium sulfate, but it is not clear whether these differences were statistically significant. In separate experiments with iron seed alone, the investigators determined that it contributed 2% to 12% of the total response, leading them to conclude that higher carbon oxidation state may also be responsible for the effect.

EFFECT OF SECONDARY ORGANIC AEROSOL CARBON OXIDATION STATE

The oxidation state of the SOA formed from the different anthropogenic and biogenic precursors was derived from elemental ratios of O:C and H:C measured during each experiment. The investigators reported that there was a significant positive correlation between ROS production and carbon oxidation state ($R = 0.64$) as shown in Figure 12. However, no correlation was observed between oxidation state and cytokine levels (see Appendix Figure C.3) or between oxidation state and oxidative potential (see Appendix Figure C.7).

COMPARISON OF OXIDATIVE POTENTIAL AND ROS PRODUCTION FOR ALL PM EXTRACTS

The investigators compared the oxidative potential and ROS response for extracts from ambient PM and SOA (see Figure 12 in the Investigators' Report). They concluded that "with the exception of naphthalene SOA…, the oxidative potentials of all SOA systems investigated were comparable to those observed in the ambient aerosol samples" and that "for ROS/RNS production, SOA systems induced comparable or higher levels of ROS/RNS compared with the levels induced by ambient aerosol samples." The investigators did not provide any tables summarizing these results quantitatively. Taking the ambient PM and SOA results together, the investigators found that "no simple trend was observed between chemical and cellular assay results for both ambient and laboratory-generated aerosol."

HEI REVIEW COMMITTEE EVALUATION

In its independent review of the study, the HEI Review Committee thought that the study addressed an important question, namely, whether components or characteristics of PM influence ROS generation differently in an acellular versus a cellular assay. This was an ambitious multidisciplinary project. The Review Committee was glad to see that the investigator of this study, Dr. Nga (Sally) Ng, who is trained in atmospheric chemistry, undertook an investigation that spanned both her field and toxicology. A strength of this study was the use of both ambient PM (which included primary particles and SOA) and SOA generated from photochemical reactions of selected VOCs in an environmental chamber across a range of atmospherically relevant conditions. Additionally, Dr. Ng tested the toxicological characteristics of the reaction products in both a chemical and a cellular assay, another important strength of her work.

However, the use of aqueous extracts of particles collected on filters and resuspended in aqueous solution, while less complex and more practical than a flow-through system, limits the ability to translate the findings to real-world situations. The use of an immortalized cell line and submerged cell cultures also limits the interpretation of this work from a biological standpoint.

The investigators conducted a systematic comparison of different aerosols' ability to generate ROS in the two assays. In the C-DCFH cellular assay, for every extract of ambient PM and SOA, the investigators tested a range of concentrations, because the initial results showed that each sample had a different dose–response curve. This is an important finding that highlights the need to test multiple doses. The investigators derived various response metrics from the dose–response curves using the Hill equation: maximum response, minimum response, EC_{50} (50% response), slope of the curve, and AUC (reported in Appendix D). Because significant associations between the DTT and the C-DCFH assays were observed only for AUC, the investigators focused on this metric alone. The Review Committee noted, however, that the Hill equation describes the binding of a ligand to a receptor and may not be appropriate to describe ROS formation. The Committee was also concerned that the choice of which response metric to report — namely, AUC — appeared to be driven by the results, limiting the confidence in the results.

The Review Committee commented that deriving intrinsic and extrinsic AUC metrics could be helpful, because the extrinsic metric accounts for the PM concentration in the air that was sampled. However, in order for the extrinsic normalization to be meaningful, the flow rates and collection times must be constant, so that the total volume of air passing through each filter is the same for all the samples. For the ambient PM filters, the total volume of air sampled was constant; however, for the SOA filters, the volume of air differed across the filters (as can be seen in Table C.2 in Appendix C, available on the HEI website). Therefore, the investigators reported only the intrinsic AUC for the SOA extracts in the report (the extrinsic values can be found in Appendix D).

Regarding the statistical approach, the Committee noted that the Monte Carlo approach was not well enough defined to comment on.

AMBIENT PM EXPERIMENTS

The Committee agreed with the investigators' conclusion that there was an association between both intrinsic and extrinsic oxidative potential (DTT assay) and ROS response (C-DCFH assay) for ambient PM collected in summer, but not for PM collected in winter. However, the Committee noted that the DTT assay was conducted as part of an earlier study (Fang et al. 2015; Verma et al. 2014), which showed that the intrinsic DTT activity (and for some sites also the extrinsic activity) of PM samples collected at various sites was higher in winter than in summer (Fang et al. 2015). Therefore, the Committee found the results in this report showing a correlation between DTT and ROS responses in summer samples difficult to interpret and was not convinced that the DTT assay could serve as "a screening tool" for cellular responses associated with PM exposure.

The Committee agreed that some constituents of summer PM (WSOC, BrC, iron, and titanium), but not of winter PM, were correlated with increased extrinsic ROS production in the C-DCFH assay. Because there are seasonal differences in source contributions, the investigators' hypothesis that seasonal variability in composition may be associated with different cellular responses is reasonable and consistent with other studies. For example, one study of alveolar macrophages exposed to an extract of fine PM from the Denver area showed that ROS production was highest in samples collected during the summer months (Prasch Landreman et al. 2008). Michael and colleagues (2013) showed that urban traffic PM and rural PM induced different toxicological responses. The evidence for a role of metals — and iron in particular — as well as organic compounds in this study is also in agreement with the results of other studies (Delfino et al. 2013; Ghio et al. 2012; Hu et al. 2008; Prasch Landreman et al. 2008).

SECONDARY ORGANIC AEROSOL EXPERIMENTS

The Review Committee thought that the use of SOA generated from six organic compounds emitted by anthropogenic and biogenic sources was novel and an important strength of this study. The Committee agreed with the investigators that naphthalene elicited the largest intrinsic response in both the DTT and C-DCFH assays under different chamber conditions and also the highest inflammatory response. Isoprene had the lowest DTT activity. For the other compounds, the DTT activities were low and similar to each other. The Committee agreed that, although there was more variability in the ROS and inflammatory responses than in the DTT across the SOA extracts, and the chamber conditions (high and low NO_x and high and low humidity) influenced the ROS response to some extent, there was no clear trend for either precursor identity or formation conditions. The Committee thought that the investigators' interpretation that different inflammatory response patterns were related to the structure and functionalities of the SOA was reasonable. The Committee also agreed with the investigators that a high ROS production was not always associated with a high production of inflammatory mediators. Regarding the correlation between the DTT and the C-DCFH assays, the Committee was not convinced that there was an exponential trend because the results seemed to be driven by the naphthalene SOA extract.

The Committee agreed that naphthalene SOA extract generated in the presence of iron sulfate seed did not differ in its DTT activity compared with SOA generated in the presence of ammonium sulfate. Although the Committee thought that the results of the C-DCFH assay were suggestive of a greater effect on the ROS response of iron sulfate SOA, it did not think that (based on experiments with high NO_x and high humidity — conditions that were not used in any of the other experiments) they convincingly showed a clear association.

Regarding the correlation between SOA carbon oxidation state and oxidative properties in the C-DCFH assay, the Committee thought that the result was intriguing, but may have been confounded by the solubility of the aerosol in water (which would be correlated with the average carbon oxidation state).

OVERALL COMMENTS

The Review Committee thought that Ng and colleagues conducted a comprehensive study of the oxidative potential and ROS cellular response associated with both ambient PM and chamber-generated SOA that produced a large data set. However, because the results are based on only one response metric out of several that were calculated, caution should be exercised in interpretation of the results.

The Committee agreed that, overall, the results indicate that both ambient PM and SOA have oxidative potential and the ability to induce ROS production. Within the SOA tested, naphthalene-derived SOA induced the largest effects. The results of this study are in agreement with results reported by others using various types of PM (see, for example, Charrier and Anastasio 2012; Ghio et al. 2012; Hu et al. 2008; McWhinney et al. 2013; and Saffari et al. 2014). The Committee agreed that a relation between the DTT and the C-DCFH results for the ambient PM was observed for the summer samples but did not think the data and the analyses presented were sufficient to make the assertion that the DTT could be used as a screening tool. For the laboratory-generated SOA samples, the Committee thought that the correlation was likely driven by SOA produced by one precursor, namely, naphthalene, and thus not generalizable.

Only a few studies have quantified the correlation between different assays of oxidative activity. Li and colleagues (2003) found a good correlation ($R = 0.97$) between the DTT assay and the expression of heme oxygenase (a marker of oxidative stress) in two cell lines for combined extracts of ultrafine, fine, and coarse PM (collected at two sites in the Los Angeles area using particle concentrators). The same group of researchers (Hu et al. 2008) found a significant correlation ($R = 0.61$) between the DTT and the C-DCFH assays for extracts of size-fractionated ambient PM collected at four sites in the Los Angeles–Long Beach port area, with quasi-ultrafine particles having the highest activity; these results led the authors to conclude that both assays may be driven, at least in part, by variations in the concentration of similar compounds. Because the chemical and cellular assays measure different aspects of oxidative activity, a correlation should not necessarily be expected.

In this study, the experiments with SOA also show that ROS production is accompanied by production of inflammatory mediators, with naphthalene having the highest responses (especially for the inflammatory mediators), and is correlated with the SOA oxidative state. Because no attempt was made to put the results of the SOA assay in the context of their respective ambient levels and because a link between these assays and effects in humans has not been established, it is difficult to assess the biological relevance of these results. However, SOA is a major component of fine particulate matter in many areas of the country, and the results of this study underscore the need to better understand the effects of SOA on human health.

ACKNOWLEDGMENTS

The Review Committee thanks the ad hoc reviewers for their help in evaluating the scientific merit of the Investigators' Report. The Committee is also grateful to Geoffrey Sunshine for his oversight of the study, to Maria Costantini for her assistance in preparing its Critique, to Mary K. Brennan for science editing of this Report and its Critique, and to Hope Green, Fred Howe, Hilary Selby Polk, and Ruth Shaw for their roles in preparing this Research Report for publication.

REFERENCES

Carslaw KS, Lee LA, Reddington CL, Pringle KJ, Rap A, Forster PM, et al. 2013 Large contribution of natural aerosols to uncertainty in indirect forcing. Nature 503:67–71.

Delfino RJ, Staimer N, Tjoa T, Gillen DL, Schauer JJ, Shafer MM. 2013. Airway inflammation and oxidative potential of air pollutant particles in a pediatric asthma panel. J Exp Sci Environ Epidemiol 23(5):466–473.

Fang T, Verma V, Guo H, King LE, Edgerton ES, Weber RJ. 2015. A semi-automated system for quantifying the oxidative potential of ambient particles in aqueous extracts using the dithiothreitol (DTT) assay: Results from the

Southeastern Center for Air Pollution and Epidemiology (SCAPE). Atmos Meas Tech 8(1):471–482.

Ghio AJ, Carraway MS, Madden MC. 2012. Composition of air pollution particles and oxidative stress in cells, tissues, and living systems. J Toxicol Environ Health B Crit Rev 15(1):1–21.

Hallquist M, Wenger JC, Baltensperger U, Rudich Y, Simpson D, Claeys M, et al. 2009. The formation, properties and impact of secondary organic aerosol: Current and emerging issues. Atmos Chem Phys 9:5155–5236.

Hedayat F, Stevanovic S, Miljevic B, Bottle S, Risotvski ZD. 2015. Review — Evaluating the molecular assays for measuring the oxidative potential of particulate matter. Chem Ind Chem Eng Q21:201–210.

Henze DK, Seinfeld JH, Ng, NL, Kroll JH, Fu T-M, Jacob DJ, et al. 2008. Global modeling of secondary organic aerosol formation from aromatic hydrocarbons: High- versus low-yield pathways. Atmos Chem Phys 8:2405–2421.

Hodzic A, Kasibhatla PS, Jo, DS, Cappa CD, Jimenez JL, Madronich S, et al. 2016. Rethinking the global secondary organic aerosol (SOA) budget: Stronger production, faster removal, shorter lifetime. Atmos Chem Phys 16:7917–7941.

Hu S, Polidori A, Arhami M, Shafer MM, Schauer JJ, Cho A, et al. 2008. Redox activity and chemical speciation in size fractionated PM in the communities of the Los Angeles-Long Beach harbor. Atmos Chem Phys 8:6439–6451.

Kalyanaraman B, Darley-Usmar V, Davies KJ, Dennery PA, Forman HJ, Grisham MB, et al. 2012. Measuring reactive oxygen and nitrogen species with fluorescent probes: Challenges and limitations. Free Radic Biol Med 52:1–6.

Kroll JH, Seinfeld JH. 2008. Chemistry of secondary organic aerosol: Formation and evolution of low-volatility organics in the atmosphere. Atmos Environ 42:3593–3624.

Li N, Sioutas C, Cho A, Schmitz D, Misra C, Sempf J, et al. 2003. Ultrafine particulate pollutants induce oxidative stress and mitochondrial damage. Environ Health Perspect 111:455–460.

Mather JH, Stevens PS, Brune WH. 1997. OH and HO_2 measurements using laser-induced fluorescence. J Geophys Res 102:6427–6436.

McWhinney RD, Badali K, Liggio J, Li S-M, Abbatt JPD. 2013. Filterable redox cycling activity: A comparison between diesel exhaust particles and secondary aerosol constituents. Environ Sci Technol 47:3362–3369.

Michael S, Montaga M, Dotta W. 2013 Pro-inflammatory effects and oxidative stress in lung macrophages and epithelial cells induced by ambient particulate matter. Environ Pollution 183:19–29.

Miller MR, Shaw CA, Langrish JP. 2012. From particles to patients: Oxidative stress and the cardiovascular effects of air pollution. Future Cardiol 8:577–602.

Nel A. 2005. Atmosphere. Air pollution-related illness: Effects of particles. Science 308:804–806.

Ng NL, Kroll JH, Chan AWH, Chhabra PS, Flagan RC, Seinfeld JH. 2007. Secondary organic aerosol formation from *m*-xylene, toluene, and benzene. Atmos Chem Phys 7:3909–3922.

Patel RP, McAndrew J, Sellak H, White CR, Jo H, Freeman BA, et al. 1999. Biological aspects of reactive nitrogen species. Biochim Biophys Acta 1411:385–400.

Prasch Landreman A, Shafer MM, Hemming JC, Hannigan MP, Schauer JJ. 2008. A macrophage-based method for the assessment of the reactive oxygen species (ROS) activity of atmospheric particulate matter (PM) and application to routine (daily-24 h) aerosol monitoring studies. Aerosol Sci Tech 42:946–957.

Robinson AL, Donahue NM, Shrivastava MK, Weitkamp EA, Sage AM, Grieshop AP, et al. 2007 Rethinking organic aerosols: semivolatile emissions and photochemical aging. Science 315:1259–1262.

Saffari A, Daher N, Shafer MM, Schauer JJ, Sioutas C. 2014. Global Perspective on the oxidation potential of airborne particulate matter: A synthesis of research findings. Environ Sci Technol 48: 7576–7563.

Sylvester PW. 2011. Optimization of the tetrazolium dye (MTT) colorimetric assay for cellular growth and viability. Methods Mol Biol 716:157–168.

Tuet WY, Fok S, Verma V, Tagle Rodriguez MS, Grosberg A, Champion JA, et al. 2016. Dose-dependent intracellular reactive oxygen and nitrogen species (ROS/RNS) production from particulate matter exposure: Comparison to oxidative potential and chemical composition. Atmos Environ 144:335–344.

Verma V, Fang T, Guo H, King L, Bates JT, Peltier RE, et al. 2014. Reactive oxygen species associated with water-soluble $PM_{2.5}$ in the southeastern United States: Spatiotemporal trends and source apportionment. Atmos Chem Phys 14:12915–12930

Volckens J, Dailey L, Walters G, Devlin RB. 2009. Direct particle-to-cell deposition of coarse ambient particulate matter increases the production of inflammatory mediators from cultured human airway epithelial cells. Environ Sci Technol 43:4595–4599.

Xu L, Suresh S, Guo H, Weber RJ, Ng NL. 2015. Aerosol characterization over the southeastern United States using high-resolution aerosol mass spectrometry: Spatial and seasonal variation of aerosol composition and sources with a focus on organic nitrates. Atmos Chem Phys 15:7307–7336.

ABBREVIATIONS AND OTHER TERMS

AMS	high-resolution time-of-flight aerosol mass spectrometer
AUC	area under the dose–response curve
BBOA	biomass burning organic aerosol
BrC	brown carbon
C-DCF	carboxy-2′,7′-dichlorofluorescein
carboxy-DCFH	carboxy-2′,7′-dichlorodihydro-fluorescein
carboxy-DCF	carboxy-2′,7′-dichlorofluorescein
carboxy-H_2DCFDA	carboxy-2′,7′-dichlorodihydro-fluorescein diacetate
CO_2	carbon dioxide
DCFH-DA	2′,7′-dichlorofluorescein diacetate
DTT	dithiothreitol
EC_{50}	dose at which 50% of the response is attained
ELISA	enzyme-linked immunosorbent assay
FBS	fetal bovine serum
FS	iron (II) sulfate
GTEC	Georgia Tech Environmental Chamber
H_2O_2	hydrogen peroxide
H_2SO_4	sulfuric acid
HO_2•	hydroperoxyl radical
HONO	nitrous acid
IL-6	interleukin-6
LO-OOA	less-oxidized organic aerosols
LPS	lipopolysaccharide
MO-OOA	more-oxidized oxygenated organic aerosol
MS	magnesium sulfate
MTT	3-(4,5-dimethylthiazol-2-yl)-2, 5-diphenyltetrazolium bromide
NADH	nicotinamide adenine dinucleotide
NADPH	nicotinamide adenine dinucleotide (phosphate)
$NaNO_2$	sodium nitrite
NO	nitric oxide
NO_2	nitrogen dioxide
NO_3•	nitrate radical
NO_x	nitrogen oxides
NRVM	neonatal rat ventricular myocyte
•OH	hydroxyl radical
•OH_2	hydroxyperoxyl radical
$\overline{OS}_c$	average carbon oxidation state
PBS	phosphate buffered saline
PM	particulate matter
PMF	positive matrix factorization
POA	primary organic aerosol
RO•	alkoxy radical
RO_2•	peroxy radical
$RONO_2$	organic nitrate
ROS/RNS	reactive oxygen and nitrogen species
SA	sulfuric acid
SCAPE	Southeastern Center for Air Pollution and Epidemiology (U.S. EPA)
SOA	secondary organic aerosol
TNF-α	tumor necrosis factor-α
VOC	volatile organic compound
WSOC	water-soluble organic carbon

RELATED HEI PUBLICATIONS

Number	Title	Principal Investigator	Date
Research Reports			
177	National Particle Component Toxicity (NPACT) Initiative: Integrated Epidemiologic and Toxicologic Studies of the Health Effects of Particulate Matter Components	M. Lippmann	2013
	NPACT Study 1. Subchronic Inhalation Exposure of Mice to Concentrated Ambient $PM_{2.5}$ from Five Airsheds	L.-C. Chen	
174	Cardiorespiratory Biomarker Responses in Healthy Young Adults to Drastic Air Quality Changes Surrounding the 2008 Beijing Olympics	J. Zhang	2013
155	The Impact of the Congestion Charging Scheme on Air Quality in London	F. Kelly	2011
	Part 1. Emissions Modeling and Analysis of Air Pollution Measurements		
	Part 2. Analysis of the Oxidative Potential of Particulate Matter		
136	Uptake and Inflammatory Effects of Nanoparticles in a Human Vascular Endothelial Cell Line	I.M. Kennedy	2009
112	Health Effects of Acute Exposure to Air Pollution	S.T. Holgate	2003
	Part I. Healthy and Asthmatic Subjects Exposed to Diesel Exhaust		
	Part II. Healthy Subjects Exposed to Concentrated Ambient Particles		
110	Particle Characteristics Responsible for Effects on Human Lung Epithelial Cells	A.E. Aust	2002
84	Evaluation of the Potential Health Effects of the Atmospheric Reaction Products of Polycyclic Aromatic Hydrocarbons	A.J. Grosovsky	1999
HEI Perspectives			
3	Understanding the Health Effects of Ambient Ultrafine Particles	HEI Review Panel on Ultrafine Particles	2013
1	Airborne Particles and Health: HEI Epidemiologic Evidence	Health Effects Institute	2001

Copies of these reports can be obtained from HEI; PDFs are available for free downloading at www.healtheffects.org/publications.

HEI BOARD, COMMITTEES, and STAFF

Board of Directors

Richard F. Celeste, Chair *President Emeritus, Colorado College*

Sherwood Boehlert *Of Counsel, Accord Group; Former Chair, U.S. House of Representatives Science Committee*

Enriqueta Bond *President Emerita, Burroughs Wellcome Fund*

Jo Ivey Boufford *President, New York Academy of Medicine*

Homer Boushey *Emeritus Professor of Medicine, University of California, San Francisco*

Michael T. Clegg *Professor of Biological Sciences, University of California, Irvine*

Jared L. Cohon *President Emeritus and Professor, Civil and Environmental Engineering and Engineering and Public Policy, Carnegie Mellon University*

Stephen Corman *President, Corman Enterprises*

Alan I. Leshner *CEO Emeritus, American Association for the Advancement of Science*

Henry Schacht *Managing Director, Warburg Pincus; Former Chairman and Chief Executive Officer, Lucent Technologies*

Research Committee

David Savitz, Chair *Professor of Epidemiology, School of Public Health, and Professor of Obstetrics and Gynecology, Alpert Medical School, Brown University*

Jeffrey R. Brook *Senior Research Scientist, Air Quality Research Division, Environment Canada, and Assistant Professor, University of Toronto, Canada*

Francesca Dominici *Professor of Biostatistics and Senior Associate Dean for Research, Harvard T.H. Chan School of Public Health*

David E. Foster *Phil and Jean Myers Professor Emeritus, Department of Mechanical Engineering, Engine Research Center, University of Wisconsin, Madison*

Amy H. Herring *Sara & Charles Ayres Professor of Statistical Science, Duke University, Durham, North Carolina*

Barbara Hoffmann *Professor of Environmental Epidemiology, Institute of Occupational, Social, and Environmental Medicine, University of Düsseldorf, Germany*

Allen L. Robinson *Raymond J. Lane Distinguished Professor and Head, Department of Mechanical Engineering, and Professor, Department of Engineering and Public Policy, Carnegie Mellon University*

Ivan Rusyn *Professor, Department of Veterinary Integrative Biosciences, Texas A&M University*

Review Committee

James A. Merchant, Chair *Professor and Founding Dean Emeritus, College of Public Health, University of Iowa*

Kiros Berhane *Professor of Biostatistics and Director of Graduate Programs in Biostatistics and Epidemiology, Department of Preventive Medicine, Keck School of Medicine, University of Southern California*

Frank Kelly *Professor of Environmental Health and Director of the Environmental Research Group, King's College London*

Jana B. Milford *Professor, Department of Mechanical Engineering and Environmental Engineering Program, University of Colorado, Boulder*

Jennifer L. Peel *Professor of Epidemiology, Colorado School of Public Health and Department of Environmental and Radiological Health Sciences, Colorado State University*

Roger D. Peng *Professor of Biostatistics, Johns Hopkins Bloomberg School of Public Health*

HEI BOARD, COMMITTEES, and STAFF

Officers and Staff

Daniel S. Greenbaum *President*
Robert M. O'Keefe *Vice President*
Rashid Shaikh *Director of Science*
Jacqueline C. Rutledge *Director of Finance and Administration*
Emily Alden *Corporate Secretary*

Hanna Boogaard *Consulting Senior Scientist*
Aaron J. Cohen *Consulting Principal Scientist*
Philip J. DeMarco *Compliance Manager*
Hope Green *Editorial Project Manager*
Kathryn Liziewski *Research Assistant*
Kethural Manokaran *Research Assistant*
Lissa McBurney *Science Administrative Assistant*
Pallavi Pant *Staff Scientist*
Allison P. Patton *Staff Scientist*
Hilary Selby Polk *Managing Editor*
Lindy Raso *Executive Assistant*
Anna S. Rosofsky *Staff Scientist*
Robert A. Shavers *Operations Manager*
Annemoon M.M. van Erp *Managing Scientist*
Eleanne van Vliet *Staff Scientist*
Donna J. Vorhees *Director of Energy Research*
Katherine Walker *Principal Scientist*

HEALTH
EFFECTS
INSTITUTE

75 Federal Street, Suite 1400
Boston, MA 02110, USA
+1-617-488-2300
www.healtheffects.org

RESEARCH
REPORT

Number 197
March 2019